

Hydrologic Components for Model Development

By Carma A. San Juan, Wayne R. Belcher, Randell J. Laczniak, and Heather M. Putnam

Chapter C of

Death Valley Regional Ground-Water Flow System, Nevada and California—Hydrogeologic Framework and Transient Ground-Water Flow Model

Edited by Wayne R. Belcher

Prepared in cooperation with the
U.S. Department of Energy
Office of Environmental Management, National Nuclear Security Administration, Nevada Site Office,
under Interagency Agreement DE-AI52-01NV13944, and
Office of Repository Development,
under Interagency Agreement DE-AI08-02RW12167

Scientific Investigations Report 2004-5205

U.S. Department of the Interior
U.S. Geological Survey

Contents

| | |
|---|-----|
| Introduction | 103 |
| Water Budget | 103 |
| Ground-Water Discharge | 103 |
| Natural Ground-Water Discharge | 105 |
| Evapotranspiration | 105 |
| Springs..... | 108 |
| Staininger and Grapevine Springs..... | 108 |
| Texas, Travertine, and Nevares Springs..... | 108 |
| Indian and Cactus Springs..... | 109 |
| Bennetts and Manse Springs..... | 109 |
| Pumpage | 110 |
| Ground-Water Recharge | 115 |
| Lateral Flow..... | 118 |
| Balance of Components | 118 |
| Hydraulic Properties | 120 |
| Hydraulic Conductivity..... | 120 |
| Probability Distributions | 121 |
| Depth Decay | 121 |
| Hydraulic Head | 122 |
| Head Observations | 122 |
| Head-Observation Uncertainty | 128 |
| Well-Altitude Error | 128 |
| Well-Location Error | 128 |
| Nonsimulated Transient Error | 130 |
| Measurement Error | 130 |
| Total Head-Observation Error | 130 |
| Summary | 132 |
| References Cited | 133 |

Figures

| | |
|--|-----|
| C-1. Map showing major areas of ground-water recharge, natural discharge, and pumpage, and model boundary segments of lateral flow in the Death Valley regional ground-water flow system region..... | 104 |
| C-2. Map showing major areas of natural ground-water discharge in the Death Valley regional ground-water flow system model domain..... | 106 |
| C-3. Graph showing annual discharge from regional springs in Pahrump Valley, Bennetts and Manse Springs, 1875–1978..... | 110 |
| C-4. Map showing spatial distribution of pumping wells by water-use class and total pumpage for 1913–98 by hydrographic area..... | 111 |
| C-5. Graph showing annual ground-water pumpage estimates developed by water-use class from Death Valley regional ground-water flow system model domain, 1913–98..... | 113 |
| C-6. Graph of uncertainty in annual ground-water pumpage estimates developed for Death Valley regional ground-water flow system model domain, 1913–98 | 114 |

| | | |
|------------|---|-----|
| C-7—C-9. | Maps showing: | |
| C-7. | Simulated average annual precipitation and stream-gaging stations used to calibrate the net-infiltration model in the Death Valley regional ground-water flow system model region | 116 |
| C-8. | Simulated net infiltration used to estimate recharge to the Death Valley regional ground-water flow system model region, 1950–99 | 117 |
| C-9. | Regional ground-water potentiometric surface and lateral flow across boundary segments of the Death Valley regional ground-water flow model domain | 119 |
| C-10. | Annotated hydrograph showing general- and detailed-condition attributes assigned to water-level measurements from a well in Pahrump Valley..... | 125 |
| C-11—C-13. | Maps showing: | |
| C-11. | Spatial distribution and altitude of head observations in wells representing regional, steady-state conditions used in calibration of the Death Valley regional ground-water flow system model | 126 |
| C-12. | Spatial distribution and maximum drawdown of head observations in wells representing regional, transient conditions used in calibration of the Death Valley regional ground-water flow system model..... | 127 |
| C-13. | Spatial distribution and bottom depth of opening in head-observation wells (steady-state and transient conditions) used in calibration of the Death Valley regional ground-water flow system model | 129 |
| C-14. | Graphs showing uncertainty of 700 head observations computed to represent prepumped, steady-state conditions in the Death Valley regional ground-water flow system model domain. <i>A</i> , Cumulative frequency. <i>B</i> , Source of error..... | 131 |

Tables

| | | |
|------|---|-----|
| C-1. | Estimates of mean annual ground-water discharge from major evapotranspiration-dominated discharge areas in Death Valley regional ground-water flow system model domain..... | 107 |
| C-2. | Estimates of mean annual natural ground-water discharge from major spring areas not included in evapotranspiration-based discharge estimates in the Death Valley regional ground-water flow system model domain | 109 |
| C-3. | Number of wells and estimated total pumpage for 1913–98 by hydrographic area for the Death Valley regional ground-water flow system model domain | 112 |
| C-4. | Estimates of flow across lateral boundary segments of the Death Valley regional ground-water flow system model domain for prepumped conditions..... | 120 |
| C-5. | Annual volumetric flow estimates of major water-budget components of Death Valley regional ground-water flow system model domain for prepumped conditions and 1998 conditions | 121 |
| C-6. | Horizontal hydraulic-conductivity estimates of hydrogeologic units in the Death Valley regional ground-water flow system | 122 |
| C-7. | Description of attributes assigned to water levels retrieved from Ground-Water Site Inventory (GWSI) for simulation of ground-water flow in the Death Valley regional ground-water flow system model domain..... | 124 |
| C-8. | Bottom depth of open interval for wells used to calibrate the Death Valley regional ground-water flow system model..... | 128 |

CHAPTER C. Hydrologic Components for Model Development

By Carma A. San Juan, Wayne R. Belcher, Randell J. Laczniak, and Heather M. Putnam

Introduction

Hydrologic components of the Death Valley regional ground-water flow system (DVRFS) were evaluated to support development of a ground-water flow model. The components evaluated are those affecting the water budget: the distribution and volume of natural ground-water discharge, ground-water pumpage, ground-water recharge, and lateral inflow and outflow; the hydraulic conductivity values of the major hydrogeologic units (HGUs); and water levels (fig. C-1). This information is used in Chapter D to conceptualize ground-water flow through the Death Valley region and in Chapter F to develop discharge and hydraulic-head observations for model calibration.

Although previous investigators have attempted to quantify all or some of these major flow components in parts of the DVRFS region (Malmberg and Eakin, 1962; Walker and Eakin, 1963; Hunt and others, 1966; Malmberg, 1967; Glancy, 1968; Rush, 1968; Miller, 1977; Waddell, 1982; Rice, 1984; Harrill, 1986; Harrill and others, 1988; Dettinger, 1989), only a few have developed comprehensive estimates for the entire DVRFS region (IT Corporation, 1996a and b; D'Agnesse and others, 1997). Attempts to combine results from past investigations often are complicated by uncertainties and differences in the definition of basin and study area boundaries (D'Agnesse and others, 2002).

A series of studies was conducted to reassess previous estimates of the major flow components and hydraulic properties of the DVRFS region to improve the data for the conceptual model and for model calibration as part of the DVRFS investigation. These studies, the results of which are described in this chapter, focused on refining estimates of natural ground-water discharge by developing local estimates of evapotranspiration (ET), and compiling and making additional spring-flow measurements; compiling ground-water pumpage information to estimate the history of ground-water development; estimating ground-water recharge from numerical simulations of net infiltration; estimating boundary inflow and outflow by using regional hydraulic gradients and water budgets of areas adjacent to the DVRFS model domain; estimating hydraulic properties from available literature and aquifer-test data; and evaluating available water-level data to estimate representative pre- and post-pumping hydraulic head

information. In general, existing and newly acquired data were evaluated using current technology and concepts, analyses were refined or new algorithms were implemented for making interpretations, and values appropriate for the regional extent and scale of the model were estimated.

Water Budget

A water budget is developed to evaluate the balance between the flow into and flow out of a ground-water flow system. The primary components of the water budget are natural discharge, recharge, and lateral flow into and out of an area across its boundary. The introduction of pumping as a discharge from the flow system initially decreases hydraulic heads and ultimately affects one or more flow components either by decreasing natural discharge or increasing recharge. The following sections describe these major flow components and provide estimates of each component as used in the development of the transient flow model of the DVRFS. Ground-water discharge estimates derived from estimates of ET computed from micrometeorological measurements and from spring-flow measurements are the primary mass-balance observations used to calibrate the transient flow model. Estimates of recharge and boundary flow, although quantified and discussed in this chapter, are based on model simulations or on less direct measurements. Together, these flow components also were used to develop a general water budget for pre-pumped and pumped conditions.

Ground-Water Discharge

Ground-water discharge from the DVRFS model domain occurs both naturally and nonnaturally. Natural ground water recharge occurs as ET and spring flow and, to a small extent, as lateral flow to adjacent basins. Nonnaturally, ground water discharges as artesian flow from wells (1913–45) or as pumpage from wells in agricultural areas such as Pahrump and Penoyer Valleys and the Amargosa Desert. Moreo and others (2003) estimated that by 1998 pumpage was equivalent to nearly 75 percent of the natural discharge estimated for the DVRFS model domain prior to ground-water development.

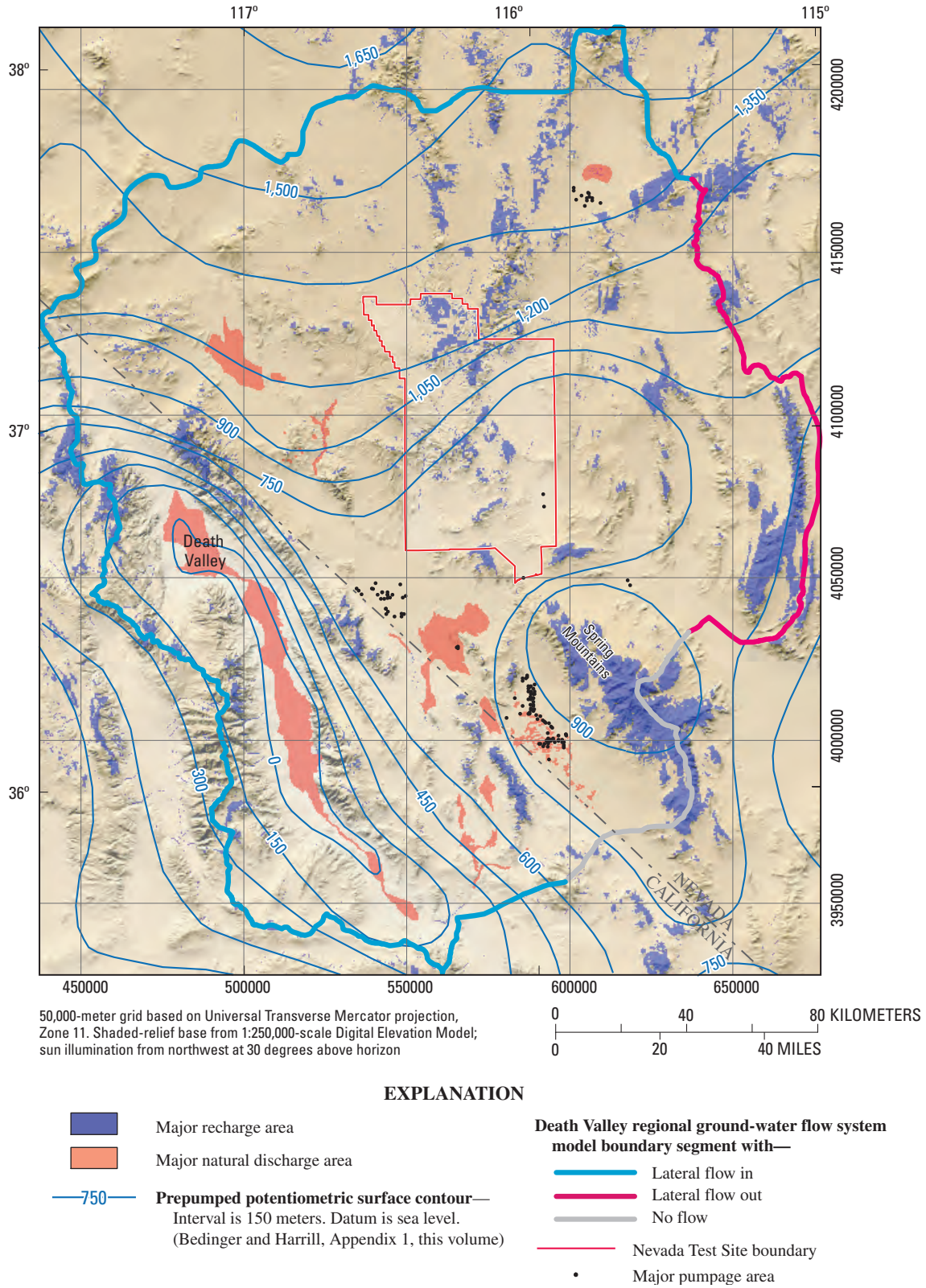


Figure C-1. Major areas of ground-water recharge, natural discharge, and pumpage, and model boundary segments of lateral flow in the Death Valley regional ground-water flow system region.

The following sections describe estimates of natural discharge and pumping as developed for simulating ground-water flow in the DVRFS model domain.

Natural Ground-Water Discharge

Areas of natural discharge cover less than 5 percent of the DVRFS model domain (fig. C-2). These areas include wet playas, wetlands with free-standing water or surface flow, narrow drainages lined with riparian vegetation, and broad areas of phreatophytic shrubs and grasses. The largest discharge areas by flow volume are Death Valley, Ash Meadows, and Sarcobatus Flat, respectively (fig. C-2). Each of these discharge areas represents a unique environment and together they include most of the different types of local habitat supported by ground-water discharge throughout the DVRFS region. Death Valley is dominated by a saltpan surrounded by alluvial fans and by numerous locally and regionally fed springs fringed with a variety of desert shrubs, trees, and grasses. Ash Meadows is a unique desert oasis that consists of broad wetlands fed by orifice-type springs. These large-volume springs are surrounded by extensive grass meadows interspersed with moderately dense to sparse stands of trees and shrubs. Sarcobatus Flat is a broad playa surrounded by moderately dense grasses and sparse shrubs that are supported by a few small springs and seeps and a moderately shallow water table.

The quantity of ground water discharging from most of the major discharge areas in the DVRFS model domain (fig. C-2) has been estimated in previous studies. These estimates were developed primarily from spring-flow measurements, ET estimates, or a combination of both. Usually, ground-water discharge was estimated only for an individual discharge area or at a specific location, and not for the entire flow system. Reports estimating ground-water discharge are Malmberg and Eakin (1962), Walker and Eakin (1963), Pistrang and Kunkel (1964), Hunt and others (1966), Malmberg (1967), Glancy (1968), Rush (1968), Van Denburgh and Rush (1974), Winograd and Thordarson (1975), Miller (1977), Harrill (1986), Czarnecki (1997), D'Agnese and others (1997), Laczniaik and others (1999), Reiner and others (2002), and DeMeo and others (2003). Discrepancies in discharge estimates between more recent and previous reports typically reflect differences in the delineation of the area contributing to ET, the number of springs measured, ET rates estimated for vegetation types, or some combination thereof (Laczniaik and others, 2001, p. 31; D'Agnese and others, 2002, p. 26).

Evapotranspiration

Recent investigations of natural ground-water discharge in the DVRFS region estimate discharge by calculating ET. The underlying assumption of this approach is that most of the ground water issuing from springs and seeps within the discharge area ultimately is evaporated or transpired locally in the DVRFS region and therefore is accounted for in estimates of ET. Most of the discharge data used to develop the discharge observations presented in Chapter F (this volume) are based

on estimates of ET in recent reports by Laczniaik and others (1999 and 2001), Reiner and others (2002), and DeMeo and others (2003). The report by Laczniaik and others (2001) is the most comprehensive evaluation of ground-water discharge in that it provides estimates of ground-water discharge for 9 of the 15 major ET-dominated discharge areas in the DVRFS model domain (fig. C-2). Their estimate of discharge in Oasis Valley was revised in a subsequent study (Reiner and others, 2002). Laczniaik and others (2001) made no attempt to revise estimates of natural discharge from Pahrump and Penoyer Valleys because ground water withdrawn for irrigation had locally altered the distribution of native vegetation and decreased local spring flow. D'Agnese and others (2002, p. 26) provide an estimate of natural discharge from Pahrump Valley but state that their estimate was based on an ET analysis that used a map delineating the native phreatophyte distribution in 1959-61 (Malmberg, 1967, pl. 3)—a time by which vegetation already had been significantly affected by local pumping. These same authors present an estimate of natural discharge from Penoyer Valley that was first documented in a reconnaissance report by Van Denburgh and Rush (1974, p. 23) and later reported by IT Corporation (1996a). A recent study by DeMeo and others (2003) was the primary source used to develop estimates of ground-water discharge from the floor of Death Valley.

The more recent investigations were similar in that continuous micrometeorological data were collected to estimate local ET rates, and remotely sensed multi-spectral data were used to distribute measured ET rates over the area evaluated. Micrometeorological data were collected continuously at 15 stations for 1 to 3 years each in Ash Meadows and Oasis Valley (Laczniaik and others, 1999; Reiner and others, 2002) and at 6 sites in Death Valley over a 4-year period (DeMeo and others, 2003). Remotely sensed images, aerial photographs, and soils and wetland maps were integrated using geographic information system (GIS) techniques and were used in these studies to delineate ET units (areas of similar vegetation and moisture conditions) and distribute calculated ET rates over respective discharge areas. This process resulted in more consistent and generally improved estimates of ground-water discharge than in previous studies.

Most ET-based estimates of ground-water discharge assume that in addition to ground water, all precipitation falling on a discharge area, any surface water flowing into a discharge area, and all local infiltration to the shallow flow system ultimately are evaporated or transpired by the local vegetation. Accordingly, mean annual ground-water discharge (estimated from ET) is the difference between the mean annual ET and the sum of mean annual precipitation and any surface-water inflow. In more recent studies, mean annual ET is computed by multiplying the area of an ET unit by the mean annual ET rate calculated for a unit. Mean annual ET rates for individual ET units range from less than 0.06 meter (m) for bare and salt-encrusted soil (DeMeo and others, 2003) to 2.75 m for open water (Laczniaik and others, 2001). Adjustments made for precipitation were typically small because mean annual precipitation ranges from less than 0.08 m in

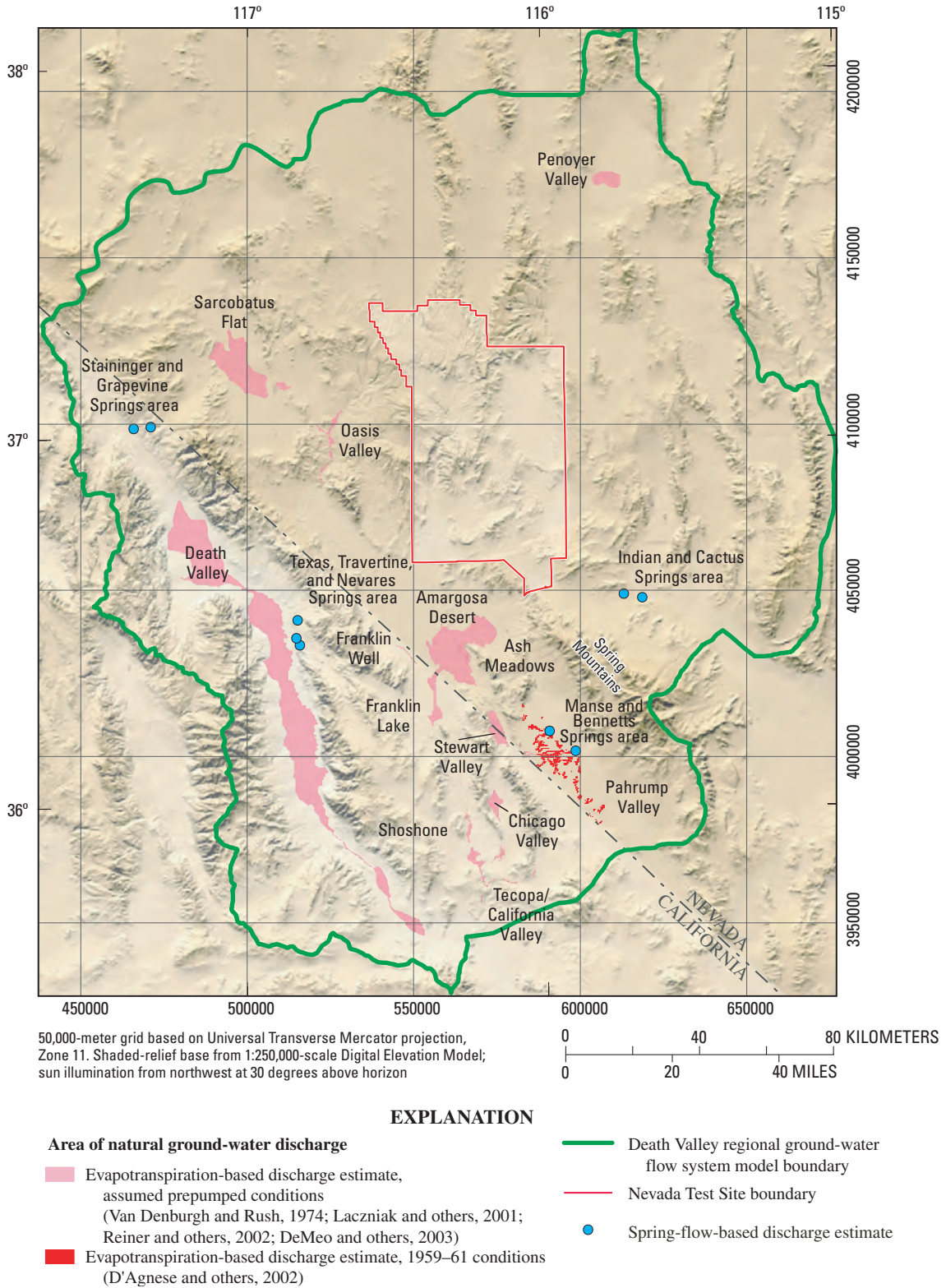


Figure C-2. Major areas of natural ground-water discharge in the Death Valley regional ground-water flow system model domain.

Death Valley (DeMeo and others, 2003) to about 0.15 m in Sarcobatus Flat and Oasis Valley (Laczniaik and others, 2001). Runoff into major discharge areas from adjacent highlands was assumed to be minimal and was not calculated. Accordingly, ground-water discharge for most major ET-dominated discharge areas (fig. C-2) was calculated as the difference between mean annual ET and mean annual precipitation.

Accurate mapping of soil and vegetation in discharge areas was critical to improving estimates of the size of ET units. These more recent studies identified most of the vegetation, soil, and water-dominated ET units in major discharge areas using remotely sensed, spectral imagery acquired during 1989–96. Wetland maps produced by the U.S. Fish and Wildlife Service for the National Wetlands Inventory Project were used to delineate two soil-dominated ET units—bare and salt encrusted—in Death Valley (DeMeo and others, 2003). Other ET units included areas of open playa; sparse to dense vegetation; moist, bare soil; and open water (Laczniaik and others, 2001; Reiner and others, 2002). Death Valley, the largest discharge area, has an estimated area of about 445.5 square kilometers (km²) and is dominated by extensive flats of moist, bare, and salt-encrusted soil. Sarcobatus Flat has an estimated area of about 138.6 km² and is predominantly sparse to moderately dense shrubland. The fourth largest ET area, Ash Meadows, has an area of about 50.5 km² and ranges from

broad, sparse grassland to dense, riparian wetland adjacent to spring pools. The estimated sizes of the other major ET-dominated major discharge areas are given in table C-1.

Micrometeorological data were collected continuously and averaged over 20-minute periods. These 20-minute averages were used to compute ET rates for the different ET units delineated throughout the DVRFS region. Microclimate stations were operated at 10 sites in Ash Meadows from 1993 to 1997 (Laczniaik and others, 1999, table 6), at 5 sites in Oasis Valley from 1996 to 2000 (Reiner and others, 2002, table 3), and at 6 sites in Death Valley from 1997 to 2001 (DeMeo and others, 2003, table 3). Annual ET rates were computed from the micrometeorological data using the Bowen ratio solution of the energy-budget equation (Bowen, 1926). Average annual ET rates for ET-dominated discharge areas ranged from 0.20 meter per year (m/yr) in Stewart Valley to 0.79 m/yr in Pahrump Valley (table C-1).

Mean annual ground-water discharge for each major ET-dominated discharge area was calculated as the product of the adjusted-annual ET rate and the area of the ET unit (table C-1). Annual ET rates were adjusted by removing water contributed by local precipitation. Although a comparison of these and previous discharge estimates is complicated by differences in the procedures used to estimate ET rates and in the mapped extent of individual discharge

Table C-1. Estimates of mean annual ground-water discharge from major evapotranspiration-dominated discharge areas in Death Valley regional ground-water flow system model domain.

[Ground-water discharge rounded to nearest thousand. Rates rounded to nearest hundredth. Mean annual ground-water discharge may not equal product of precipitation-adjusted ET rate and area because of rounding. Dash (--) indicates that no value was reported in referenced source or that the information given was insufficient to compute a value. Abbreviations: ET, evapotranspiration; m/yr, meters per year; km², square kilometer; m³, cubic meter; Mm³, million cubic meters]

| Discharge area (shown in fig. C-2) | Estimated mean annual ET rate (m/yr) | Area (km ²) | Annual precipitation rate (m/yr) | Estimated precipitation- adjusted annual ET rate (m/yr) | Estimated mean annual ground-water discharge (m ³) |
|--|---|----------------------------|---|---|--|
| Ash Meadows ¹ | 0.55 | 50.5 | 0.11 | 0.44 | 22,203,000 |
| Chicago Valley ¹ | 0.34 | 2.48 | 0.11 | 0.23 | 530,000 |
| Franklin Lake ¹ | 0.23 | 9.43 | 0.10 | 0.13 | 1,234,000 |
| Franklin Well area ¹ | 0.46 | 1.20 | 0.11 | 0.35 | 432,000 |
| Oasis Valley ² | 0.70 | 13.9 | 0.15 | 0.55 | 7,401,000 |
| Pahrump Valley ³ | 0.79 | 12.2 | 0.12 | 0.67 | ³ 8,082,000 |
| Penoyer Valley ⁴ | -- | 76.9 | -- | 0.06 | 4,650,000 |
| Sarcobatus Flat ¹ | 0.27 | 138.6 | 0.15 | 0.12 | 16,035,000 |
| Shoshone area ¹ | 0.55 | 5.62 | 0.09 | 0.46 | 2,590,000 |
| Stewart Valley ¹ | 0.20 | 12.2 | 0.11 | 0.09 | 1,234,000 |
| Tecopa/California Valley area ¹ | 0.64 | 14.2 | 0.09 | 0.55 | 7,894,000 |
| Death Valley floor ⁵ | -- | 445.5 | -- | 0.01 | ⁶ 43,172,000 |
| Total | | | | | 115,457,000 |

¹Laczniaik and others (2001, tables 5 and 10).

²Reiner and others (2002, table 5).

³D'Agnesse and others (2002, table 3). Mean annual ground-water discharge during the period 1959–61.

⁴Van Denburgh and Rush (1974, table 8 and p. 23); D'Agnesse and others (2002, p. 26).

⁵DeMeo and others (2003, table 4).

⁶Estimate varies from about 27.1–43.2 Mm³ as adjusted for different flood recurrence intervals (DeMeo and others, 2003, p. 24). Flood-adjusted ET estimate reported by DeMeo and others (2003, p. 24) is 40.7 Mm³.

areas, Laczniaik and others (2001, p. 29–30) state that their estimates, in general, are greater than those reported in the literature for the more northern discharge areas and less than those previously reported for the more southern discharge areas.

The mean annual ground-water discharge given for Death Valley (DeMeo and others, 2003, p. 24) is considered a partial estimate because evaporation, transpiration, and flow diversions associated with a series of regional springs along the northeastern margin of the valley are not included. The total mean annual ground-water discharge from Death Valley is equal to the sum of ET estimated for the valley floor and reported flow from valley-margin springs discussed in the following section. This method may account twice for underflow from these valley-margin springs into sediment beneath the valley floor. The error resulting from any double accounting of underflow is expected to be small because most of the water discharged from these springs is transpired, evaporated, or diverted for local water supply.

All discharge estimates given in table C–1, except those for Pahrump and Penoyer Valleys, are assumed to represent discharge for both prepumped and current conditions. This assumption is reasonable considering that pumping from these major discharge areas is negligible and climate has been relatively stable over the period. The total amount of ground water discharging annually from the DVRFS model domain (computed by summing all estimates in table C–1) is about 115.5 million cubic meters (Mm³).

Limitations inherent in an ET-based approach for estimating ground-water discharge can be attributed to errors in delineating the extent of ET units and errors in calculating ET rates (Laczniaik and others, 2001, p. 31). Other factors potentially affecting the accuracy of ET-based estimates of ground-water discharge include (1) the assumption that all spring flow ultimately is evaporated or transpired from within the discharge area, (2) the assumption that surface-water inflow is minimal, (3) the short period of record used to compute mean annual ET rates, (4) the limited number of local sites used to estimate mean annual ET rates, (5) uncertainties associated with estimating ET on the basis of relative differences in vegetation density, and (6) uncertainties in the amount of water contributed by precipitation and surface flow to the ET estimates (Laczniaik and others, 2001, p. 31).

Springs

Most of the ground water discharged naturally from the DVRFS region flows from springs and seeps. Regional high-volume springs having flows greater than 1,500 cubic meters per day (m³/d) discharge in Oasis Valley, Ash Meadows, Pahrump Valley, the Shoshone and Tecopa areas, and on the floor of Death Valley (fig. C–2). Typically, these regional springs discharge water with temperatures greater than 30 degrees Celsius (°C) (U.S. Geological Survey, National Water Information System, retrieved June 2003) directly from the rocks that make up the regional aquifer. Because most flow from

springs and seeps in major ET-dominated discharge areas is evaporated and(or) transpired by the local riparian vegetation, ET estimates are assumed to be inclusive of spring and seep flow (table C–1; Laczniaik and others, 2001; Reiner and others, 2002).

Spring discharge cannot always be quantified accurately using ET-based methods. For example, ET-based methods are not well suited for estimating discharge in areas where springs support limited vegetation or where local pumping has decreased spring flow. Estimates of ground-water discharge from areas of spring flow not estimated by an ET technique were derived solely on the basis of spring-flow measurements and are presented in table C–2. Areas of discharge not included in ET-based estimates are the Staininger and Grapevine Springs areas near Scotty's Castle in Death Valley; Texas, Travertine, and Nevares Springs areas near Furnace Creek Ranch in Death Valley; Indian and Cactus Springs areas near Indian Springs, Clark County, Nev.; and the Manse and Bennetts Springs areas in Pahrump Valley (fig. C–2). All discharge estimates, except those for Pahrump Valley (Bennetts and Manse Springs), were based on flow measurements made or compiled by C.S. Savard (U.S. Geological Survey, written commun., 2001). Thus any nonreferenced discharge values in the following sections are attributed to Savard's unpublished work. The total annual discharge from spring flow summarized in table C–2 is about 16.8 Mm³.

Staininger and Grapevine Springs

Mean ground-water discharge from Staininger Spring, the water supply for Scotty's Castle area in Death Valley, is estimated at 1,035 m³/d±15 percent (table C–2). This estimate was based on four historical flow measurements, three of which were reported by Miller (1977): 1,019 m³/d in 1924, 981 m³/d in 1958, 1,025 m³/d in 1971, and the fourth, 1,090 m³/d in 1967 by Rush (1968). Other reported values of discharge from this spring—2,271 m³/d (Ball, 1907), 54 m³/d (Waring, 1915), and 163 m³/d (Waring, 1965)—were considered to be unreliable because they did not measure the entire spring flow.

The aggregate discharge from about 12 springs and seeps in the Grapevine Springs area is estimated at 2,450 m³/d±20 percent (table C–2). This estimate was originally made by Miller (1977) on the basis of discharge measurements made at a few accessible springs and a cursory quantification of ET. Previous reports by Ball (1907) and Mendenhall (1909) mention these springs but do not provide a discharge estimate. Rush (1968) reports discharge from a single unnamed spring at 109 m³/d.

Texas, Travertine, and Nevares Springs

Discharge from Texas Spring from 1989 to 1996 is estimated at 1,220 m³/d±15 percent (table C–2). This estimate is based on measurements reported in LaCamera and Westenburg (1994), Hale and Westenburg (1995), Westenburg and LaCamera (1996), LaCamera and others (1996), and

Table C-2. Estimates of mean annual natural ground-water discharge from major spring areas not included in evapotranspiration-based discharge estimates (table C-1) in the Death Valley regional ground-water flow system model domain.[--, no value reported; m³/d, cubic meters per day; discharge rate rounded to nearest five; ground-water discharge rounded to nearest hundred]

| Spring name/area | General location | Estimated mean discharge rate (m ³ /d) | Estimated mean annual ground-water discharge (m ³) | Estimated percent accuracy |
|---|---|---|--|----------------------------|
| Staininger Spring ¹ | Scotty's Castle, Death Valley, Calif. | 1,035 | 378,000 | 15 |
| Grapevine Springs ¹ | Scotty's Castle, Death Valley, Calif. | 2,450 | 894,900 | 20 |
| Texas Spring ¹ | Furnace Creek Ranch, Death Valley, Calif. | 1,220 | 445,600 | 15 |
| Travertine Spring ¹ | Furnace Creek Ranch, Death Valley, Calif. | 4,630 | 1,691,100 | 10 |
| Nebares Spring ¹ | Furnace Creek Ranch, Death Valley, Calif. | 1,885 | 688,500 | -- |
| Indian and Cactus Springs ¹ | Indian Springs, Clark County, Nev. | 2,240 | 818,200 | 10 |
| Bennetts and Manse Springs ² | Pahrump, Nev. | 32,400 | 11,834,100 | 25 |
| Total | | 45,860 | 16,750,400 | -- |

¹Estimate based on flow measurements made or compiled by C.S. Savard (U.S. Geological Survey, written commun., 2001).²Estimate of ground-water discharge based on flow measurements from Bennetts and Manse Springs made before 1913 when ground-water pumping began (Maxey and Jameson, 1948; Malmberg, 1967; and Harrill, 1986).

LaCamera and Locke (1997). Earlier reports give discharge rates from Texas Spring that range from 136 m³/d in 1915 (Waring, 1915) to 685 m³/d in 1926 (Pistrang and Kunkel, 1964). A tunnel constructed into the spring between 1926 and 1941 nearly doubled spring discharge. Reported discharge measurements taken after tunnel construction were 930 m³/d in 1941 (Pistrang and Kunkel, 1964); 1,150 to 1,223 m³/d from 1956 to 1963 (Pistrang and Kunkel, 1964); and 1,145 m³/d in 1976 (Miller, 1977).

Mean discharge from the Travertine Spring area is estimated at 4,630 m³/d±10 percent. This estimate is based on measurements made from 1956 to 1972 (table C-2; Miller, 1977). Estimates developed by summing measurements made at 10 springs in the Travertine Springs area between 1955 and 1965 ranged from 4,111 to 4,747 m³/d (Pistrang and Kunkel, 1964). The aggregate discharge estimate of 3,815 m³/d given in Miller (1977) was based on measurements made at only three springs in 1977. Other periodic measurements made at individual springs are difficult to composite into an estimate of discharge for the entire area because of differences in measurement dates.

Natural discharge from the Nebares Spring area is estimated at 1,885 m³/d (table C-2; Pistrang and Kunkel, 1964). This estimate includes discharge from nearby Cow (100 m³/d) and Salt Springs (25 m³/d). Early measurements of discharge from the main area of Nebares Spring averaged 1,470 m³/d for the period 1956 to 1957, while discharge from other nearby springs in the Nebares Spring area totaled 290 m³/d (Pistrang and Kunkel, 1964). Hunt and others (1966) report combined discharge from the five major springs in the area at 1,790 m³/d in 1951 and 1,760 m³/d in 1957. An aggregate discharge of about 1,420 m³/d was reported by Miller (1977) for Nebares Spring and a nearby, unnamed spring.

Indian and Cactus Springs

Discharge from the Indian and Cactus Springs area is estimated at 2,240 m³/d±10 percent (table C-2). The first reported estimate of discharge at Indian Springs, 2,230 m³/d (Carpenter, 1915), was made in 1912. Subsequent estimates of 2,180 m³/d (Maxey and Jameson, 1948) and 2,365 m³/d (Malmberg, 1965) varied by less than 10 percent. Rush (1970) reports an anomalously low discharge of 1,690 m³/d. He attributes the decrease to be an effect of nearby pumping. Reported estimates of discharge from Cactus Spring are all less than 5 m³/d (Carpenter, 1915; Maxey and Jameson, 1948).

Bennetts and Manse Springs

Natural discharge from Bennetts and Manse Springs in Pahrump Valley (fig. C-2) is estimated at 32,400 m³/d±25 percent (table C-2) for the period prior to ground-water pumping. This estimate is based on reported discharges before 1913 of 17,900 m³/d from Bennetts Spring and 14,500 m³/d from Manse Spring (Maxey and Jameson, 1948). The estimates of spring flow from Bennetts and Manse Springs are based on measurements made before 1913 and represent prepumped conditions (Maxey and Jameson, 1948; Malmberg, 1967; and Harrill, 1986). The relatively large inaccuracy given to the estimate accounts for uncertainties associated with the nature of the measurements.

Bennetts and Manse Springs were the largest springs in Pahrump Valley and discharged from the base of alluvial fans at the foot of the Spring Mountains. After 1945, large-scale agricultural development accompanied by the drilling and pumping of wells to irrigate cropland drastically decreased spring flows throughout the valley (Harrill, 1986). Bennetts Spring stopped flowing in 1959. Manse Spring virtually

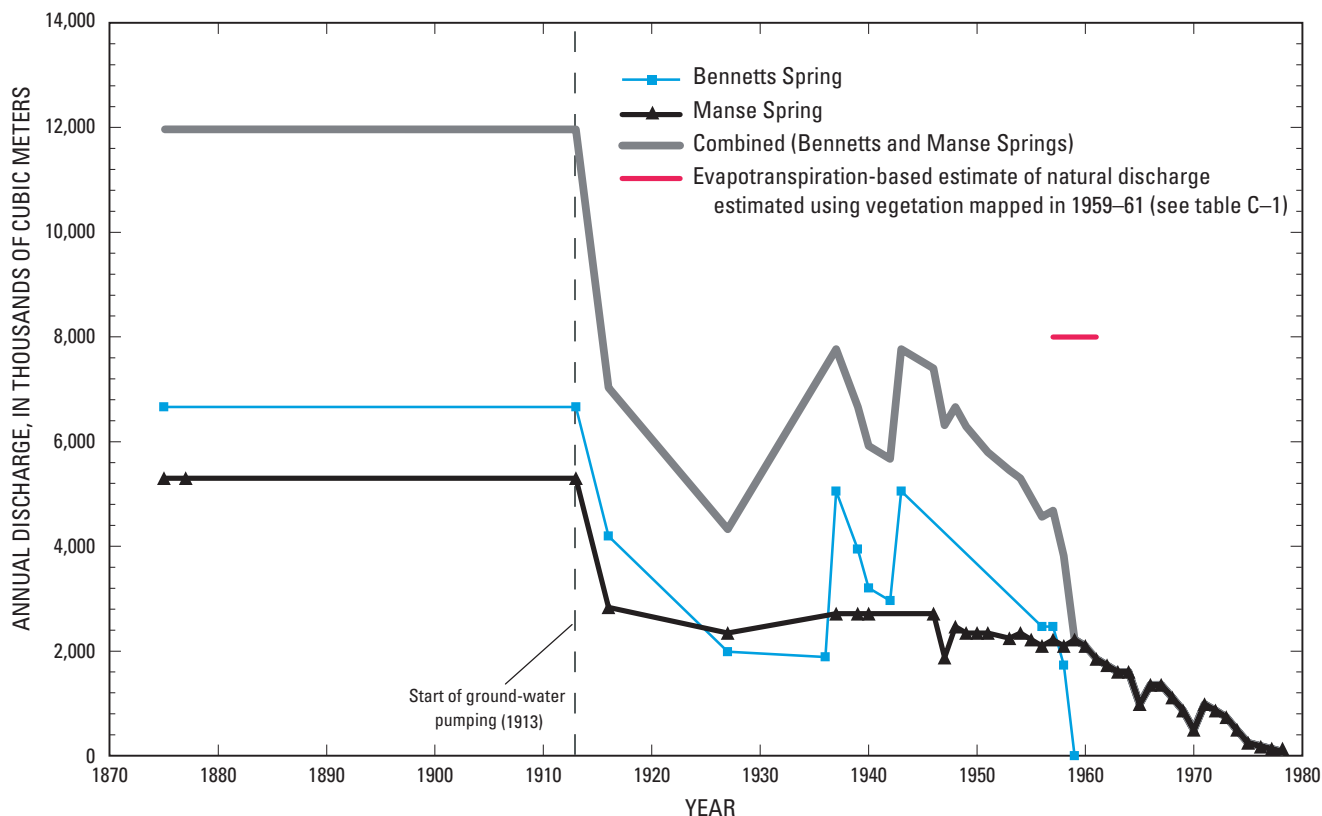


Figure C-3. Annual discharge from regional springs in Pahrump Valley, Bennetts and Manse Springs, 1875–1978.

stopped flowing in 1977 although small intermittent flows during the winter season have been reported. Estimated annual discharge from Bennetts and Manse Springs is shown in figure C-3 for 1875–1978.

The mean annual discharge in Pahrump Valley estimated from ET by D’Agnese and others (2002) also is shown in figure C-3. During 1959–61, mean annual discharge was estimated as about 8.1 Mm³.

Pumpage

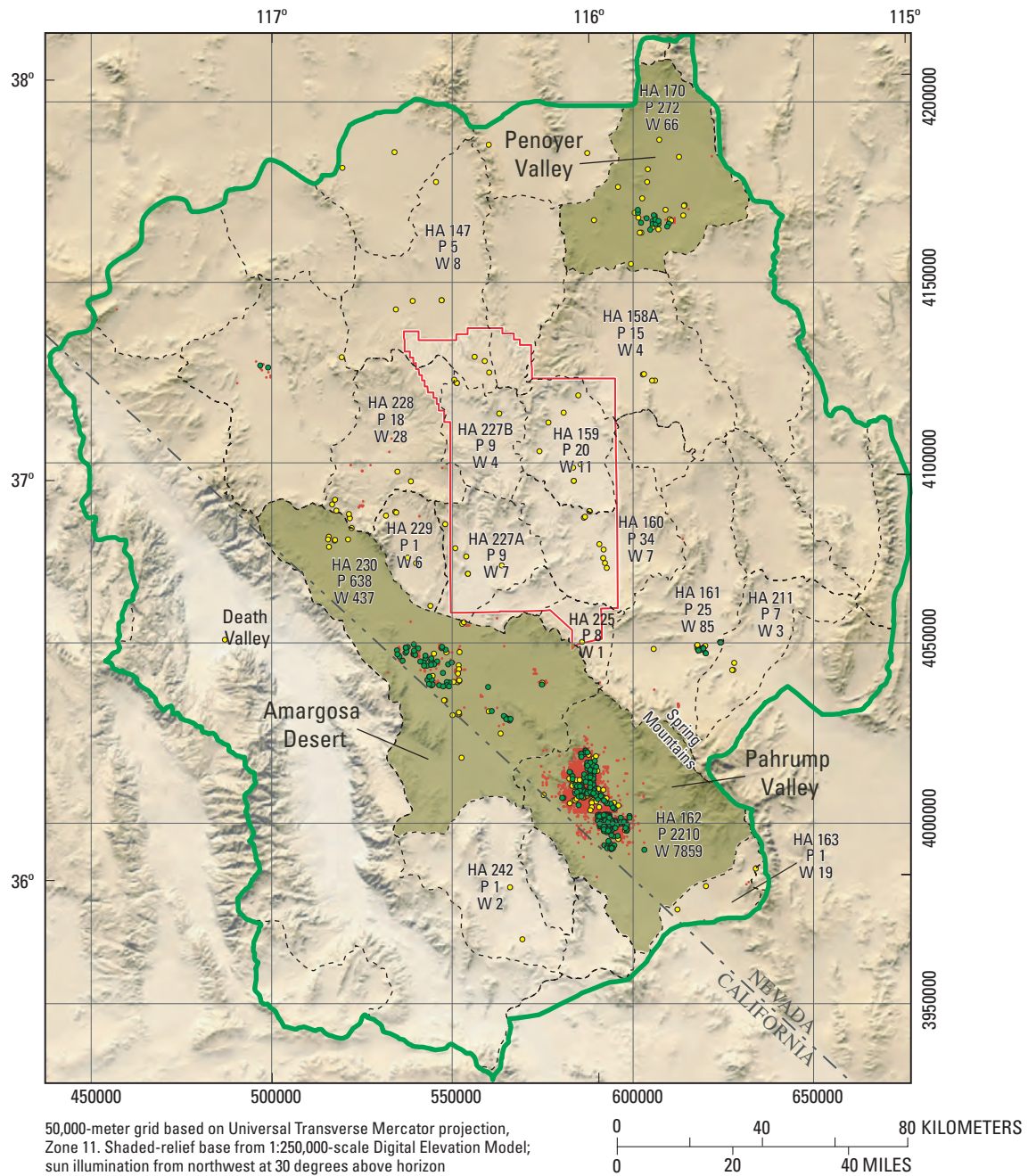
Substantial quantities of ground water have been pumped from the DVRFS region. Ground-water pumping started around 1913 in Pahrump Valley to support a small agricultural community and has continued throughout the region to support local agriculture, mining, industry, and rural and urban growth. The number of pumping wells in the DVRFS region increased substantially from only a few wells in 1913 to nearly 9,300 wells in 1998 (Moreo and others, 2003).

Pumpage from wells, and the physical description and location of pumping wells in the DVRFS region, are reported intermittently in publicly available reports and databases. These sources lack sufficient information, however, from which to develop the complete history of ground-water development for the DVRFS region. Moreo and others (2003) compiled available information and developed annual pumpage

estimates to complete the annual pumpage history for the period 1913–98. Their database contains estimates of annual ground-water withdrawal at each known pumping well in the DVRFS region and was used to develop pumping stresses for model simulation of pumped conditions (see Chapter F, this volume).

About 8,600 of the approximately 9,300 wells investigated by Moreo and others (2003) are in the DVRFS model domain (fig. C-4). A few wells included in Moreo and others (2003) that had estimated open intervals that did not match the interpolated horizons in the hydrogeologic framework model (Chapter E, this volume) were removed from the dataset. The combined pumpage from these few wells removed from the data set accounted for less than 0.001 percent (about 8,000 m³ of the total ground water pumped for the period 1913–98).

About 97 percent of the pumping wells are in the southern part of the model domain (fig. C-4 and table C-3). These wells are concentrated primarily in the southern part of Amargosa Desert and in Pahrump Valley. Penoyer Valley has the greatest concentration of pumping wells in the northern part of the model domain. About 95 percent of the pumpage estimated from 1913 to 1998 was withdrawn from these three hydrographic areas (fig. C-4 and table C-3) delineated by Cardinalli and others (1968) on the basis of topographic basins. Table C-3 presents estimates of total pumpage from the DVRFS model domain for the period 1913–98 and for



EXPLANATION

- Hydrographic areas where pumpage exceeds 100 million cubic meters (Mm^3)
- HA 242
P 1
W 2 Hydrographic areas where pumpage exceeds 1 Mm^3 —
HA, hydrographic area;
P, total pumpage in Mm^3 ;
W, number of wells.
- Hydrographic area boundary
(modified from Cardinalli and others, 1968)
- Death Valley regional ground-water flow system model boundary
- Nevada Test Site boundary
- Pumping wells by water-use class**
(Moreo and others, 2003)
- Domestic
- Mining, public supply, and commercial
- Irrigation

Figure C-4. Spatial distribution of pumping wells by water-use class and total pumpage for 1913–98 by hydrographic area.

Table C-3. Number of wells and estimated total pumpage for 1913–98 by hydrographic area for the Death Valley regional ground-water flow system model domain.

[Annual pumpage estimates computed from data in Moreo and others (2003) for 22 hydrographic areas having reported pumpage; m³, cubic meters; pumpage values for 1913–98 are rounded to the nearest thousand and for 1998 to the nearest ten]

| Hydrographic area | | Number of wells 1913–98 | Estimated pumpage | |
|-------------------|------------------------------------|-------------------------|---------------------------|------------------------|
| Number | Name | | 1913–98 (m ³) | 1998 (m ³) |
| 144 | Lida Valley | 1 | 12,000 | 860 |
| 146 | Sarcobatus Flat | 15 | 850,000 | 25,160 |
| 147 | Gold Flat | 8 | 4,561,000 | 43,170 |
| 148 | Cactus Flat | 2 | 866,000 | 56,740 |
| 158A | Emigrant Valley | 4 | 15,196,000 | 345,380 |
| 159 | Yucca Flat | 11 | 20,023,000 | 91,280 |
| 160 | Frenchman Flat | 7 | 34,272,000 | 534,100 |
| 161 | Indian Springs Valley | 85 | 25,422,000 | 789,680 |
| 162 | Pahrump Valley | 7,859 | 2,210,135,000 | 43,855,360 |
| 163 | Mesquite Valley ¹ | 19 | 1,059,000 | 31,080 |
| 170 | Penoyer Valley | 66 | 272,390,000 | 15,669,790 |
| 173A | Railroad Valley ¹ | 2 | 197,000 | 4,930 |
| 211 | Three Lakes Valley (southern part) | 3 | 6,986,000 | 410,750 |
| 225 | Mercury Valley | 1 | 8,479,000 | 3,700 |
| 226 | Rock Valley | 1 | 38,000 | 860 |
| 227A | Fortymile Canyon (Jackass Flats) | 7 | 8,510,000 | 184,650 |
| 227B | Fortymile Canyon (Buckboard Mesa) | 4 | 8,674,000 | 117,180 |
| 228 | Oasis Valley | 28 | 17,880,000 | 309,600 |
| 229 | Crater Flat | 6 | 1,094,000 | 171,450 |
| 230 | Amargosa Desert | 437 | 637,619,000 | 30,729,610 |
| 242 | Lower Amargosa Desert | 2 | 1,132,000 | 33,300 |
| 243 | Death Valley | 1 | 497,000 | 40,700 |
| Total | | 8,569 | 3,275,892,000 | 93,449,330 |

¹Only part of hydrographic area contained in Death Valley regional ground-water flow system model domain.

1998 by hydrographic area. Of the 38 hydrographic areas in the DVRFS model domain, 16 have no reported pumping during this period.

Moreo and others (2003) grouped pumping wells into three water-use categories: (1) irrigation; (2) mining, public supply, and commercial; and (3) domestic. Although nearly 93 percent of the wells are for domestic use, 90 percent of the water pumped was for irrigation. Pumpage determined for each water-use category was estimated using different methods. The results and techniques used to develop a pumpage history for the DVRFS region are summarized in the following paragraphs. Moreo and others (2003) provide more detail.

Well-construction information was used to estimate the open-interval depths of each pumping well. Approximately 85 percent of the irrigation wells, 97 percent of the mining, public supply, and commercial wells, and 98 percent of the domestic wells had reported completion intervals (Moreo and others, 2003). For wells for which construction information was absent, open intervals were estimated using construction data from nearby wells of the same water-use category. Moreo

and others (2003) reported that most pumping wells are open to basin-fill deposits and were drilled to depths of less than about 150 m, with less than 1 percent having depths exceeding about 300 m.

Irrigation accounted for 90 percent of the ground water pumped from the DVRFS model domain during 1913–98. Irrigation gradually declined from about 100 percent (about 4,940 Mm³) of the ground water used in 1913 to about 80 percent (about 74,710 of 93,450 Mm³) in 1998 (fig. C-5). Moreo and others (2003) estimated annual irrigation by multiplying an irrigated acreage by a crop application rate. These investigators identified the extent and years that a field was irrigated from pumping inventories and remotely sensed data available since 1972; the crop type from pumping inventories and field visits; and the application rate of the representative crop from published sources. Application-rate estimates for alfalfa had the greatest effect on estimated pumpage. The high sensitivity of application rates, particularly that of alfalfa, is not unexpected considering that 75 percent of the ground water withdrawn from 1913–98 was used to irrigate alfalfa (Moreo

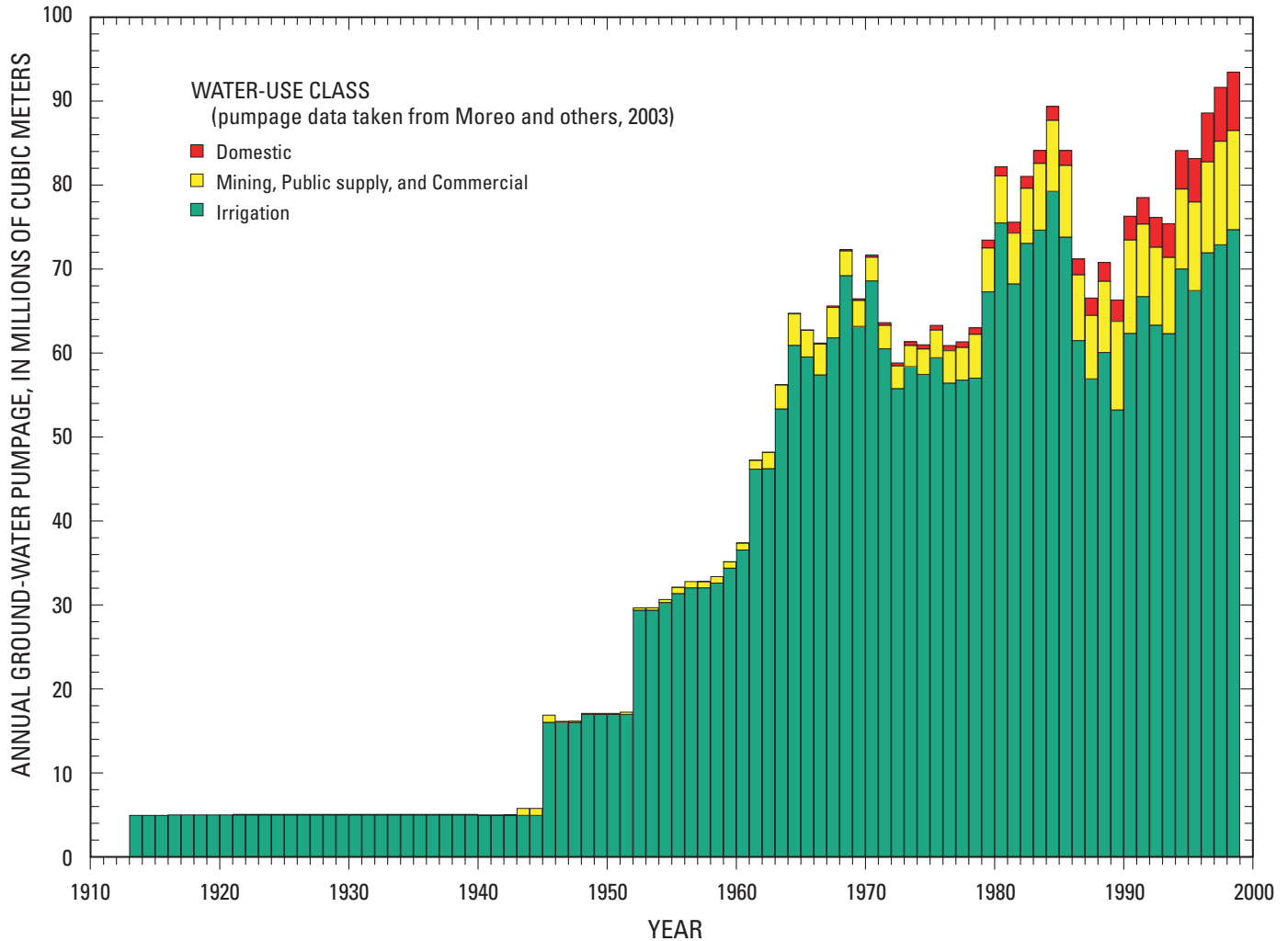


Figure C-5. Annual ground-water pumpage estimates developed by water-use class from Death Valley regional ground-water flow system model domain, 1913–98.

and others, 2003). The uncertainty in annual irrigation was expressed by Moreo and others (2003) as a range between a minimum and maximum estimate, with the most likely value closer to the minimum.

Mining, public supply, and commercial pumpage accounted for about 8 percent of all the ground water pumped from 1913–98. By 1998 pumpage in this category increased, accounting for nearly 13 percent of the annual total (fig. C-5). Pumpage for mining, public supply, and commercial use was estimated primarily from metered and inventoried data. Estimates for this water-use category were considered accurate within 5 percent (Moreo and others, 2003).

Pumpage for domestic use accounted for about 2 percent of the total amount of ground water pumped from 1913 to 1998. The percentage of water pumped for domestic use gradually increased over the years and by 1998 accounted for more than 7 percent of the annual total (fig. C-5). Moreo and others (2003) estimated domestic pumpage as the product of the average annual rate (per household) of domestic consumption and

the number of domestic wells permitted for use. The number of domestic wells may have been slightly overestimated because the history of well abandonment is not known. The uncertainty in the domestic-use estimate was expressed as a range defined by a minimum and maximum value that reflects, primarily, the uncertainty in the per household consumption rate. The minimum estimate of domestic pumpage was based on an annual per household consumption of 616.5 m³ and the maximum estimate on an annual per household consumption of 1,233 m³ (Moreo and others, 2003).

Annual ground-water pumpage estimates from the DVRFS model domain increased from about 5 Mm³ in 1913 to about 93.5 Mm³ in 1998 (fig. C-5 and table C-3). The greatest number of wells and the largest withdrawals are in Pahrump Valley, Amargosa Desert, and Penoyer Valley (fig. C-4). During 1913–45, ground water was used primarily for irrigation and was supplied by about 30 flowing wells in Pahrump Valley (Moreo and others, 2003). After 1945, local water use relied on pumps and continued to increase as access to the region

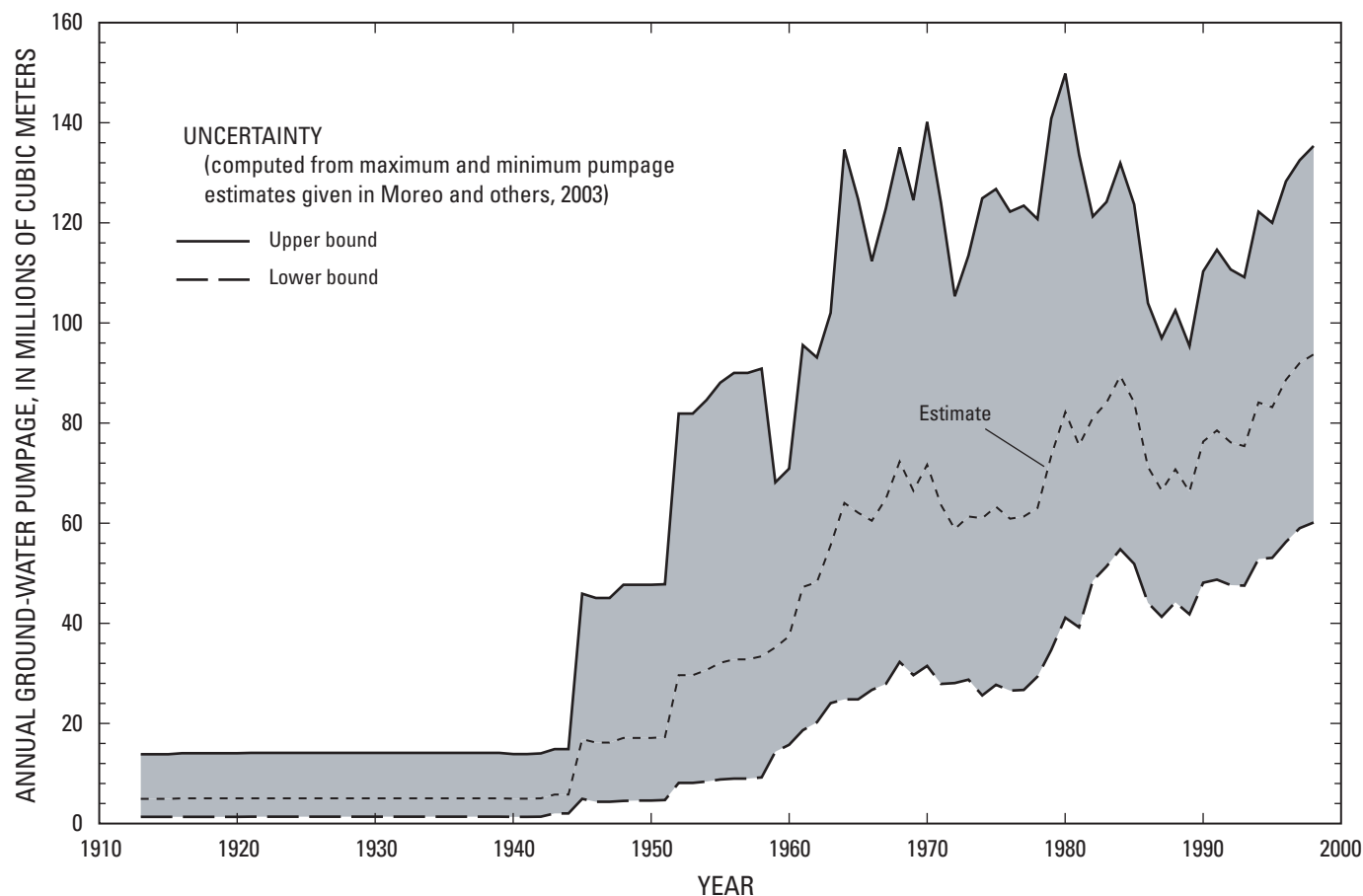


Figure C-6. Uncertainty in annual ground-water pumpage estimates developed for Death Valley regional ground-water flow system model domain, 1913–98.

improved (fig. C-5; Moreo and others, 2003). The percentage of ground water pumped for nonirrigation uses (domestic, mining, public supply, and commercial) began to increase from only a small percentage in 1960 to about 20 percent of the annual total in 1998. This trend is expected to continue as the population of Pahrump Valley and Amargosa Desert increases as a consequence of continued urbanization.

The total amount of ground water pumped from the DVRFS model domain during the period 1913–98 is estimated at 3,276 Mm³ (table C-3). Moreo and others (2003) expressed uncertainty in their estimate of annual pumpage as a range defined by a minimum and maximum estimate (fig. C-6). Accordingly, the uncertainty in their estimate of total pumpage from the DVRFS model domain during the period 1913–98 ranges from 1,616 to 6,081 Mm³. This large uncertainty is attributed to incomplete pumping records, misidentification of crop type, and errors associated with estimating annual domestic consumption, the irrigated area, and crop application rates (Moreo and others, 2003). The error associated with the uncertainty in the application rate, which differs spatially and temporally with variations in potential ET, length of growing season, irrigation systems, crop type, and management practices, exceeds that of all other uncertainties combined (Moreo and others, 2003).

Moreo and others (2003) did not adjust estimates of annual pumpage for water potentially returned to the flow system through subsequent infiltration of excess irrigation, lawn water, or septic tank wastewater. Although some return flow is likely to occur in the DVRFS model domain, the magnitude and timing of these returns have not been precisely quantified. Harrill (1986, p. 19) estimates return flows for Pahrump Valley as 70 percent of domestic pumpage, 50 percent of public-supply and commercial pumpage, and 25 percent of irrigation pumpage and states that the returns depend on the timing and method by which the water is returned to the flow system.

Stonstrom and others (2003) estimate return flows beneath three irrigated fields in the southern part of the Amargosa Desert. These estimates are made using the chloride mass-balance method and downward velocities inferred from peaks of chloride and nitrate concentrations noted in borehole depth profiles. Estimates of the rate at which irrigation water percolates downward through the unsaturated zone toward the water table ranged from 0.1 to 0.5 m/yr. On the basis of these rates and the depth to water beneath the fields, irrigation returns would take between 10 and 70 years to reach the water table. The water returned to the water table beneath individual irrigated fields was estimated to be 8 to 16 percent of the irrigation (Stonstrom and others, 2003, p. 19).

Many difficulties are associated with estimating return flows. These include uncertainties in pumpage, in the hydraulic properties of unsaturated zone sediment, and delineating the actual areas where water is or was returned to the environment. For example, ground water pumped for irrigation does not return to the flow system at the well (point of withdrawal) but rather to the water table beneath the field or fields irrigated by the well. The actual location of these fields, especially those of historical significance, can be highly uncertain. Despite these uncertainties, a method was developed to compute informal estimates of return flow. Return flows were computed as the product of the estimated annual pumpage and a user-defined return-flow percentage, and could be lagged in time by a user-defined value. All computed return flows were assumed to return to the water table at the location of the pumped well. Return flows were evaluated using the transient model in Chapter F of this volume.

Ground-Water Recharge

Ground-water recharge is defined as water that infiltrates downward through the unsaturated zone into the water table. Most of the ground-water recharge in the DVRFS region originates from precipitation that falls on mountainous areas throughout the DVRFS region (fig. C-7). The distribution and quantification of recharge for basins in the DVRFS region have been evaluated using empirical (Maxey and Eakin, 1950; Malmberg and Eakin, 1962; Walker and Eakin, 1963; Malmberg, 1967; Winograd and Thordarson, 1975; Miller, 1977; Harrill, 1986; IT Corporation, 1996a; D'Agnesse and others, 1997), water-balance (Rice, 1984; West, 1988), chloride mass-balance (Dettinger, 1989; Lichty and McKinley, 1995; Russell and Minor, 2002), and distributed-parameter (Hevesi and others, 2002; Hevesi and others, 2003) methods. Each of these methods attempts to capture the complex array of factors that control recharge.

The distributed-parameter method described by Hevesi and others (2003) provided an estimate of the potential recharge based on net infiltration, and was used primarily to distribute recharge in the model domain. The potential recharge estimated by their method was adjusted across the model domain to better balance with discharge (Chapter F, this volume). Hevesi and others (2003) estimated potential recharge using a net-infiltration model, INFILv3. Net infiltration is considered a reasonable indicator of ground-water recharge because most of the net infiltration and surface runoff that originates as precipitation in the model domain eventually moves downward through the unsaturated zone to recharge the ground-water flow system (Hevesi and others, 2003). In general, the uncertainty of approximating potential recharge from net infiltration increases as the thickness and heterogeneity of the unsaturated zone increases. INFILv3 simulates surface-water flow, snowmelt, transpiration, and ground-water drainage in the root zone and has as a climate algorithm that simulates daily climate conditions in local watersheds. Topography, geology, soils, and vegetation data are input to represent

local drainage-basin characteristics. Improved vegetation distributions were delineated from a western region vegetation map developed by the U.S Geological Survey Gap Analysis Program (WESTVEG GAP) and soil distributions from the U.S. Department of Agriculture (1994) State Soils Geographic Database (STATSGO).

On a daily basis, INFILv3 simulated major components of the mass-balance equation within the unsaturated zone to a depth of 6 m, the depth at which the seasonal effects of ET become insignificant. Net infiltration equaled the sum of snowmelt, precipitation, and infiltrating surface flow minus the sum of ET, runoff, and changes in root-zone storage. Each of these components was estimated on a cell-by-cell basis by using secondary governing equations (Hevesi and others, 2003). Runoff was generated in the model when and where available water exceeded the root-zone storage capacity or the saturated hydraulic conductivity of the soil or bedrock. A surface-water routing process was used to move runoff downstream through a simulated drainage basin and allow the surface water potentially to infiltrate through the root zone.

Net-infiltration simulations were calibrated by fitting the simulated daily discharge from modeled watersheds to stream-flow records at 31 gaged sites in the DVRFS region (fig. C-7). Model fit was evaluated both qualitatively and quantitatively by comparing simulated to measured daily and annual hydrographs. Model calibration was complicated by sparse daily climate records and information regarding stream-channel characteristics and base-flow contributions, the absence of collocated climate stations and stream-gaging stations in a watershed, and the nonuniqueness of model results (Hevesi and others, 2003). To increase the confidence in the net-infiltration estimates, model results were constrained by prior estimates of recharge that were calculated using alternative methods.

The calibrated net-infiltration model (model 1 in Hevesi and others, 2003) was used to simulate daily net infiltration from 1950 through 1999 across the DVRFS model domain (fig. C-8). This period was selected for simulation primarily because of the availability of climate and streamflow records. An average annual net infiltration of 2.8 millimeters (mm) was estimated over the entire model domain by averaging simulated daily net infiltration over the 50-year simulation period. This estimate is less than 2 percent of the average annual precipitation computed for the same period (Hevesi and others, 2003). An annual potential recharge of about 125 Mm³ was computed by multiplying the average annual infiltration by the area of the model domain. Results presented by Hevesi and others (2003) indicate a wide range in the simulated rate of net infiltration across the model domain. Local net-infiltration rates ranged from near zero to a maximum of about 1,262 millimeters per year (mm/yr) beneath a stream channel. The simulated average annual runoff over the 50-year simulation period was 2.2 mm, of which 0.2 mm eventually flowed into lowland playas where it was evaporated or infiltrated into the subsurface (Hevesi and others, 2003). About 14 percent of the total net infiltration simulated over the 50-year period was from overland flow, but locally the overland flow accounted for as much as 40 percent (Hevesi and others, 2003).

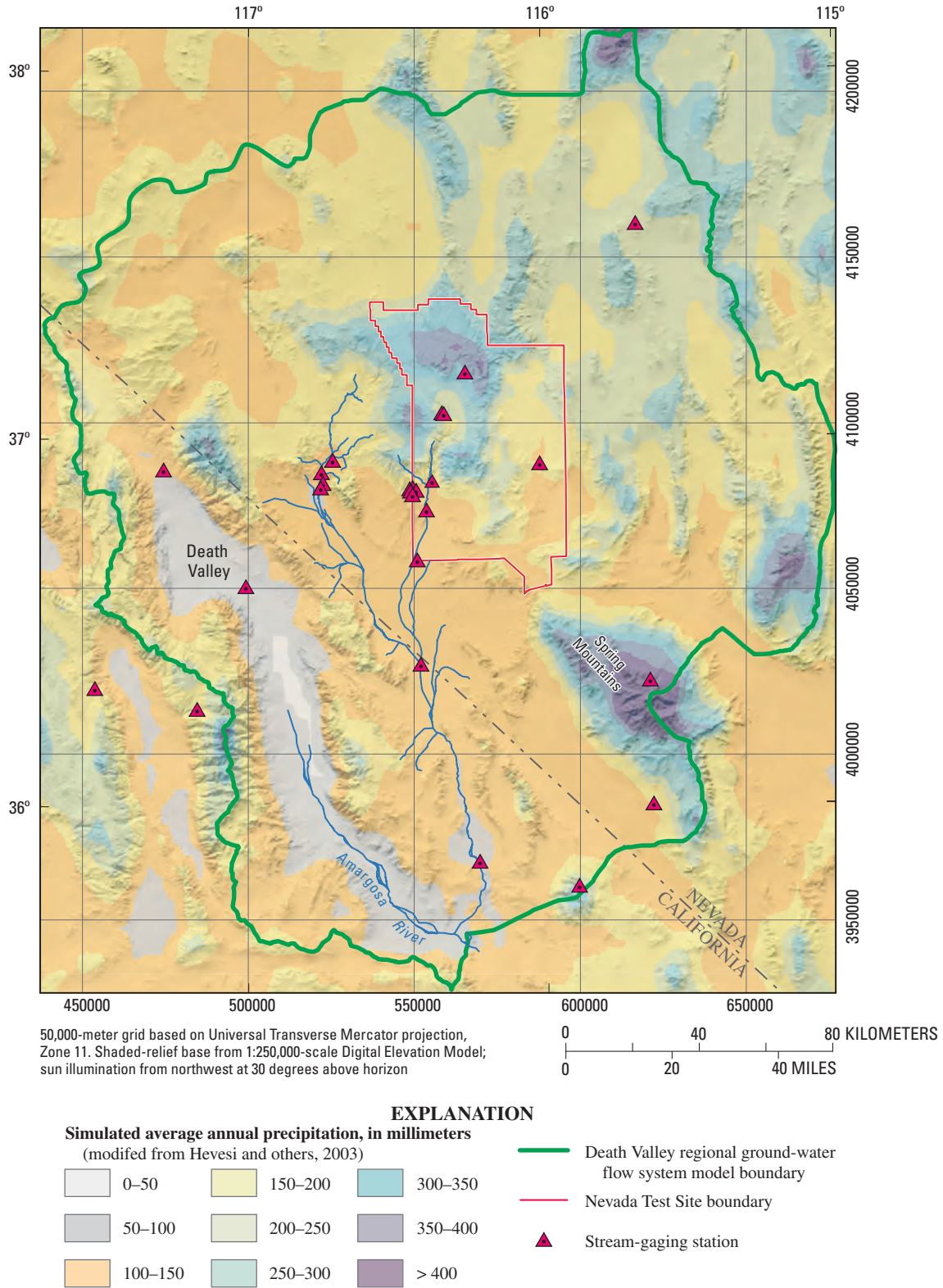
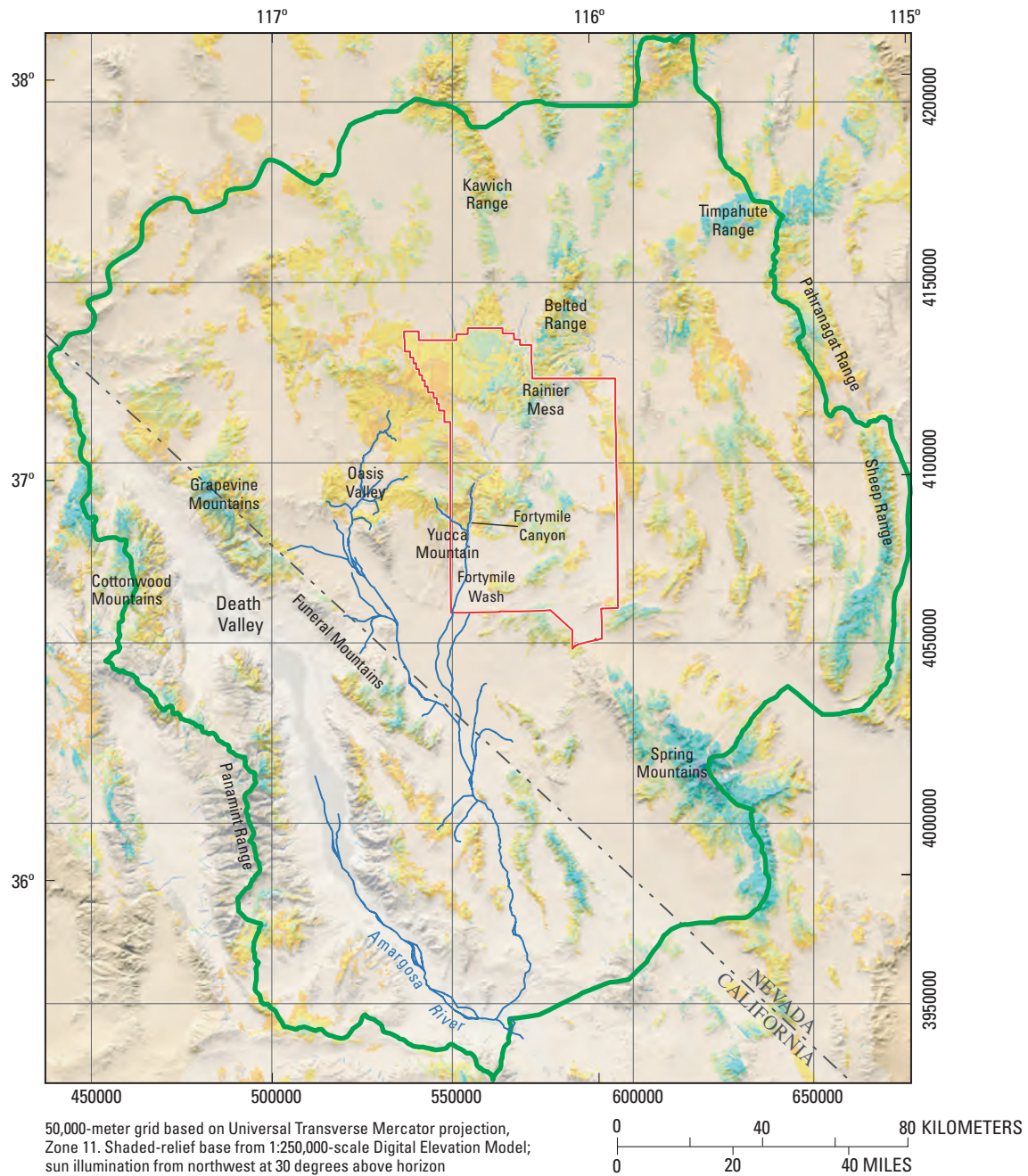


Figure C-7. Simulated average annual precipitation and stream-gaging stations used to calibrate the net-infiltration model in the Death Valley regional ground-water flow system model region.



EXPLANATION

Net infiltration, in millimeters per year (based on model 1 simulation of Hevesi and others, 2003)

| | | |
|-------|--------|---------|
| 0–0.1 | 5–10 | 100–500 |
| 0.1–1 | 10–20 | > 500 |
| 1–2 | 20–50 | |
| 2–5 | 50–100 | |

- Death Valley regional ground-water flow system model boundary
- Nevada Test Site boundary

Figure C-8. Simulated net infiltration used to estimate recharge to the Death Valley regional ground-water flow system model region, 1950–99.

Simulated net-infiltration rates, averaged over the period 1950–99, were generally consistent with published (Hevesi and others, 2003, table 1) estimates of recharge in the DVRFS region. The reported annual estimate of recharge from 42 conterminous hydrographic areas including most of the DVRFS region was about 157 Mm^3 (Hevesi and others, 2003). The simulated annual net infiltration for this same area was 4 percent less at 151 Mm^3 .

The uncertainty in model-generated net infiltration estimates was related to uncertainties associated with the representation of the near-surface environment and the unsaturated zone processes. Hevesi and others (2003) presented model uncertainty qualitatively because the results of their study could not support a rigorous quantification of uncertainty. Model uncertainty remained high for many model inputs such as bedrock permeability, soil thickness, root density as a function of depth, stream-channel properties, spatial distribution of climate by month (computed from daily records), and potential evapotranspiration coefficients. Although the general magnitude of the simulated net-infiltration volume was consistent with prior discharge and recharge estimates for the DVRFS region, substantial differences were observed in some local basins. Nonetheless, the spatial distribution of estimated net infiltration was considered a reasonable indication of the spatial distribution of the potential recharge across the model domain under current climate conditions (Hevesi and others, 2003).

On the basis of the net infiltration simulated by Hevesi and others (2003), the major areas of the model domain receiving recharge are along the eastern model boundary beneath the Timpahute, Pahrnat, and Sheep Ranges and the Spring Mountains; along the western part of the model boundary beneath the Panamint Range and Cottonwood Mountains; beneath the Kawich and Belted Ranges and Rainier Mesa, near the northern part of the NTS area; and beneath the Grapevine Mountains and the southern part of the Funeral Mountains, along the eastern margin of Death Valley (fig. C–8). In addition, small concentrated areas of recharge occur beneath major drainages, such as Fortymile Canyon and Fortymile Wash near Yucca Mountain and the Amargosa River near Oasis Valley, and beneath channels draining the Panamint Range and along well-developed drainages that incise major alluvial fans in Death Valley.

Lateral Flow

Areas of potential inflow and outflow, or lateral ground-water flow, along the DVRFS model boundary were defined for prepumped conditions (Appendix 2, this volume). Hydraulic gradients determined from a regional potentiometric map (plate 1 and Appendix 1, this volume) indicate that one boundary segment has no flow and that flow occurs across 11 of 12 lateral boundary segments of the model domain—7 boundary segments have inflow (Eureka and Saline are combined) and 3 have outflow (fig. C–9).

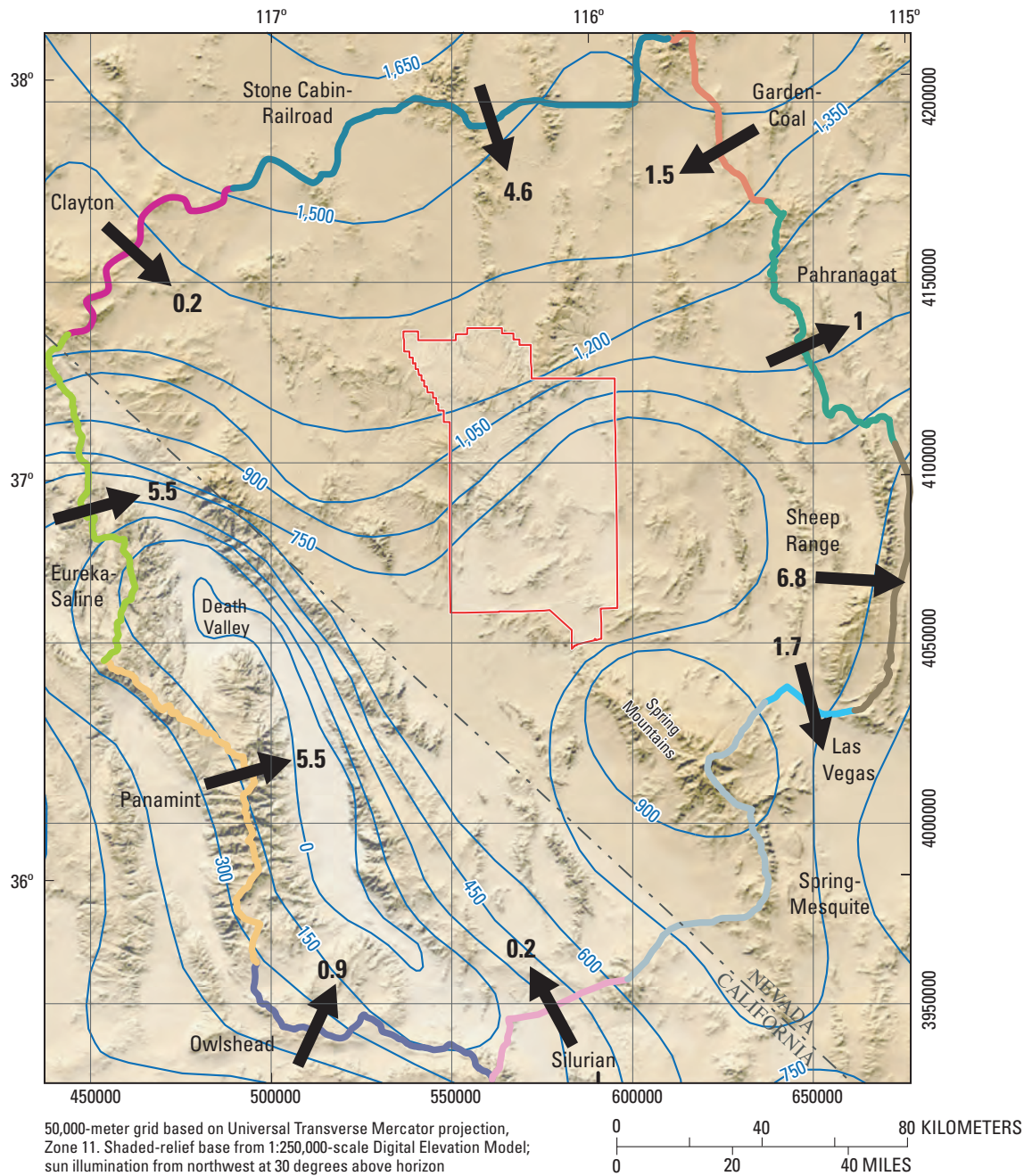
Lateral flow was estimated using the Darcy equation with hydraulic gradients defined by regional water levels, and estimates of hydraulic conductivity and the cross-sectional area of HGUs along the model boundary. Where possible, lateral-flow estimates were constrained by inflows and outflows estimated from available water-budget information for areas adjacent to the model domain. Where discrepancies between Darcy and water-budget flow estimates were great, alternative interpretations of the data, such as local adjustments to the composite hydraulic conductivity or reappraisals of the surrounding area water budgets, were used to further develop a reasonable estimate of lateral-boundary flow for the boundary segment.

Lateral-flow estimates for each boundary segment are given in table C–4. The table includes Darcy and water-budget estimates and the estimate considered most reasonable for prepumped conditions (Appendix 2, this volume). On the basis of these estimates of lateral flow, nearly 18.4 Mm^3 of ground water flows into the model domain annually, primarily along the western and northern parts of the model boundary, and 9.5 Mm^3 flows out, primarily along the eastern part of the model boundary (fig. C–9 and table C–4). The greatest inflow occurs from the area west of Death Valley, and the greatest outflow to the area east of the Sheep Range. The estimated annual net lateral flow is about 8.8 Mm^3 into the model domain.

Balance of Components

The water budget commonly is used to assess the significance of individual flow components in the ground-water system and to evaluate the balance between inflows and outflows. The volumetric flows estimated for the major water-budget components of the DVRFS from data previously presented in this chapter are summarized in table C–5. For prepumped conditions, annual recharge accounted for about 87 percent of the total inflow (143.4 Mm^3), and natural discharge (ET and spring flow) about 93 percent of the total outflow (133.8 Mm^3). The remainder (less than 10 percent) of the inflow and outflow is accounted for by lateral flows into and out of the model domain. The difference between estimated prepumped inflows and outflows is less than 7 percent of the estimated inflow. By 1998, pumpage was about 93.5 Mm^3 , which equates to about 70 percent of the total outflow estimated for prepumped conditions. It should be noted that this pumpage estimate is not adjusted for any potential return flow and that table C–5 does not include return flow as a potential inflow to the 1998 water budget.

Water naturally discharging as spring flow and(or) ET and water stored in pore spaces of subsurface rock units are two likely sources for the ground water pumped from the DVRFS. A decrease in estimated spring discharge—from 16.8 Mm^3 for prepumped conditions to 5 Mm^3 in 1998 (table C–5)—indicates that ground-water pumping has affected natural discharge. The water budget given in table C–5 also indicates that ET in 1998 is likely to be less than that estimated for prepumped conditions and possibly



EXPLANATION

Death Valley regional ground-water flow system model boundary segment

- Lateral-flow boundary—
- Colors delineate segments
- No-flow boundary

1 **Lateral flow**—Arrow indicates direction; number indicates annual volume in millions of cubic meters from table C-4.

—750— **Regional potentiometric-surface contour**—
Interval is 150 meters. Datum is sea level.
(Bedinger and Harrill, Appendix 1, this volume)

— Nevada Test Site boundary

Figure C-9. Regional ground-water potentiometric surface and lateral flow across boundary segments of the Death Valley regional ground-water flow model domain.

Table C-4. Estimates of flow across lateral boundary segments of the Death Valley regional ground-water flow system model domain for prepumped conditions.

[+ values, flow into model domain; – values, flow out of model domain; --, no value was reported or estimate was unreliable; m³/d, cubic meter per day; m³, cubic meter]

| Boundary segment (shown in fig. C-9) | Boundary flow estimate (m ³ /d) | | | Estimate of annual boundary flow ¹ (m ³) |
|---|---|-----------------------------|-----------------------------|---|
| | Darcy calculation | Water-budget calculation | Most reasonable estimate | |
| Silurian | -125 | -11,400 | 500 ² | 183,000 |
| Spring-Mesquite | -782 | -- | 0 ³ | 0 |
| Las Vegas | -4,575 | -- | -4,575 | -1,671,000 |
| Sheep Range | -18,747 | -- | -18,747 | -6,847,000 |
| Pahrnanagat | -2,783 | -- | -2,783 | -1,016,000 |
| Garden-Coal | 4,139 | -- | 4,139 | 1,512,000 |
| Stone Cabin-Railroad | 12,476 | -- | 12,476 | 4,557,000 |
| Clayton | 667 | -- | 667 | 244,000 |
| Eureka-Saline ⁴ | 20,873 | 14,600–15,600 | 15,100 | 5,515,000 |
| Panamint | 14,050 | 14,000–16,000 | 15,000 | 5,479,000 |
| Owlshead | 2,382 | -- | 2,382 | 870,000 |
| Total | 27,576 | | 24,193 | 8,826,000 |

¹Volume calculated using most reasonable estimate of boundary flow; from data analyses in Appendix 2 (this volume), rounded to the nearest 1,000 m³.

²See Appendix 2 (this volume) for explanation of method used to determine most reasonable estimate.

³No significant flow estimated across boundary because segment closely coincides with natural no-flow boundary.

⁴Estimate is sum of flows across Saline and Eureka boundary segments.

represents a source of natural discharge reduced by local pumpage. Given the relatively short time period (less than a century), this decrease in discharge is probably not due to climatic influences. Accordingly, this interpretation would support a higher estimate of prepumped discharge than that presented in table C-5.

The other potential source of ground water pumped from the DVRFS model domain is water stored in the pores of sub-surface rock. This water, when removed from the flow system, decreases the hydraulic head in the aquifer. Although the actual volume of stored ground water is uncertain, preliminary estimates, based on sparse available data on storage properties, indicate that storage accounts for the largest amount of the available water (Harrill, 1986, p. 18; Dettinger, 1989, p. 22). Measured declines in hydraulic head and only small decreases in spring discharge relative to the total amount of ground water being pumped from the DVRFS strongly indicate that the primary source of water pumped from the DVRFS model domain is stored ground water.

Hydraulic Properties

Belcher and others (2001) compiled published and unpublished hydraulic-property data to estimate hydraulic properties of the major HGUs defined for the DVRFS (see Chapter B, this volume). The hydraulic-property estimates included those for transmissivity, hydraulic conductivity, storage coefficient, and anisotropy ratios. With the exception of the lower elastic-rock confining unit (LCCU), however, only

aquifer tests were used to estimate the hydraulic properties of an HGU. Belcher and others (2001) evaluated these data to characterize the hydraulic properties of the major HGUs. Hydraulic conductivity was the only property with a sufficient number of estimates to generate statistical distributions for specific HGUs. Belcher and others' (2001) compilation provided the data set from which hydraulic properties, primarily hydraulic conductivity, were estimated for the transient flow model. Storage coefficients are not discussed because field data are extremely limited (Harrill, 1986, p. 31; Belcher and others, 2001; Carroll and others, 2003). Consequently, values given in standard hydrogeology textbooks were considered adequate for purposes of this investigation.

Hydraulic Conductivity

Belcher and others (2001) estimated horizontal hydraulic conductivity (hereinafter referred to as hydraulic conductivity) by dividing transmissivity calculated from an aquifer test by the total thickness of the aquifer material being tested. Because an HGU is typically stratified and the individual aquifers or confining units have unknown thicknesses, Belcher and others (2001) used the length of the open interval of the well or borehole as the unit thickness. Belcher and others (2001) indicate that while this simplifying approach is not optimal, it is considered appropriate given the available data and nature of the units tested. This approach also was used in previous regional modeling studies in the DVRFS region (IT Corporation, 1996b).

Table C-5. Annual volumetric flow estimates of major water-budget components of the Death Valley regional ground-water flow system model domain for prepumped conditions and 1998 conditions.

[--, no estimate was made or available; Mm³, millions of cubic meters; ET, evapotranspiration]

| Water-budget component | Estimated annual volumetric flow (Mm ³) | |
|--------------------------------------|---|---------------------|
| | Prepumped conditions | 1998 |
| Inflow | | |
| Recharge (net infiltration) | 125 | 125 |
| Boundary inflow (table C-4) | 18.4 | -- |
| Total | 143.4 | |
| Outflow | | |
| Natural discharge: ET ¹ | 107.5 | ³ <107.5 |
| Spring flow ² (table C-2) | 16.8 | 5 |
| Boundary outflow (table C-4) | 9.5 | -- |
| Pumpage (table C-3) | 0 | 93.5 |
| Total | 133.8 | |
| Difference (inflow-outflow) | 9.6 | |
| Difference (percent) | 6.7 | |

¹Estimate for prepumped conditions not included in estimate given in table C-1 for Pahrump Valley.

²Bennetts and Manse Springs were reported dry after 1975.

³"Less than" symbol is not intended to quantify discharge, but only to indicate that the component likely is less than the prepumped natural discharge.

Pumping and companion observation wells commonly are constructed in water-producing zones of an HGU in the model domain. Data collected from these wells may represent the more transmissive zones of an HGU; therefore, transmissivities calculated from these data may be biased to larger values. This bias may be compounded further by the assumption that the thickness of a unit is limited to the length of the open interval of the well when calculating hydraulic conductivity. Thus, the means and variances presented by Belcher and others (2001) may be most representative of the hydraulic properties of the more productive zones in an HGU.

Variability inherent in the HGUs across the DVRFS region increases the uncertainty of the estimated hydraulic conductivity values. Lithologic factors, such as facies changes in sedimentary rock, changes in welding in volcanic rock, and degree of fracturing, can cause hydraulic conductivity values to vary substantially over relatively short distances. Variability also can result from sampling bias. Variability for estimates of the matrix permeability commonly depends upon the variable lithology and interval penetrated by the well within a particular unit. Sampling variability also can be a factor in fractured rocks if boreholes intersect rocks with different degrees of fracturing.

Probability Distributions

Data from Belcher and others (2001) were used to estimate probability distributions and to provide reasonable ranges of hydraulic conductivity for the major HGUs in the DVRFS region (Belcher and others, 2002). Fracturing appears to have the greatest influence on the permeability of bedrock HGUs—the greater the degree of fracturing, the greater the permeability. Alteration and welding in the Cenozoic volcanic rocks also greatly influence hydraulic conductivity. Alteration decreases hydraulic conductivity, and welding forms brittle rocks that fracture more easily, thereby increasing hydraulic conductivity. In Chapter B (this volume), these relations are used to establish hydraulic-conductivity zones. Table C-6 presents probability distributions of hydraulic conductivity for the major HGUs in the DVRFS region.

Depth Decay

Intuitively, hydraulic conductivity decreases with depth as the geostatic load increases, compressing favorably oriented fractures, faults, and sedimentary units. Analyses of covariance confirmed the assumption that depth was a significant factor in the variability of hydraulic conductivity in the DVRFS region, but variability in hydraulic-conductivity estimates because of other factors prevents a rigorous quantification of a depth decay function.

The relation between hydraulic conductivity and depth in the DVRFS region has been postulated by Bedinger and others (1989), IT Corporation (1996b), and D'Agnesse and others (1997). Bedinger and others (1989) developed a series of curves defining the distribution of hydraulic conductivity for hydrogeologic units in the region. The hydraulic-conductivity values of each unit were affected by the variation of rock properties by depth and degree of faulting. Using these findings, D'Agnesse and others (1997) indicate qualitatively that the hydraulic conductivity decreases rapidly for most rocks between depths of 300 to 1,000 m across the model domain. At depths greater than 1,000 m, matrix permeability probably dominates, except in regional fault zones. At depths greater than 5,000 m, the geostatic load probably keeps faults and fractures closed (D'Agnesse and others, 1997). The study by the IT Corporation (1996b, p. 29) postulated a relation of exponentially decreasing hydraulic conductivity with depth in the alluvial aquifer (equivalent to the AA and ACU units in table C-6), in the volcanic aquifer (equivalent to part of the Cenozoic volcanic-rock HGUs), and in the lower carbonate-rock aquifer (LCA). Decreasing trends in hydraulic conductivity are evident in the data presented in this study (IT Corporation, 1996b, figs. 6-1, 6-2, and 6-3), despite a great deal of apparent scatter in the data.

On the basis of regression analysis, Belcher and others (2001) found the best relation was between log₁₀-transformed hydraulic conductivity and depth. The logarithmic values of hydraulic conductivity were used for statistical calculations because this parameter tends to be log-normally distributed

Table C-6. Horizontal hydraulic-conductivity estimates of hydrogeologic units in the Death Valley regional ground-water flow system (modified from Belcher and others, 2001; 2002).

[Abbreviations: AA, alluvial aquifer; ACU, alluvial confining unit; BRU, Belted Range unit; CFBCU, Crater Flat–Bullfrog confining unit; CFPPA, Crater Flat–Prow Pass aquifer; CFTA, Crater Flat–Tram aquifer; CHVU, Calico Hills volcanic-rock unit; ICU, intrusive-rock confining unit; LCA, lower carbonate-rock aquifer; LCCU, lower elastic-rock confining unit; LFU, lava-flow unit; OAA, older alluvial aquifer; OACU, older alluvial confining unit; OVU, older volcanic-rock unit; PVA, Paintbrush volcanic-rock aquifer; SCU, sedimentary-rock confining unit; TMVA, Thirsty Canyon–Timber Mountain volcanic-rock aquifer; UCA, upper carbonate-rock aquifer; UCCU, upper elastic-rock confining unit; VSU, volcanic- and sedimentary-rock unit; XCU, crystalline-rock confining unit; YAA, younger alluvial aquifer; YACU, younger alluvial confining unit; YVU, younger volcanic-rock unit; NA, not applicable]

| Hydrogeologic unit or subunit | Hydraulic conductivity (meters per day) | | | | 95-percent confidence interval | Number of measurements |
|-------------------------------|---|-----------------|--------------------|---------|--------------------------------|------------------------|
| | Geometric mean ¹ | Arithmetic mean | Minimum | Maximum | | |
| AA ² | 1.5 | 10.8 | 0.00006 | 130 | 0.005–430 | 52 |
| ACU ³ | 3 | 10.5 | 0.003 | 34 | 0.02–470 | 15 |
| LFU | NA | NA | 0.002 | 4 | NA | 2 |
| YVU & VSU | 0.06 | 1.5 | 0.00004 | 6 | 0.00005–80 | 15 |
| TMVA | 0.01 | 2 | 0.0002 | 20 | 0.00001–18 | 11 |
| PVA | 0.02 | 4 | 0.000007 | 17 | 0.0000003–1300 | 9 |
| CHVU | 0.2 | 0.55 | 0.008 | 2 | 0.007–5 | 14 |
| BRU | 0.3 | 1.03 | 0.01 | 4 | 0.006–17 | 6 |
| CFTA | 0.05 | 0.4 | 0.003 | 2 | 0.0004–5.3 | 11 |
| CFBCU | 0.4 | 6.8 | 0.0003 | 55 | 0.0006–240 | 34 |
| CFPPA | 0.3 | 13 | 0.001 | 180 | 0.000006–2.4 | 19 |
| OVU | 0.004 | 0.07 | 0.000001 | 1 | 0.00002–5 | 46 |
| ICU | 0.01 | 0.3 | 0.0006 | 1.4 | 0.00002–5 | 7 |
| SCU | 0.002 | 0.02 | 0.0002 | 0.3 | 0.00004–0.09 | 16 |
| UCA & LCA | 2.5 | 90 | 0.0001 | 820 | 0.0008–7700 | 53 |
| fractured | 19 | 150 | 0.01 | 820 | 0.03–11,000 | 32 |
| unfractured | 0.1 | 1.6 | 0.0001 | 14 | 0.0002–70 | 21 |
| UCCU & LCCU ⁴ | 0.00002 | 0.2 | 3×10 ⁻⁸ | 5 | 1×10 ⁻¹⁰ –3 | 29 |
| shale | 0.01 | 0.07 | 0.0002 | 0.4 | 0.0001–1.4 | 9 |
| quartzite | 0.000001 | 0.24 | 3×10 ⁻⁸ | 5 | 1×10 ⁻¹⁰ –0.006 | 19 |

¹Values determined from log-transformed distribution.

²AA is the combined YAA and OAA.

³ACU is the combined YACU and OACU.

⁴One measurement could not be classified as shale or quartzite.

(Neuman, 1982). The Cunnane plotting position method was used to assess the normality of the logarithms of hydraulic-conductivity estimates for each major HGU (Helsel and Hirsch, 1992, p. 27–29). In most cases, the assumption of a normal distribution for log hydraulic conductivity was true.

For the major HGUs, 14 of the 15 relations between depth and log hydraulic conductivity had a correlation coefficient that ranged from virtually zero to 0.52. Depth and log hydraulic conductivity possibly are correlated for the Belted Range unit ($r^2=0.78$), although the regression was determined with only six data pairs.

Despite poor results from the regression analysis, a relation between depth and hydraulic conductivity might exist at the scale of this investigation. Hydraulic-conductivity estimates were available only to depths of less than 3,600 m, and the average depth investigated was only 700 m. A possible relation between depth and hydraulic conductivity could be investigated further through calibration of regional models.

Hydraulic Head

Hydraulic-head measurements at each measurement site were composited to develop hydraulic-head observations. Errors in well altitude and location, nonsimulated transient stress, and water-level measurement were estimated to quantify the uncertainty of the head observations.

Head Observations

Periodic depth-to-water measurements and continuous down-hole water pressure measurements made in wells throughout the DVRFS model domain were used to develop hydraulic-head observations. The observations for each well, which composite one or more water-level measurements, were used in calibrating the ground-water flow model. These data were acquired as part of activities associated with many historical and currently active water-level monitoring networks,

each of which was established to address a specific interest in a study area. Active monitoring networks include those funded or operated by Nye County, the States of Nevada and California, U.S. Geological Survey, National Park Service, U.S. Fish and Wildlife Service, and the U.S. Department of Energy Yucca Mountain Project and Underground Test Area Program. Much of these data and other water-level information available from local mining operations have been included in the U.S. Geological Survey's National Water Information System (NWIS). NWIS, specifically its ground-water component, the Ground-Water Site Inventory (GWSI), served as the primary source and repository for water levels and associated borehole information used to develop and calibrate the DVRFS ground-water flow model. Temporal and spatial gaps in water-level data were evaluated and, where possible, addressed by making additional measurements and by entering any previously omitted water-level information into the GWSI.

The GWSI, although comprehensive and complete in terms of water-level measurements and borehole and well information, has limited options for assigning ancillary information to individual water-level measurements. Thus, a project database was designed to retrieve site, construction, borehole, and water-level information directly from GWSI and store additional information about each water-level measurement.

Ancillary information about each water level was incorporated into the project database by assigning attributes. This information included one general-condition attribute and multiple detailed-condition attributes for each water-level measurement (table C-7). The general-condition attribute indicates the appropriateness of the measurement as a steady-state or transient head observation. The detailed-condition attribute provides additional information about the condition or state of the measurement or of the well at the time the measurement was made.

The general-condition attribute identifies measurements determined acceptable as head observations for calibration of the regional ground-water flow model. Measurements representative of regional ground-water conditions were identified as regional-scale measurements. All other general-condition attributes indicate that the measurement is unacceptable for developing head observations for calibration of the regional ground-water flow model. These regional measurements were attributed as either steady state or transient. A regional transient designation is assigned only to those water levels in which the measured response is considered to be the result of ground-water pumpage. Detailed-condition attributes provide information to support the general condition assigned to the measurement. These attributes include information about the condition and location of the well, observed trends in the water level, and reported and likely explanations for measured water-level changes.

Attributes assigned to each category were determined by analyzing hydrographs, reviewing reports pertaining to water levels measured nearby, and evaluating the well location relative to centers of pumping and underground nuclear tests. Reports include mainly those published as part of previously

mentioned monitoring networks. Open-interval depth information for wells also was evaluated to assess whether measured fluctuations result from precipitation variations or evapotranspiration. Measurements from wells having insufficient information from which to determine or estimate an open interval were not used to develop head observations. This attributing procedure is illustrated by an annotated hydrograph of water levels from a well in Pahrump Valley (fig. C-10).

Nearly 40,000 water levels measured in about 2,100 wells were evaluated in the model domain. Of these, about 12,000 water levels in 700 wells were assigned attributes indicating that the water level represented regional, steady-state conditions. Head observations for calibration of prepumped conditions were computed at each of the 700 wells as the average of all measurements attributed as representing regional, steady-state conditions. The spatial distribution of the 700 steady-state head observations is shown in figure C-11. Head observations range from about 2,500 m above sea level in the Spring Mountains to nearly 100 m below sea level in Death Valley. In general, head decreased from north to south. Local areas of higher head are coincident with mountainous areas where regional aquifers receive recharge from precipitation.

Nearly 15,000 water levels measured in about 350 wells were attributed to indicate that the measurements represented regional, transient (pumped) conditions (fig. C-12). These measurements, along with those attributed as regional steady-state water-level measurements, were used to develop the set of transient-head observations used to calibrate the ground-water flow model. Water-level records for individual wells spanned periods from 1 to about 50 years. Water levels attributed as representing regional steady-state or transient conditions were averaged by year and by well to compute the almost 5,000 head observations used to calibrate the transient ground-water flow model.

The earliest reported water level usable for the DVRFS ground-water flow model was measured in 1907. Most wells having longer term water-level records are in Pahrump Valley (fig. C-12). Nearly 100 wells in the DVRFS model domain have a record of 20 years or longer. The greatest drawdown measured in the DVRFS model domain is 76 m, which was measured in a well in the Beatty area just north of Amargosa Desert (fig. C-12). Most wells have less than 15 m of measured drawdown; wells having the greatest drawdown (>15 m) typically are in areas of concentrated irrigation use, primarily the Amargosa Desert and Pahrump and Penoyer Valleys (fig. C-12).

Every well in which a water level was measured was attributed to indicate the depth of the interval contributing water to the well. Two depth attributes were assigned to each well—one representing the top of the uppermost open interval, and the other, the bottom of the lowermost open interval. Depth attribute values were determined from well-construction and borehole information stored in GWSI. For wells in which specific screen- or open-interval information was not known, top and bottom interval values were estimated from reported well depths, hole depths, casing information, and water levels.

Table C-7. Description of attributes assigned to water levels retrieved from Ground-Water Site Inventory (GWSI) for simulation of ground-water flow in the Death Valley regional ground-water flow system model domain.

| General-condition attribute | | |
|-------------------------------------|---|---|
| Attribute name | Description | Considered appropriate for regional evaluation |
| Duplicate | Measurement entered under another site identifier. | NO |
| Insufficient data | Measurement does not have sufficient supporting information to determine general condition. | NO |
| Localized | Measurement represents localized hydrologic conditions. | NO |
| None | Water level not measured because well was dry or obstructed. | NO |
| Nonstatic level | Measurement affected by sampling, testing, construction, or some other local activity. | NO |
| Steady state-LOCAL | Measurement represents prepumped, equilibrium conditions in a local-scale flow system. | NO |
| Steady state-REGIONAL | Measurement represents prepumped, equilibrium conditions in regional ground-water flow system. | YES |
| Superseded | Measurement replaced by another that more accurately represents ground-water conditions at the site. | NO |
| Suspect | Measurement is erroneous or affected by unnatural conditions. | NO |
| Transient-LOCAL | Measurement reflects transient conditions in or near borehole. | NO |
| Transient-REGIONAL | Measurement reflects changes caused by pumping from the regional ground-water flow system. | YES |
| Detailed-condition attribute | | |
| Attribute name | Description | |
| Erratic/Unstable | Measurement appears to be erratic and unstable. | |
| Evapotranspiration response | Measurement appears to be responding to evapotranspiration. | |
| Flowing | Measurement is above land surface. In some cases an accurate water level could not be determined due to flowing conditions. | |
| Insufficient data | Measurement does not have sufficient information to determine detailed conditions. | |
| Limited data | Measurement is one of a limited number, but general condition is assumed to represent regional conditions. | |
| Missing | Measurement not assigned a value. | |
| No date | Measurement not associated with a date. | |
| Obstruction | Measurement not assigned a value because of an obstruction in borehole. | |
| Nuclear test effect | Measurement appears to be responding to nearby nuclear test (1951-92). | |
| Not adjusted for temperature | Measurement not adjusted for a reported temperature effect. | |
| Precipitation response | Measurement appears to be responding to a recent precipitation event. | |
| Pumping area | Site is located in an area that may have been affected by ground-water pumping. | |
| Pumping steady state | Measurement appears to represent steady- or near steady-state conditions during sustained pumping. | |
| Pumping/recovery | Measurement appears to be responding to pumping in the borehole or in a nearby borehole. | |
| Reported perched water | Measurement is reported to represent local perched-water conditions. | |
| Rising trend | Measurement appears to be part of a discernible, overall, rising trend. Possible causes include decrease in nearby pumping and a local precipitation event. | |
| Seasonal pumping | Measurement appears to be responding to nearby seasonal pumpage. | |
| Suspect | Measurement is suspect. | |
| Suspected perched water | Measurement assumed to represent local perched-water conditions. | |
| Testing area | Well located in area of past nuclear testing. | |
| Undeveloped | Well not sufficiently developed. | |

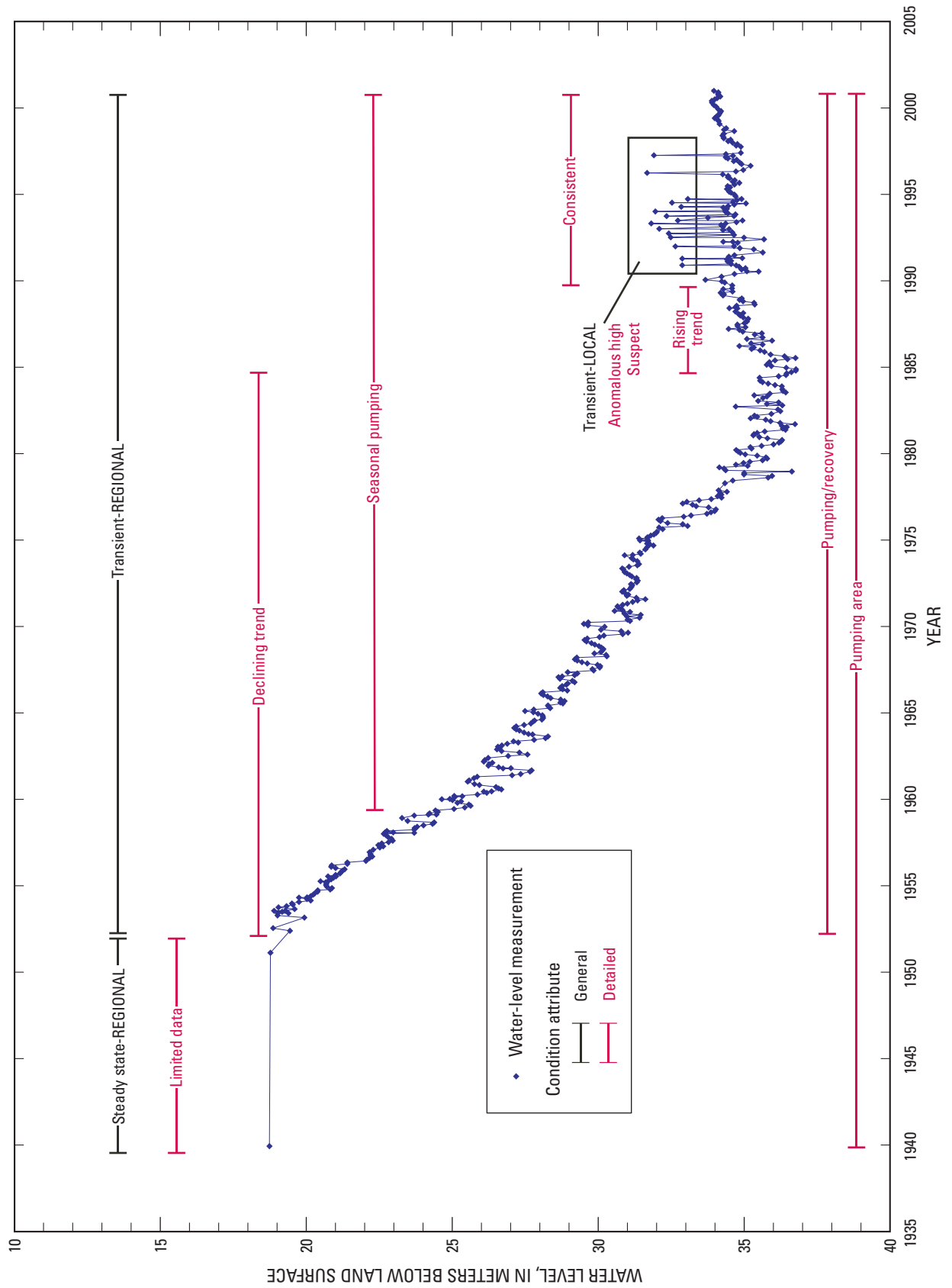
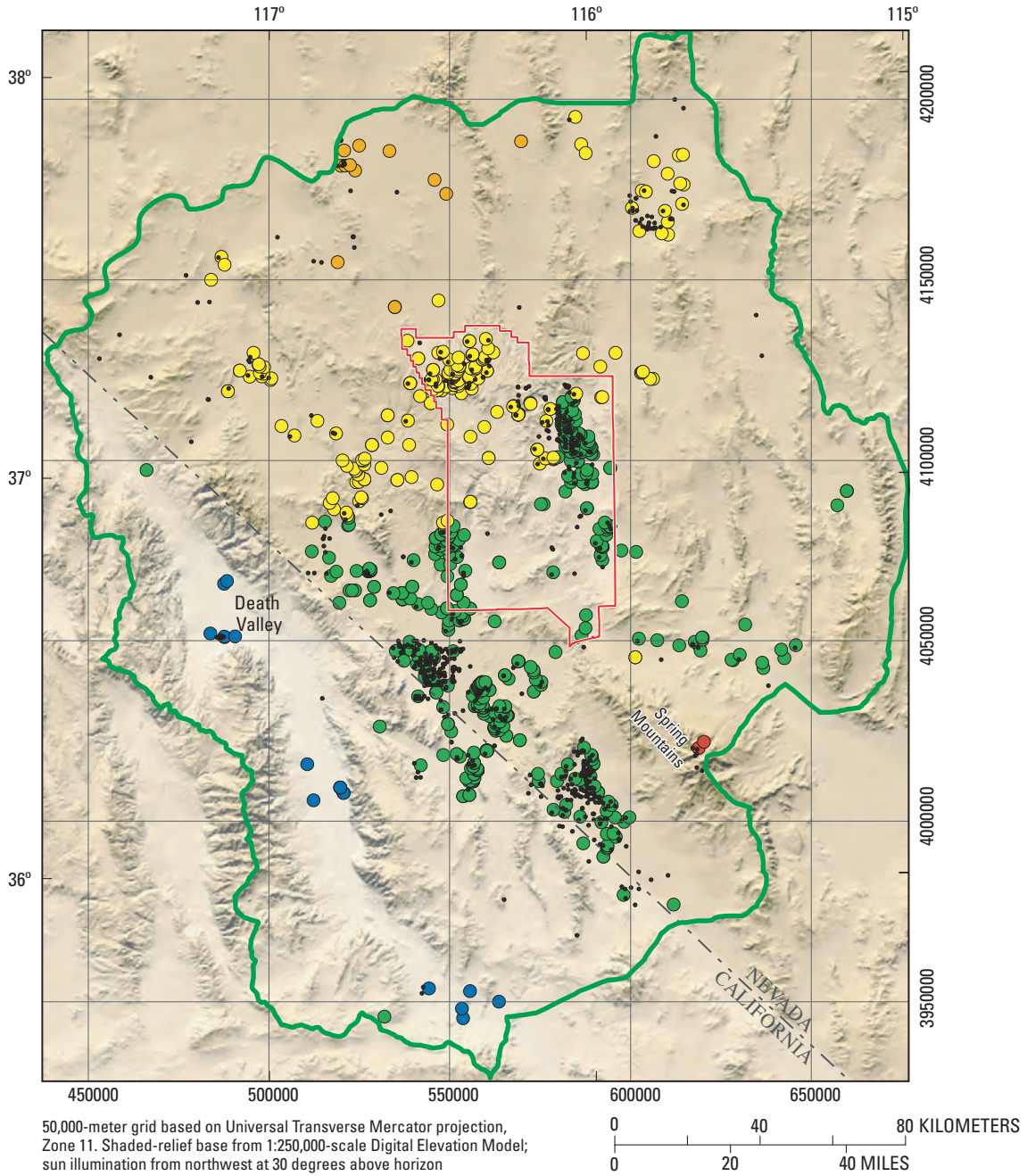


Figure C-10. Annotated hydrograph showing general- and detailed-condition attributes assigned to water-level measurements from a well in Pahrump Valley.



EXPLANATION

- Death Valley regional ground-water flow system model boundary
 - Nevada Test Site boundary
 - Water-level measurements not representative of regional, steady-state conditions
- Head-observation altitude in well representing regional, steady-state conditions—In meters above sea level**
- < 500
 - 500–1,000
 - 1,000–1,500
 - 1,500–2,000
 - 2,000–2,500

Figure C-11. Spatial distribution and altitude of head observations in wells representing regional, steady-state conditions used in calibration of the Death Valley regional ground-water flow system model.

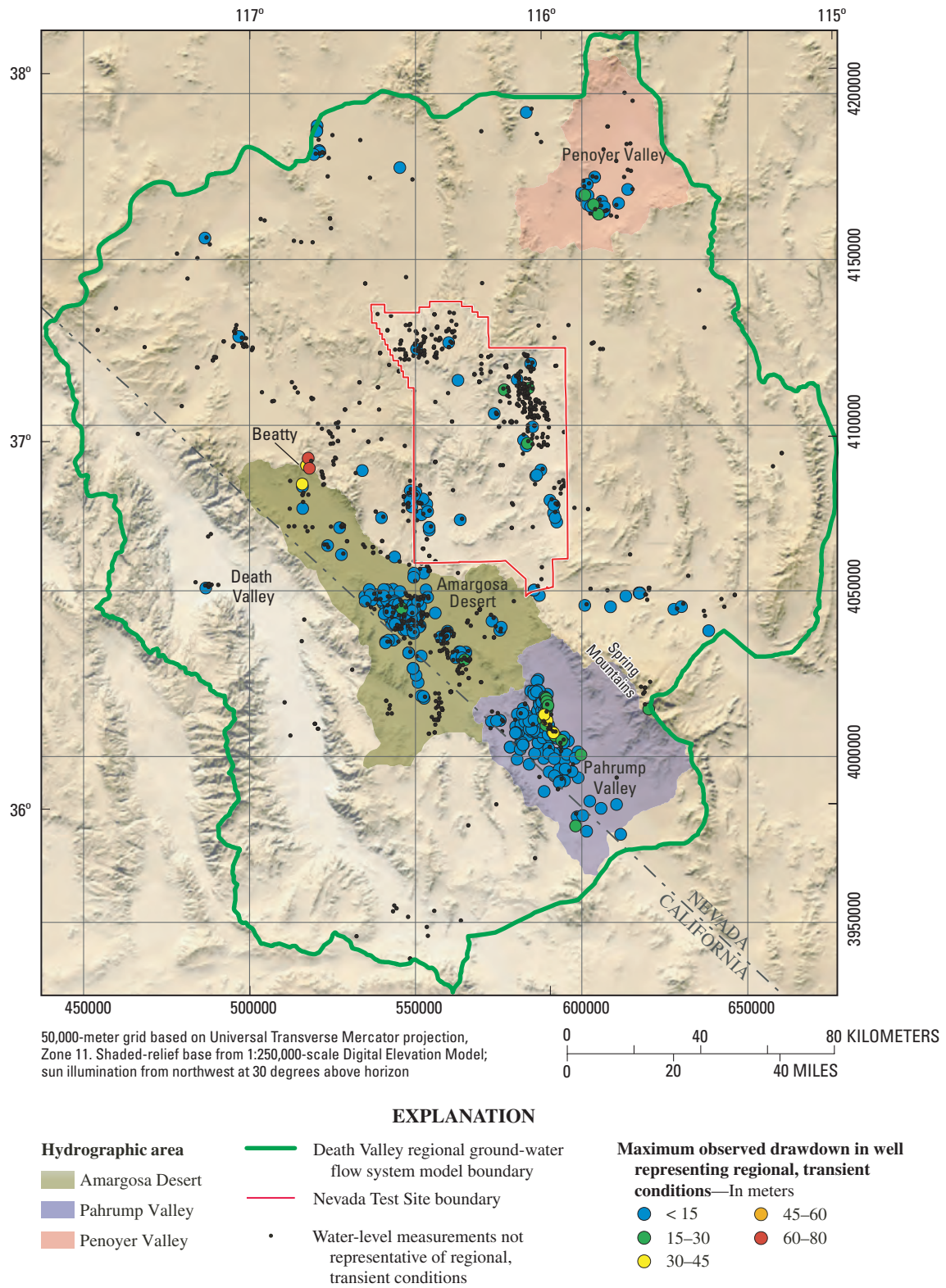


Figure C–12. Spatial distribution and maximum drawdown of head observations in wells representing regional, transient conditions used in calibration of the Death Valley regional ground-water flow system model.

As previously stated, measurements from wells for which information was insufficient to determine or estimate an open interval were not used to calibrate the transient ground-water flow model. Wells used to calibrate the transient flow model are summarized in table C-8. The table lists wells in depth ranges based on the depth of the bottom of the open interval. About 43 percent of the wells have open intervals at depths less than 100 m, and less than 10 percent at depths greater than 1,000 m. The spatial distribution of wells with shallow and deep openings is shown in figure C-13. Most wells having deeper openings are in or near the NTS. The typical depth of the open interval of wells in major agricultural areas of the DVRFS model domain (Amargosa Desert and Penoyer and Pahrump Valleys) is less than 100 m.

Head-Observation Uncertainty

Errors that contribute most to the uncertainty of head observations are associated with potential inaccuracies in the altitude and location given for a well and in the measurement of a water level, and fluctuations introduced by variations in climate or any other nonsimulated transient stress. These errors were estimated from available information and were used to quantify the uncertainty of a head observation.

Table C-8. Bottom depth of open interval for wells used to calibrate the Death Valley regional ground-water flow system model.

[≤, less than or equal to]

| Bottom depth of open interval (meters) | Number of wells | Percentage of wells |
|--|-----------------|---------------------|
| ≤100 | 369 | 42.5 |
| ≤500 | 642 | 74. |
| ≤1,000 | 803 | 92.5 |
| ≤5,000 | 868 | 100. |

Well-Altitude Error

Well-altitude error directly affects the calculation of the hydraulic head as referenced to a common datum. The error associated with the potential inaccuracy in well altitude was computed from the altitude accuracy code given in GWSI, expressed as a plus/minus (±) range related directly to the method by which the altitude was determined. This range varies from ±0.03 m for high-precision methods, such as spirit level and differential global positioning system (GPS) surveys, to ±25 m for estimates determined from topographic maps having large (50 m) contour intervals. The range defined by the altitude accuracy code is assumed to represent, with 95 percent confidence (two standard deviations), the true well-altitude uncertainty. Assuming that the head observation represents the mean value and that the error is normally distributed,

the uncertainty of the head observation, with respect to the well-altitude error, can be expressed as a standard deviation by the following equation:

$$sd = AAC / 2 \tag{1}$$

where

sd is the standard deviation,

and

AAC is the value of the GWSI altitude accuracy code, in meters.

Accordingly, the standard deviation for well-altitude error could range from 0.015 to 12.5 m.

Well-Location Error

Well-location errors can cause a discrepancy between observed and simulated heads. The magnitude of this discrepancy depends directly on the hydraulic gradient at the well—the steeper the gradient, the greater the discrepancy. Well-location error was calculated as the product of the distance determined from the coordinate accuracy code values given in GWSI and the hydraulic gradient estimated for a given well location. Latitude and longitude coordinate accuracy codes given for wells in the DVRFS range from about 0.1 to 100 seconds. In the DVRFS region, a second represents about 33 m. Accordingly, the largest distance accuracy that could be computed for a well in the DVRFS model domain would be about ±3,300 m. The hydraulic gradient at a well was estimated from a regional potentiometric surface map developed by D’Agnese and others (1998). The largest gradient estimated from their map was nearly 15 percent and the smallest about 2 percent. The range defined by the value of the coordinate accuracy code is assumed to represent, with 95 percent confidence (or two standard deviations), the true error in the head observation as related to well-location uncertainty. Assuming that the head observation represents the mean value and that the error is normally distributed, the uncertainty of the head observation, with respect to the well-location error, can be expressed as a standard deviation calculated by the following equation:

$$sd = (CAC / 2) \times HG, \tag{2}$$

where

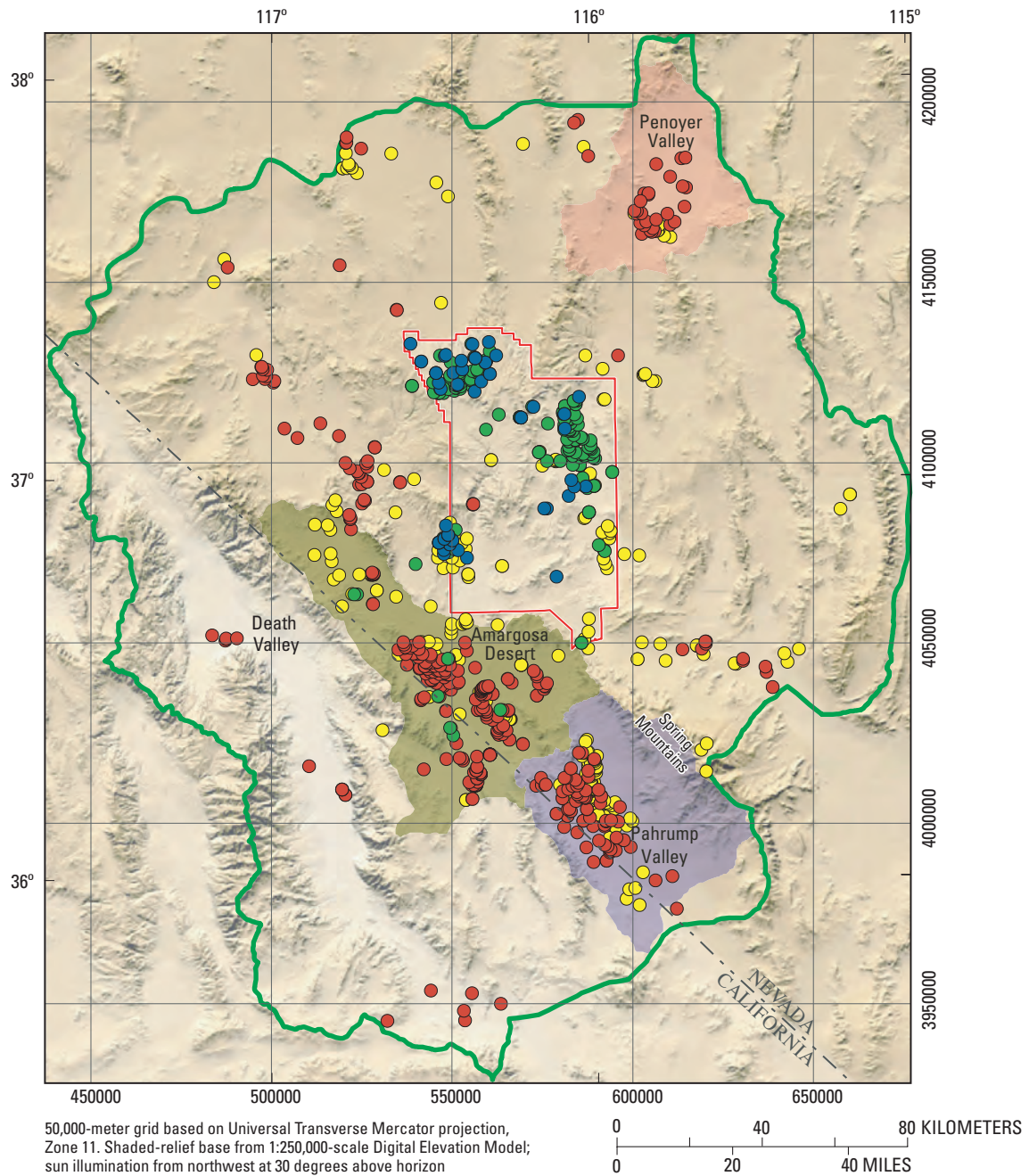
sd is the standard deviation;

CAC is the value of the GWSI coordinate accuracy code, in meters;

and

HG is hydraulic gradient, in percent slope divided by 100.

Accordingly, the standard deviation for well-location error could range from about 0.03 to 250 m.



EXPLANATION

Hydrographic area

- Amargosa Desert
- Pahrump Valley
- Penoyer Valley

- Death Valley regional ground-water flow system model boundary
- Nevada Test Site boundary

Bottom depth of opening in

- head-observation well—In meters below land surface**
- ≤100
 - >100 and ≤500
 - >500 ≤1,000
 - >1,000 ≤5,000

Figure C-13. Spatial distribution and bottom depth of opening in head-observation wells (steady-state and transient conditions) used in calibration of the Death Valley regional ground-water flow system model.

Nonsimulated Transient Error

Nonsimulated transient errors result from uncertainty in the magnitude of water-level response caused by stresses not simulated in the flow model, which are typically seasonal and long-term climate changes. Seasonal water-level fluctuations of nearly 5 m have been measured in shallow wells in the DVRFS model domain. These seasonal fluctuations decrease as the depth of the open interval increases. The quantification of uncertainty associated with seasonal fluctuations in the water level requires a sufficient number of measurements made over an entire year. For observations computed with less than 7 measurements per year, the seasonal fluctuation was set to 5 m for wells with open intervals less than 15 m below land surface and 1.5 m for open intervals greater than 15 m below land surface. For observations computed from seven or more measurements per year, the fluctuation is computed as the difference between the highest and lowest water-level measurement. It was assumed that if at least seven measurements were made per year, then these measurements spanned the entire year.

The long-term climatic response in the water-level record is much more difficult to discern and commonly is masked by pumping effects. On the basis of an analysis of available water-level data, long-term climatic response is relatively small throughout the DVRFS region (less than 1.5 m). The potential error associated with long-term climate response at a well was not calculated independently but instead was accounted for by adding 1 m to the seasonal fluctuation assigned to each well. The range defined by this sum is assumed to represent, with 95-percent confidence (or two standard deviations), the true error in the head observation as related to nonsimulated transient uncertainty. Assuming that the head observation represents the mean value and that the error is normally distributed, the uncertainty of the head observation, with respect to the nonsimulated transient error, can be expressed as a standard deviation calculated by the following equation:

$$sd = (SF + LTC) / 4, \quad (3)$$

where

sd is the standard deviation;

SF is seasonal fluctuation as defined by water-level measurements, in meters;

and

LTC is the long-term climate trend defined as 1 m.

Accordingly, the maximum standard deviation for nonsimulated transient error is 1.5 m for wells having less than 7 measurements and an open interval within 15 m of land surface, and 0.625 m for deeper wells.

Measurement Error

Measurement errors result from inaccuracies in the measurement of the depth to water. Measurement accuracy depends primarily on the device being used to make the

measurement. Typically, the accuracies of measurement devices are less than a meter and are defined as a percentage of the depth of the measurement—the deeper the depth-to-water measurement, the greater the potential error. Errors associated with most devices used to measure water levels in the DVRFS region are described in a standard operating procedure report for water-level measurements at the NTS (U.S. Geological Survey, Las Vegas, Nev., written commun., 2001). The greatest error associated with any of these devices equates to about ± 1 m per 1,000 m or 0.1 percent. Water-level depths measured in the region range from near land surface to about 750 m below land surface. A value computed as 0.1 percent of the water-level measurement was used to represent the potential error in measurement accuracy. The range defined by this value is assumed to represent, with 95-percent confidence (or two standard deviations), the true error in the head observation as related to measurement uncertainty. Assuming that the head observation represents the mean value and that the error is normally distributed, the uncertainty of the head observation, with respect to the measurement-accuracy error, can be expressed as a standard deviation calculated by the following equation:

$$sd = (DOOBS \times 0.001) / 2, \quad (4)$$

where

sd is the standard deviation,

and

$DOOBS$ is depth of the observation, in meters above or below land surface.

Accordingly, the standard deviation for the measurement-accuracy error could range from near 0 to 0.375 m.

Total Head-Observation Error

The potential error associated with each head observation is the composite of all errors contributed by the different sources. This uncertainty, expressed as a standard deviation, was computed as:

$$(sd_1^2 + sd_2^2 + sd_3^2 + sd_4^2)^{1/2}, \quad (5)$$

where

sd_1 is standard deviation of well-altitude error,

sd_2 is standard deviation of well-location error,

sd_3 is standard deviation of nonsimulated transient error,

and

sd_4 is standard deviation of measurement-accuracy error.

Accordingly, the standard deviations representing the uncertainty of head observations used to calibrate steady-state (pre-pumped) conditions generally range from less than 1 to about 40 m (fig. C-14A). About 95 percent of the head observations had an uncertainty of less than 10 m and nearly

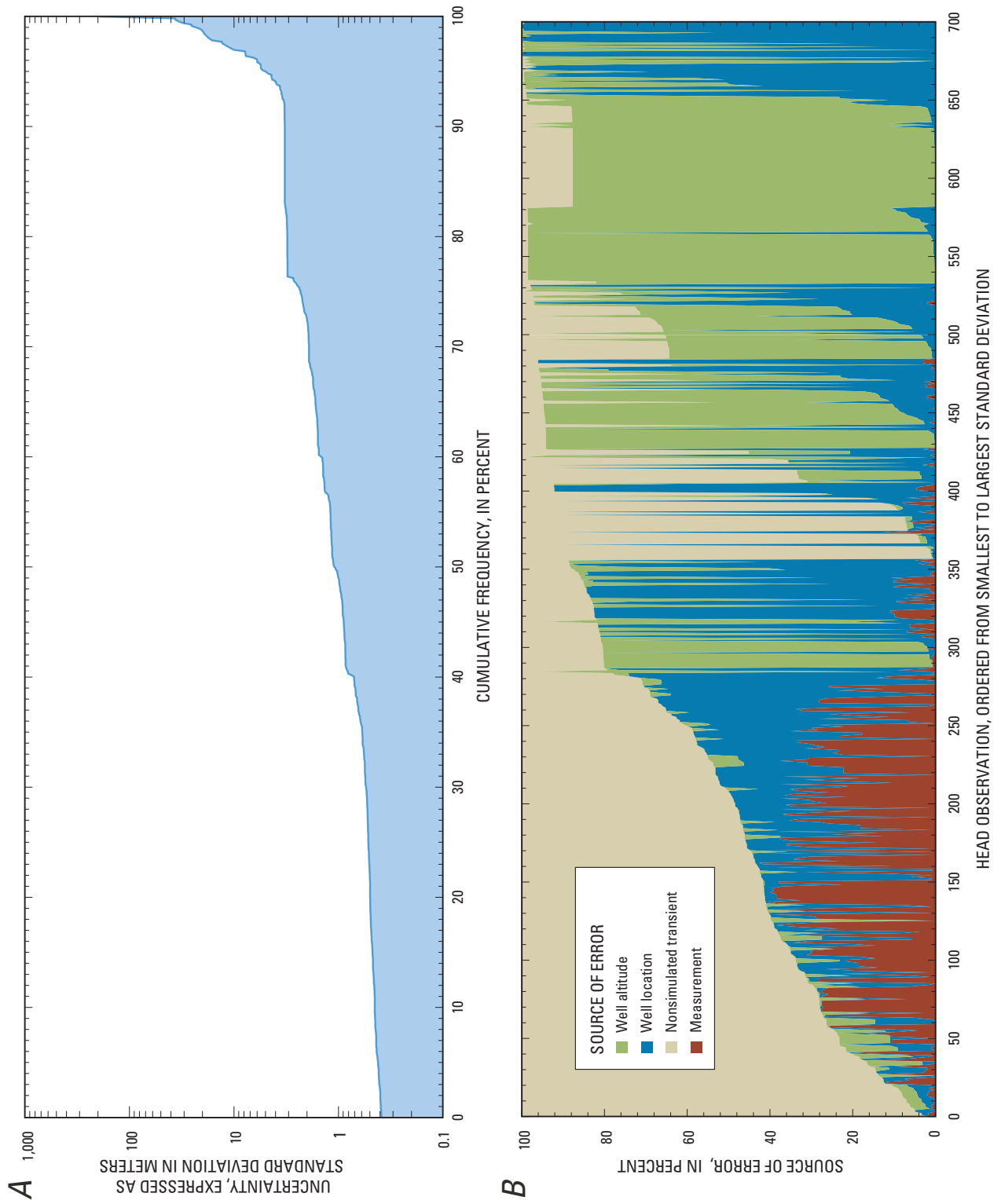


Figure C-14. Uncertainty of 700 head observations computed to represent prepumped, steady-state conditions in the Death Valley regional ground-water flow system model domain.

50 percent had an uncertainty of less than 1 m. The contribution of individual sources to head observation uncertainty varies; but in general, smaller uncertainties were dominated by nonsimulated transient and measurement errors and larger uncertainties by well-altitude and well-location errors (fig. C-14B).

Summary

Information from a series of investigations was compiled to conceptualize and quantify hydrologic components of the ground-water flow system in the Death Valley regional ground-water flow system (DVRFS) model domain and to provide hydraulic-property and head-observation data to be used in the calibration of the transient-flow model. These studies, completed as part of the overall DVRFS investigation, reevaluated natural ground-water discharge occurring through evapotranspiration (ET) and spring flow; the history of ground-water pumping from 1913 through 1998; ground-water recharge simulated as net infiltration; model boundary inflows and outflows based on regional hydraulic gradients and water budgets of surrounding areas; hydraulic conductivity and its relation to depth; and water levels and their appropriateness for regional simulation of prepumped and pumped conditions in the DVRFS model domain. Results appropriate for the regional extent and scale of the model were provided by acquiring additional data, by reevaluating existing data using current technology and concepts, and by refining interpretations using new analyses or algorithms.

Estimates of natural ground-water discharge were evaluated for Death Valley, Oasis Valley, and the other major discharge areas in the DVRFS model domain. Natural ground-water discharge was estimated from evaporation from open water and moist, bare soil and from transpiration by the phreatophytes growing in the discharge area. Discharge from the many regional springs in these discharge areas was accounted for because most spring flow eventually is evapotranspired. In Pahrump and Penoyer Valleys, where ground water is discharged both naturally and by pumping, natural discharge estimates were based on published sources and were assumed to vary with local pumping. In discharge areas not affected by pumping, rates of natural ground-water discharge were assumed to remain fairly constant, presuming no major changes in climate. Mean annual discharge from ET for the model domain is estimated at about 115.5 million cubic meters (Mm^3).

The ET investigations did not account for spring flow where springs supported narrow bands of riparian habitat along the valley margins or where local pumping had decreased spring flow. Previously published spring-discharge rates and some additional measurements of discharge from selected springs were compiled. Annual natural discharge from springs not accounted for in ET studies is estimated at about 16.8 Mm^3 .

The composite annual discharge from Bennetts and Manse Springs, the largest springs in Pahrump Valley, is estimated at 12 Mm^3 prior to ground-water pumping. The local pumping of ground water for large-scale agricultural use in Pahrump Valley caused Bennetts Spring to stop flowing in 1959 and Manse Spring to stop flowing around 1977.

A history of ground-water use for the DVRFS region (1913–98) was developed by compiling available information and using various estimation methods to fill gaps where data were missing. In 1913, ground water used to support agriculture in Pahrump Valley was estimated at less than 5 Mm^3 . Ground-water pumping remained relatively constant through 1944 and thereafter increased steadily in response to agricultural expansion. The estimated total volume of ground water pumped from the DVRFS model domain for the period 1913–98 is about 3,276 Mm^3 and in 1998 about 93.5 Mm^3 . These estimates are not adjusted for water potentially returned to the ground-water flow system.

Recharge in the DVRFS region was estimated from net infiltration using a deterministic mass-balance method. The approach simulated daily climate changes and numerous near-surface processes controlling infiltration. The net-infiltration model, INFILv3, was calibrated to available surface-water flow measurements and constrained by prior estimates of recharge and discharge. The INFILv3 model simulated a mean annual potential recharge to the model domain of about 125 Mm^3 for the period 1950–99.

Lateral flow across the boundary of the DVRFS model domain was estimated. Flows from water-budget studies were compared to those computed by Darcy calculations by using hydraulic gradients obtained from a regional potentiometric-surface map (Appendix 1) and estimated hydraulic conductivities of the hydrogeologic units (HGUs) along the model boundary. The estimated mean annual ground-water flow into the model domain is about 18.4 Mm^3 and out of the model domain is about 9.5 Mm^3 .

A water budget for the prepumping period (pre-1913) computed for the DVRFS model domain was balanced to within about 7 percent. For prepumped conditions, annual recharge accounted for about 87 percent of the total inflow, and natural discharge (ET and spring flow) about 93 percent of the total outflow. Although natural discharge by ET was assumed to represent prepumped conditions, actual discharge may have been reduced some by local pumpage. The remainder of the inflow and outflow is accounted for by lateral flows into and out of the model domain.

The water budget for pumped conditions for the DVRFS model domain is incomplete because accurate estimates for the major hydrologic components are not available. Pumpage in 1998 was about 70 percent of the total outflow estimated for prepumped conditions. A likely source of most of the water being pumped from the DVRFS region is ground water in storage. This water, when removed from the flow system, potentially decreases the hydraulic head within aquifers and decreases natural discharge through ET and from spring flow.

These decreases are partly reflected by declining water-level measurements in areas of pumping and by estimates showing declining spring discharge in Pahrump Valley.

Previously developed reasonable ranges of hydraulic properties, primarily horizontal hydraulic conductivity, were used for the major HGUs of the DVRFS region. Fracturing appears to have the greatest influence on the permeability of bedrock HGUs—the greater the degree of fracturing, the greater the permeability. In the Cenozoic volcanic rocks by alteration decreases hydraulic conductivity, and welding forming brittle rocks that fracture more easily, increases hydraulic conductivity. Storage coefficients from the literature were used because field data necessary to develop HGU-specific values were extremely limited.

The average depth represented by hydraulic-conductivity estimates for the model domain is 700 m with a maximum depth of 3,600 m. Using these limited data, hydraulic conductivity decreased with depth. A rigorous quantification of a depth-decay function was prevented by the variability in available hydraulic-conductivity data.

Nearly 40,000 water levels measured since 1907 in about 2,100 wells were evaluated as part of the DVRFS investigation. Almost 100 wells in the DVRFS model domain have a record of 20 years or longer. Most wells having 30 or more years of water-level record are in Pahrump Valley. About 43 percent of the wells have openings at depths less than 100 m, and less than 10 percent at depths greater than 1,000 m. Wells having deeper openings are generally in or near the NTS. The depth of the open interval for wells in major areas of ground-water pumping (Amargosa Desert and Penoyer and Pahrump Valleys) is typically less than 100 m.

Head observations representing steady-state, prepumped conditions were computed from about 12,000 water levels averaged at 700 wells in the DVRFS model domain. Head observations range from about 2,500 m above sea level in the Spring Mountains to nearly 100 m below sea level in Death Valley. Transient, pumped conditions were represented by head observations computed from nearly 15,000 water levels measured in about 350 wells. Water-level records for individual wells spanned periods from 1 to about 50 years. Most wells have less than 15 m of measured drawdown. Wells having measured drawdown greater than 15 m typically are in areas of concentrated irrigation use, primarily the Amargosa Desert and Pahrump and Penoyer Valleys. The largest drawdown is 76 m, which was measured in a well located in the Beatty area just north of the Amargosa Desert.

Each head observation was assigned an uncertainty based on potential errors related to uncertainties in the altitude and location given for a well, potential inaccuracies in the measurement of a water level, and fluctuations introduced by variations in climate or any other nonsimulated transient stress. The uncertainty of each head observation was represented by a standard deviation calculated by compositing the individual source errors. Standard deviations representing the uncertainty of the head observations range from less than 1 to about 200 m with only one observation having an uncertainty exceeding 40 m.

References Cited

- Ball, S.H., 1907, A geologic reconnaissance in southwestern Nevada and eastern California: U.S. Geological Survey Bulletin 308, 218 p., 3 plates.
- Bedinger, M.S., Langer, W.H., and Reed, J.E., 1989, Hydraulic properties of rocks in the Basin and Range province, *in* Bedinger, M.S., Sargent, K.A., Langer, W.H., Sherman, F.B., Reed, J.E., and Brady, B.T., Studies of geology and hydrology in the Basin and Range province, southwestern United States, for isolation of high-level radioactive waste—Basis of characterization and evaluation: U.S. Geological Survey Professional Paper 1370–A, p. 16–18.
- Belcher, W.R., Elliott, P.E., and Geldon, A.L., 2001, Hydraulic-property estimates for use with a transient ground-water flow model of the Death Valley regional ground-water flow system, Nevada and California: U.S. Geological Survey Water-Resources Investigations Report 01–4120, 33 p.
- Belcher, W.R., Sweetkind, D.S., and Elliott, P.E., 2002, Probability distributions of hydraulic conductivity for the hydrogeologic units of the Death Valley regional ground-water flow system, Nevada and California: U.S. Geological Survey Water-Resources Investigations Report 02–4212, 24 p.
- Bowen, I.S., 1926, The ratio of heat losses by conduction and by evaporation from any water surface: *Physical Review*, v. 27, p. 779–787.
- Cardinali, J.L., Roach, L.M., Rush, F.E., and Vasey, B.J., 1968, State of Nevada hydrographic areas: Nevada Division of Water Resources map, 1:500,000 scale.
- Carpenter, Everett, 1915, Groundwater in southeastern Nevada: U.S. Geological Survey Water-Supply Paper 365, 86 p., 5 plates.
- Carroll, Rosemary W.H., Giroux, B., Pohll, G., Hershey, R.L., Russell, C.E., and Howcraft, W., 2003, Numerical simulation of groundwater withdrawal at the Nevada Test Site: Las Vegas, University and Community College System of Nevada, Desert Research Institute Publication 45163, 20 p.
- Czarnecki, J.B., 1997, Geohydrology and evapotranspiration at Franklin Lake playa, Inyo County, California, *with a section on* Estimating evapotranspiration using the energy-budget eddy-correlation technique by D.I. Stannard: U.S. Geological Survey Water-Supply Paper 2377, 75 p.

- D'Agnese, F.A., Faunt, C.C., and Turner, A.K., 1998, An estimated potentiometric surface of the Death Valley region, Nevada and California, developed using geographic information system and automated interpolation techniques: U.S. Geological Survey Water-Resources Investigations Report 97-4052, 15 p.
- D'Agnese, F.A., Faunt, C.C., Turner, A.K., and Hill, M.C., 1997, Hydrogeologic evaluation and numerical simulation of the Death Valley regional ground-water flow system, Nevada and California: U.S. Geological Survey Water-Resources Investigations Report 96-4300, 124 p.
- D'Agnese, F.A., O'Brien, G.M., Faunt, C.C., Belcher, W.R., and San Juan, C.A., 2002, A three-dimensional numerical model of predevelopment conditions in the Death Valley regional ground-water flow system, Nevada and California: U.S. Geological Survey Water-Resources Investigations Report 02-4102, 114 p. Accessed September 22, 2004, at <http://pubs.water.usgs.gov/wri024102/>.
- DeMeo, G.A., Lacznia, R.J., Boyd, R.A., Smith, J.L., and Nylund, W.E., 2003, Estimated ground-water discharge by evapotranspiration from Death Valley, California, 1997-2001: U.S. Geological Survey Water-Resources Investigations Report 03-4254, 27 p.
- Dettinger, M.D., 1989, Distribution of carbonate-rock aquifers in southern Nevada and the potential for their development, summary of findings, 1985-88—Program for the study and testing of carbonate-rock aquifers in eastern and southern Nevada, Summary Report No. 1: State of Nevada, Carson City, 37 p.
- Glancy, P.A., 1968, Water-resources appraisal of Mesquite-Ivanpah Valley area, Nevada and California: Nevada Department of Conservation and Natural Resources, Water Resources—Reconnaissance Series Report 46, 57 p.
- Hale, G.S., and Westenburg, C.L., 1995, Selected ground-water data for Yucca Mountain region, southern Nevada and eastern California, calendar year 1993: U.S. Geological Survey Open-File Report 95-0158, 67 p.
- Harrill, J.R., 1986, Ground-water storage depletion in Pah-rump Valley, Nevada-California, 1962-1975: U.S. Geological Survey Water-Supply Paper 2279, 53 p.
- Harrill, J.R., Gates, J.S., and Thomas, J.M., 1988, Major ground-water flow systems in the Great Basin region of Nevada, Utah, and adjacent States: U.S. Geological Survey Hydrologic Investigations Atlas HA-694-C, scale 1:1,000,000.
- Helsel, D.R., and Hirsch, R.M., 1992, Statistical methods in water resources: Amsterdam, Elsevier, 529 p.
- Hevesi, Joseph A., Flint, Alan L., and Flint, Lorraine E., 2002, Preliminary estimates of spatially distributed net infiltration and recharge for the Death Valley region, Nevada-California: U.S. Geological Survey Water-Resources Investigations Report 02-4010, 36 p.
- Hevesi, J.A., Flint, A.L., and Flint, L.E., 2003, Simulation of net infiltration and potential recharge using a distributed-parameter watershed model of the Death Valley Region, Nevada and California: U.S. Geological Survey Water-Resources Investigations Report 03-4090, 161 p.
- Hunt, C.B., Robinson, T.W., Bowles, W.A., and Washburn, A.L., 1966, Hydrologic basin, Death Valley, California: U.S. Geological Survey Professional Paper 494-B, 138 p.
- IT Corporation, 1996a, Underground test area subproject phase I, Data analysis task, volume II—Groundwater recharge and discharge data documentation package: Las Vegas, Nev., Report ITLV/10972-81 prepared for the U.S. Department of Energy, 8 volumes, various pagination.
- IT Corporation, 1996b, Underground test area subproject phase I, Data analysis task, volume IV—Hydraulic parameter data documentation package: Las Vegas, Nev., Report ITLV/10972-81 prepared for the U.S. Department of Energy, 8 volumes, various pagination.
- LaCamera, R.J., and Locke, G.L., 1997, Selected ground-water data for Yucca Mountain region, southern Nevada and eastern California, through December 1996: U.S. Geological Survey Open-File Report 97-821, 79 p.
- LaCamera, R.J., and Westenburg, C.L., 1994, Selected ground-water data for Yucca Mountain region, southern Nevada and eastern California, through December 1992: U.S. Geological Survey Open-File Report 94-54, 161 p.
- LaCamera, R.J., Westenburg, C.L., and Locke, G.L., 1996, Selected ground-water data for Yucca Mountain region, southern Nevada and eastern California, through December 1995: U.S. Geological Survey Open-File Report 96-553, 75 p.
- Lacznia, R.J., DeMeo, G.A., Reiner, S.R., Smith, J.L., and Nylund, W.E., 1999, Estimates of ground-water discharge as determined from measurements of evapotranspiration, Ash Meadows area, Nye County, Nevada: U.S. Geological Survey Water-Resources Investigations Report 99-4079, 70 p.
- Lacznia, R.J., Smith, J., LaRue, Elliott, P.E., DeMeo, G.A., Chatigny, M.A., and Roemer, G.J., 2001, Ground-water discharge determined from estimates of evapotranspiration, Death Valley regional flow system, Nevada and California: U.S. Geological Survey Water-Resources Investigations Report 01-4195, 51 p.

- Lichty, R.W., and McKinley, P.W., 1995, Estimates of ground-water recharge rates for two small basins in central Nevada: U.S. Geological Survey Water-Resources Investigations Report 94-4104, 31 p.
- Malmberg, G.T., 1965, Available water supply of the Las Vegas ground-water basin, Nevada: U.S. Geological Survey Water-Supply Paper 1780, 116 p.
- Malmberg, G.T., 1967, Hydrology of the valley-fill and carbonate-rock reservoirs, Pahrump Valley, Nevada-California: U.S. Geological Survey Water-Supply Paper 1832, 47 p.
- Malmberg, G.T., and Eakin, T.E., 1962, Ground-water appraisal of Sarcobatus Flat and Oasis Valley, Nye and Esmeralda Counties, Nevada: Nevada Department of Conservation and Natural Resources, Ground-Water Resources—Reconnaissance Series Report 10, 39 p.
- Maxey, G.B., and Eakin, T.E., 1950, Ground water in White River Valley, White Pine, Nye, and Lincoln Counties, Nevada: Nevada State Engineer Water Resources Bulletin No. 8, 59 p.
- Maxey, G.B., and Jameson, C.H., 1948, Geology and water resources of Las Vegas, Pahrump, and Indian Springs Valleys, Clark and Nye Counties, Nevada: Nevada State Engineer Water Resources Bulletin no. 5, 43 p.
- Mendenhall, W.C., 1909, Some desert watering places in southeastern California and southern Nevada: U.S. Geological Survey Water-Supply Paper 224, 98 p.
- Miller, G.A., 1977, Appraisal of the water resources of Death Valley, California-Nevada: U.S. Geological Survey Open-File Report 77-728, 68 p.
- Moreo, M.T., Halford, K. J., La Camera, R.J., and Lacznia, R.J., 2003, Estimated ground-water withdrawals from the Death Valley regional flow system, Nevada and California, 1913-98: U.S. Geological Survey Water-Resources Investigations Report 03-4245, 28 p.
- Neuman, S.P., 1982, Statistical characterization of aquifer heterogeneities—An overview, *in* Narasimhan, T.N., ed., Recent trends in hydrogeology: Boulder, Colo., Geological Society of America Special Paper 189, p. 81-102.
- Pistrang, M.A., and Kunkel, F., 1964, A brief geologic and hydrologic reconnaissance of the Furnace Creek Wash area, Death Valley National Monument, California: U.S. Geological Survey Water-Supply Paper 1779-Y, 35 p.
- Reiner, S.R., Lacznia, R.J., DeMeo, G.A., Smith, J.L., Elliott, P.E., Nylund, W.E., and Fridrich, C.J., 2002, Ground-water discharge determined from measurements of evapotranspiration, other available hydrologic components, and shallow water-level changes, Oasis Valley, Nye County, Nevada: U.S. Geological Survey Water-Resources Investigations Report 01-4239, 65 p.
- Rice, W.A., 1984, Preliminary two-dimensional regional hydrologic model of the Nevada Test Site and vicinity: Albuquerque, N. Mex., Sandia National Laboratories Report SAND83-7466, 89 p.
- Rush, F.E., 1968, Water-resources appraisal of Clayton Valley-Stonewall Flat area, Nevada and California: Nevada Department of Conservation and Natural Resources, Water Resources—Reconnaissance Series Report 45, 54 p.
- Rush, F.E., 1970, Regional ground-water systems in the Nevada Test Site area, Nye, Lincoln, and Clark Counties, Nevada: Carson City, Nevada Department of Conservation and Natural Resources, Ground-Water Resources—Reconnaissance Series Report 54, 25 p.
- Russell, C.E., and Minor, T., 2002, Reconnaissance estimates of recharge based on an elevation-dependent chloride mass balance approach: Las Vegas, University and Community College System of Nevada, Desert Research Institute Publication 45164, 57 p.
- Stonstrom, D.A., Prudic, D.E., Lacznia, R.L., Akstin, K.C., Boyd, R.A., and Henkelman, K.K., 2003, Estimates of deep percolation beneath native vegetation, irrigated fields, and the Amargosa River channel, Amargosa Desert, Nye County, Nevada: U.S. Geological Survey Open-File Report 03-104, 83 p.
- U.S. Department of Agriculture, 1994, State Soil Geographic (STATSGO) Data Base—Data use information: U.S. Department of Agriculture Miscellaneous Publication no. 1492.
- Van Denburgh, A.S., and Rush, F.E., 1974, Water-resources appraisal of Railroad and Penoyer Valleys, east-central Nevada: Nevada Department of Conservation and Natural Resources, Water Resources—Reconnaissance Series Report 60, 61 p.
- Waddell, R.K., 1982, Two-dimensional, steady-state model of ground-water flow, Nevada Test Site and vicinity, Nevada-California: U.S. Geological Survey Water-Resources Investigations Report 82-4085, 72 p.
- Walker, G.E., and Eakin, T.E., 1963, Geology and ground water of Amargosa Desert, Nevada-California: Nevada Department of Conservation and Natural Resources, Ground-Water Resources—Reconnaissance Series Report 14, 45 p.

- Waring, G.A., 1915, Springs of California: U.S. Geological Survey Water-Supply Paper 338, 410 p.
- Waring, G.A., revised by Blankenship, R.R., and Bentall, Ray, 1965, Thermal springs of the United States and other countries of the world—A summary: U.S. Geological Survey Professional Paper 492, 383 p.
- West, N.E., 1988, Intermountain deserts, shrub steppes, woodlands, *in* Barbour, M.G., and Billings, W.D., eds., North American terrestrial vegetation: Cambridge, Cambridge University Press, 434 p.
- Westenburg, C.L., and LaCamera, R.J., 1996, Selected groundwater data for Yucca Mountain region, southern Nevada and eastern California, through December 1994: U.S. Geological Survey Open-File Report 96-205, 73 p.
- Winograd, I.J., and Thordarson, William, 1975, Hydrologic and hydrochemical framework, south-central Great Basin, Nevada-California, with special reference to the Nevada Test Site: U.S. Geological Survey Professional Paper 712C, p. C1-C126.

Hydrology

By Claudia C. Faunt, Frank A. D’Agnese, and Grady M. O’Brien

Chapter D of

Death Valley Regional Ground-Water Flow System, Nevada and California—Hydrogeologic Framework and Transient Ground-Water Flow Model

Edited by Wayne R. Belcher

Prepared in cooperation with the
U.S. Department of Energy
Office of Environmental Management, National Nuclear Security Administration, Nevada Site Office,
under Interagency Agreement DE–AI52–01NV13944, and
Office of Repository Development,
under Interagency Agreement DE–AI08–02RW12167

Scientific Investigations Report 2004–5205

U.S. Department of the Interior
U.S. Geological Survey

Contents

| | |
|---|-----|
| Introduction | 141 |
| Hydrochemistry | 141 |
| Ground-water Hydrology | 142 |
| Source and Movement of Ground Water | 142 |
| Regional Aquifers, Flow Barriers, and Confining Units | 145 |
| Flow-System Model Boundaries | 145 |
| Flow-System Subregions | 145 |
| Northern Death Valley Subregion | 147 |
| Central Death Valley Subregion | 148 |
| Pahute Mesa-Oasis Valley Basin | 149 |
| Ash Meadows Basin | 152 |
| Alkali Flat-Furnace Creek Basin | 154 |
| Southern Death Valley Subregion | 155 |
| Surface-Water Hydrology | 156 |
| Drainage Areas | 156 |
| Springs | 156 |
| Paleohydrology | 158 |
| Summary | 159 |
| References Cited | 160 |

Figures

| | |
|--|-----|
| D-1. Schematic block diagram of Death Valley and other basins illustrating the structural relations between mountain blocks, valleys, and ground-water flow..... | 142 |
| D-2—D-5. Maps showing: | |
| D-2. Generalized areas of potential recharge and discharge based on potentiometric surfaces for the Death Valley regional ground-water flow system model..... | 143 |
| D-3. Generalized areas of recharge and discharge, and location of regional springs and pumping wells in the Death Valley regional ground-water flow system region | 144 |
| D-4. Generalized distribution of deep Cenozoic basins, southwestern Nevada volcanic field, regional carbonate-rock aquifer, and confining units at the water table for the Death Valley regional ground-water flow system region | 146 |
| D-5. Subregions and associated flow paths of the Death Valley regional ground-water flow system region | 147 |

| | |
|--|-----|
| D-6—D-8. Maps of the Death Valley regional ground-water flow system showing ground-water sections and flow directions for the: | |
| D-6. Northern Death Valley subregion | 149 |
| D-7. Central Death Valley subregion | 150 |
| D-8. Southern Death Valley subregion..... | 151 |
| D-9. Map showing hydrologic units for the Death Valley regional ground-water flow system | 157 |
| D-10. Map showing location of paleodischarge areas and regional springs in the Death Valley regional ground-water flow system region | 159 |

Table

| | |
|---|-----|
| D-1. Divisions of the Death Valley regional ground-water flow system..... | 148 |
|---|-----|

CHAPTER D. Hydrology

By Claudia C. Faunt, Frank A. D’Agnese, and Grady O’Brien

Introduction

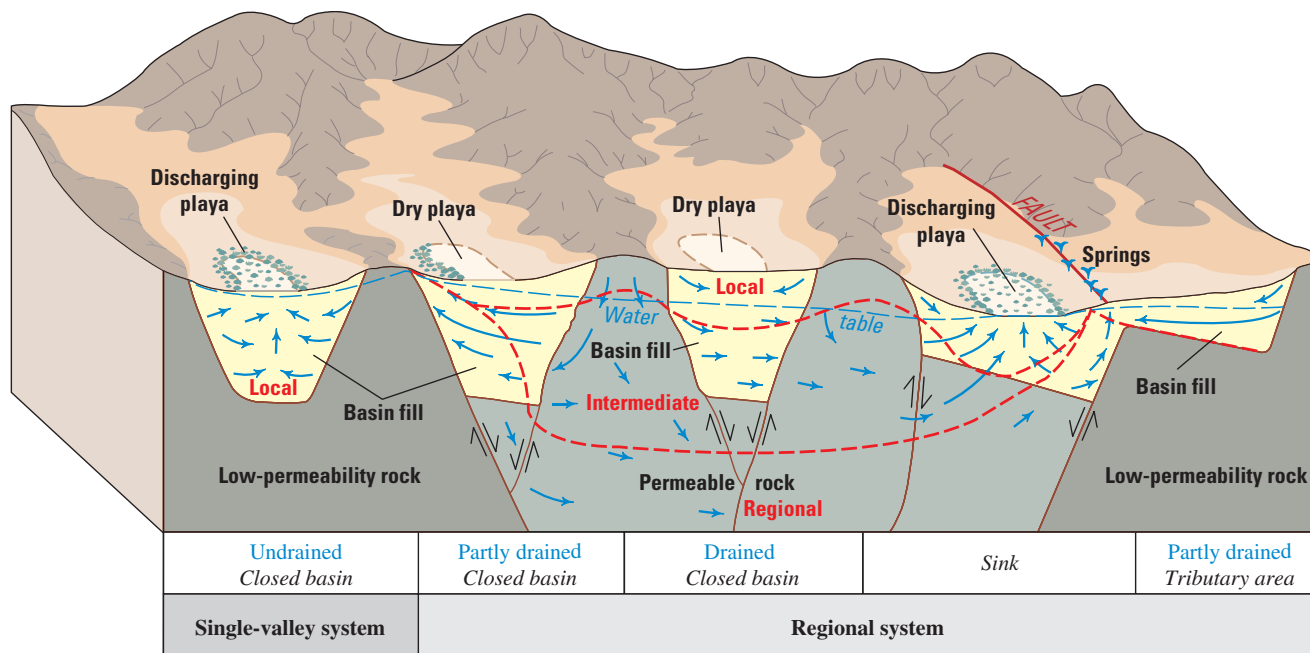
The hydrology of the Death Valley regional ground-water flow system (DVRFS), as in all flow systems, is influenced by geology and climate and varies with time. In general, ground water moves through permeable zones under the influence of hydraulic gradients from areas of recharge to areas of discharge in the regional system (fig. D–1). The topography produces numerous local subsystems within the major flow system (Freeze and Cherry, 1979, p. 196). Water that enters the flow system in a recharge area may be discharged in the nearest topographic low, or it may be transmitted to a regional discharge area.

Ground-water flow in the DVRFS region is dominated by interbasin flow with several relatively shallow and local on flow systems that are superimposed on deeper intermediate and regional flow systems (fig. D–1). The regional ground-water flow patterns do not coincide with local topographic basins. Regional ground-water flow generally follows the regional topographic gradient as water moves toward the lowest point in the region at Death Valley, Calif. (fig. D–2). Bedinger and Harrill (plate 1 and Appendix 1, this volume) developed regional potentiometric-surface contours of the areas contributing ground-water flow to the DVRFS model domain to define the regional ground-water flow across the lateral boundary of the model. For conceptualization of the ground-water flow system and for the construction of a numerical flow model (D’Agnese and others, 1997), D’Agnese and others (1998) developed an approximation of the regional potentiometric surface. This surface depicted mounds, troughs, and depressions indicating areas of recharge and discharge that may be characteristic of a relatively shallow and local flow system (fig. D–2). Differences between the potentiometric surfaces of the deep regional system (plate 1 and Appendix 1, this volume) and those in the shallower local systems depicted on D’Agnese and others (1998) are emphasized by areas of generally downward flow (recharge areas) to, and generally upward flow (discharge areas) from, the regional system (fig. D–2).

Hydrochemistry

The chemically and thermally dynamic nature of ground water can be used to help define flow systems and evaluate the relative importance of ground-water sources and pathways using chemical, isotope, temperature, and hydraulic data for ground water. For example, leakage from the carbonate-rock aquifer into overlying aquifers can be distinguished by differences in water quality along with differences in water temperature and hydraulic potential. Discharge temperatures for many modern springs commonly are higher than mean annual air temperature, indicating that the water has thermally equilibrated along deep flow paths. Cooler temperatures or lower altitude recharge are usually associated with shallower and shorter ground-water flow paths. Chemical and thermal heterogeneities are common in the DVRFS region due to fracture flow through contrasting lithologies, and these data were used, where possible, to help delineate the flow system.

Ground water of the DVRFS region may be divided into hydrochemical categories that reflect equilibration with (1) tuffaceous rocks or tuffaceous basin-fill sediments (a sodium and potassium bicarbonate type); (2) primarily carbonate rocks or carbonate basin-fill sediments (a calcium and magnesium bicarbonate type); and (3) both kinds of rocks or sediments, or a mixing of different types of water (Schoff and Moore, 1964; Winograd and Thordarson, 1975). These categories define hydrochemical signatures for the water that can be used to identify sources and flow paths. In some areas water can reflect equilibration with playa deposits. Isotopic information from water or discharge deposits can provide substantial information on the hydrochemical signature of ground water. For example, higher levels of strontium appear to be fairly common in water samples from the regional carbonate-rock aquifer (the associated carbonate rocks are relatively low in strontium), which indicates that more flow occurs through the fractured basement rocks (clastic and intrusive rocks, which are relatively high in strontium) than had been thought previously (Peterman and Stuckless, 1992a, b).



EXPLANATION

- Phreatophytes
 Approximate location of local, intermediate, and regional systems
- Ground-water flow
 Faults

Figure D-1. Schematic block diagram of Death Valley and other basins illustrating the structural relations between mountain blocks, valleys, and ground-water flow (modified from Eakin and others, 1976).

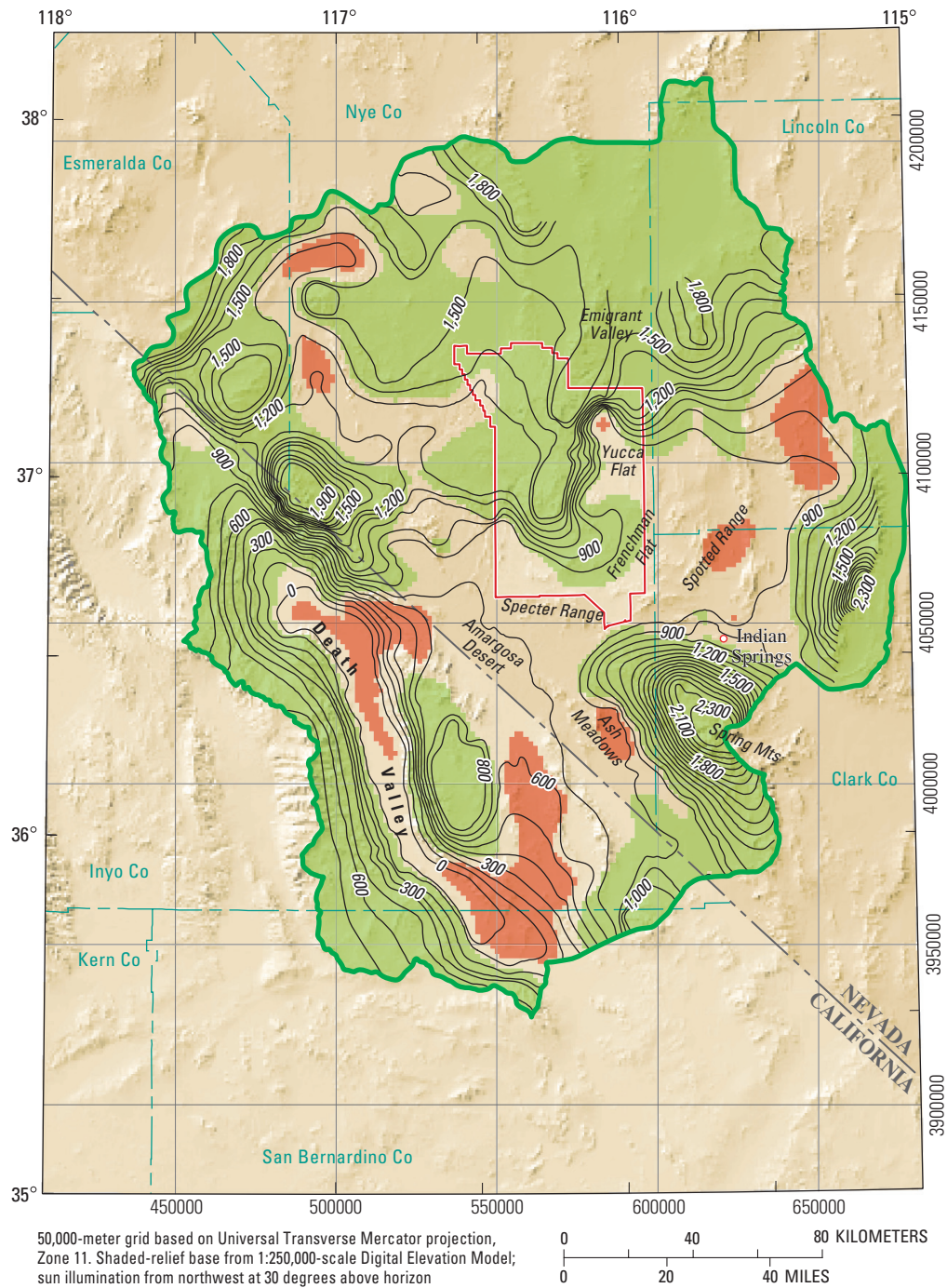
Ground-Water Hydrology

Within the DVRFS region, ground-water flow is strongly influenced by the physical framework of the system, which is characterized by aquifers, confining units, and flow barriers. In order to simulate the regional flow system, the boundaries of the system must be identified and defined for the model.

Source and Movement of Ground Water

Current sources of ground-water flow in the DVRFS region are (1) recharge from precipitation in the mountains (usually winter storms) within the model domain, and (2) lateral flow into the model boundary, predominantly through the carbonate-rock aquifer. Most ground-water recharge results from infiltration of precipitation and runoff on the mountain ranges (Bedinger and others, 1989) (fig. D-3). Water may infiltrate from melting snowpack in the mountains primarily on volcanic or carbonate rocks or adjacent to the mountains from streams flowing over alluvium (fans and channels) (Harrill and Prudic, 1998). Lateral ground-water flow across the model boundary is governed in part by regional hydraulic gradients in the DVRFS region.

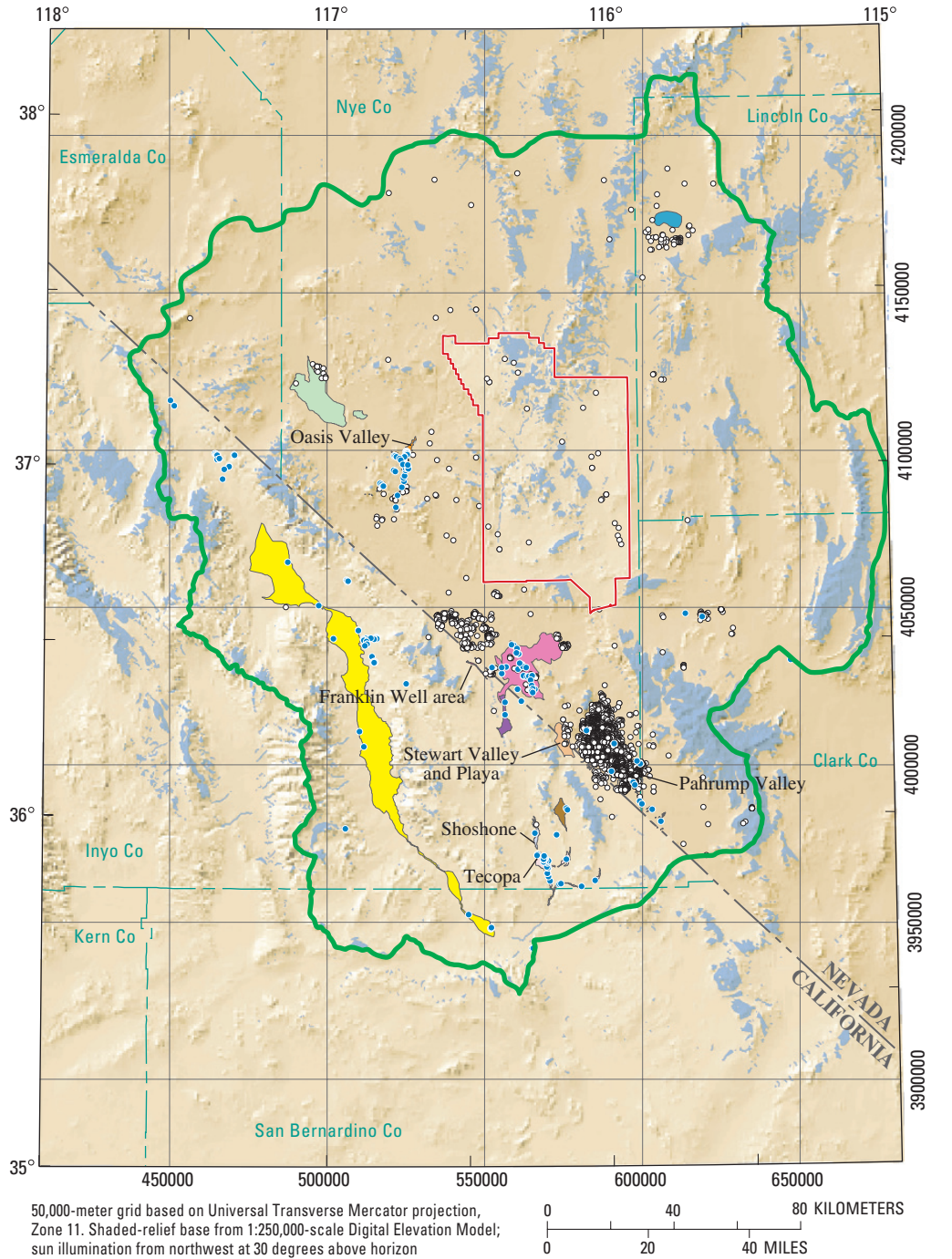
Current ground-water discharge in the DVRFS region is from (1) seeps and spring flow from the regional carbonate-rock aquifer and local systems; (2) evapotranspiration (ET); (3) pumpage for irrigation, mining, public supply, commercial, and domestic uses; and (4) subsurface flow out of the model boundary (fig. D-3 and plate 1). Most ground-water discharge today originates as spring or seep flow caused by variations in permeability created by geologic structures and varying lithologies (Winograd and Thordarson, 1975; Chapter B, this volume; fig. D-1). In particular, many of the regional (larger volume and higher temperature) springs occur along major faults (figs. D-1 and D-3). Most spring discharge is ultimately consumed by ET. Major discharge areas primarily occur in the lower part of intermontane valleys where the potentiometric surface is near or above land surface. Discharge also occurs as pumping for irrigation, mining, public supply, commercial, and domestic uses (Bedinger and others, 1989; Moreo and others, 2003; Chapter C, this volume) (fig. D-3). Lateral flow into the model domain, predominantly through the carbonate-rock aquifer, is small compared to the internal discharge (fig. D-3; Appendix 2, this volume).



EXPLANATION

- Generalized area of potential discharge from regional system**
 - Generalized area of potential recharge to regional system**
 - 300 — **Potentiometric-surface contour**—In meters above sea level. Contour interval 100 meters (D’Agnese and others, 1998)
 - Death Valley regional ground-water flow system model boundary**
 - Nevada Test Site boundary**
 - Populated place**
- Areas are delineated on the basis of differences between potentiometric surfaces in the deep regional flow system (Plate I and Appendix 1, this volume) and those in shallower, local

Figure D-2. Generalized areas of potential recharge and discharge based on potentiometric surfaces for the Death Valley regional ground-water flow system model.



EXPLANATION

- | | |
|--|--|
| Recharge area (modified from Hevesi and others, 2003) | Death Valley regional ground-water flow system model boundary |
| Discharge area (modified from Laczniaik and others, 2001 and DeMeo and others, 2003) | Nevada Test Site boundary |
| Ash Meadows | Franklin Well area |
| Carson Slough/ Franklin Lake Playa | Pahrump Valley |
| Chicago Valley | Penoyer Valley |
| Death Valley | Sarcobatus Flat |
| Shoshone | Oasis Valley |
| Stewart Valley and Playa | Tecopa |
| Regional springs | Pumping wells (modified from Moreo and others, 2003) |

Figure D-3. Generalized areas of recharge and discharge, and location of regional springs and pumping wells in the Death Valley regional ground-water flow system region.

Regional Aquifers, Flow Barriers, and Confining Units

Hydraulic compartmentalization may occur throughout the DVRFS region owing to the complex hydrogeologic framework. Ground water flows through a diverse assemblage of rocks and sediments in the region, and geologic structures exert significant control on ground-water movement as well (Chapter B, this volume).

Hydrogeologic units (HGUs) that are important to the hydrology of the DVRFS region include Cenozoic basin-fill units, Cenozoic volcanic-rock units of the southwestern Nevada volcanic field, the carbonate-rock aquifer, and confining units present at the water table (fig. D-4). Three types of aquifers exist in the region: basin-fill, volcanic-rock, and carbonate-rock aquifers (Chapter B, this volume). Some ground-water basins are part of multibasin flow systems connected by surface-water streams or by flow through the basin-fill sediments or permeable bedrock, and others are topographically and hydraulically isolated by low-permeability bedrock (figs. D-1 and D-4).

Juxtaposition of thick, low-permeability clastic-rock strata and rocks forming aquifers by folding or faulting commonly forms barriers to ground-water flow (Chapter B, this volume). Although the clastic rocks are subjected to the same deformational history as the carbonate rocks, the clastic rocks are generally relatively impermeable because of their low susceptibility to solution and their lack of significant secondary permeability. Most of the clastic rocks, when deformed, will break into fragments that reconsolidate into impermeable rock (quartzites) or will yield ductilely (shale) and, in either case, will not result in significant openings through which water can flow. In general, crystalline rocks have low permeability; however, where fractured, crystalline rocks may have significant permeability (Winograd and Thordarson, 1975).

In the DVRFS region, the relative permeability of faulted rock may vary either directly as the result of the fault orientation with respect to the present-day stress field or indirectly as zones of fracturing adjacent to the fault. The present-day stress field in the DVRFS region tends to enhance flow along northeast-southwest-trending features while decreasing the permeability along features oriented northwest-southeast (Carr, 1984; Faunt, 1997). Despite their orientation to the stress field, faults with low-permeability gouge may be barriers to ground-water flow (Winograd and Thordarson, 1968).

Flow-System Model Boundaries

The DVRFS model domain is contained within the DVRFS and can be defined by a series of boundaries. For modeling purposes, a ground-water flow system is a set of three-dimensional (3D) pathways through the subsurface rocks and sediments by which ground water moves from recharge areas to discharge areas. Below the water table, the saturated

volume of rock is bounded on all sides by a boundary surface (Franke and others, 1987). For the flow-system model, this boundary surface is represented by the upper, lower, and lateral extents of the model.

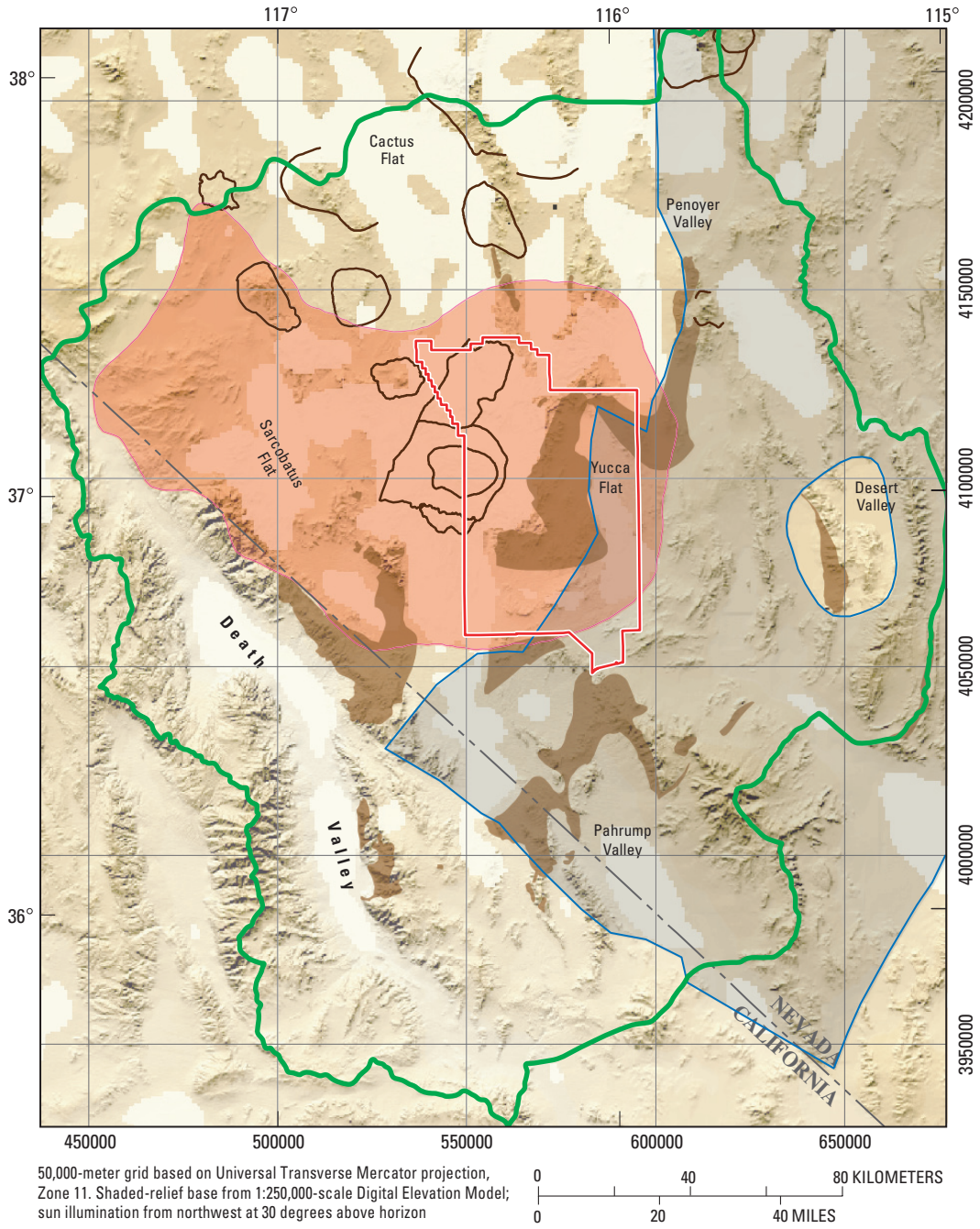
The upper boundary of the DVRFS model is the water table. Under natural (prepumping) conditions, water moves across this boundary as recharge or as discharge. When stressed (from climate change or pumping), the upper boundary may fluctuate with changes in recharge and discharge.

The lower boundary of the DVRFS model is the depth at which ground-water flow is dominantly horizontal or parallel to the boundary. Near the lower boundary, permeabilities are so low that flow near this boundary does not substantially affect regional flow. The depth of this boundary can vary and generally corresponds to the upper surface of low-permeability basement rocks.

The lateral boundary of the DVRFS model is a combination of no-flow boundaries resulting from physical barriers or hydraulic separation of flow regimes (ground-water divides and[or] regional flow lines) and arbitrary lateral-flow (throughflow) boundaries where water is allowed to flow across the model boundary. When the system is at steady state, no-flow conditions exist where ground-water movement across the boundary is impeded by physical barriers, which results in flow paths parallel to the boundary, or where ground-water flow paths diverge, which results from ground-water divides. Under transient-state conditions, the location of flow paths and ground-water divides may shift if hydraulic-head changes occur. An estimated regional potentiometric-surface map was developed for the DVRFS region to delineate areas outside the model domain that contribute inflow to or receive outflow from the DVRFS across the model boundary (Appendixes 1 and 2, this volume; plate 1).

Flow-System Subregions

Ground-water flow in the DVRFS model domain is described simply in terms of the northern, central, and southern Death Valley subregions (fig. D-5) of D'Agnes and others (1997, p. 62-67). The subregions are further subdivided into ground-water sections, with the sections in the central Death Valley region grouped into ground-water basins (table D-1). These subregions, basins, and sections are used for descriptive purposes only, and the boundaries do not define independent flow systems. The subregions, basins, and sections are delineated primarily on (1) location of recharge areas; (2) regional hydraulic gradients; (3) distribution of aquifers, structures, and confining units that affect flow; (4) location of major discharge areas; and (5) hydrochemical composition of the ground water. Flow directions across the model boundary, as indicated in figure D-5, are based on the lateral flow estimates provided in Appendix 2.



EXPLANATION

- | | |
|---|---|
| <ul style="list-style-type: none"> Cenozoic basin-fill units (lighter area) estimated to be greater than 750 meters thick (From Blakely and others, 1999) Southwestern Nevada volcanic field (SWNVF) (From Laczniaik and others, 1996) Central corridor of carbonate-rock aquifer—Area is underlain by thick sequences of carbonate rock; outside corridor, carbonate rock is thin, or present as isolated bodies (Modified from Dettinger and others, 1995, p. 38) | <ul style="list-style-type: none"> Known distribution of clastic-rock and crystalline-rock confining units at water table (Modified from Winograd and Thordarson, 1975, plate 1) Outer margin of caldera or volcanic center (From Potter and others, 2002) Death Valley regional ground-water flow system model boundary Nevada Test Site boundary |
|---|---|

Figure D-4. Generalized distribution of deep Cenozoic basins, southwestern Nevada volcanic field, regional carbonate-rock aquifer, and confining units at the water table for the Death Valley regional ground-water flow system region.

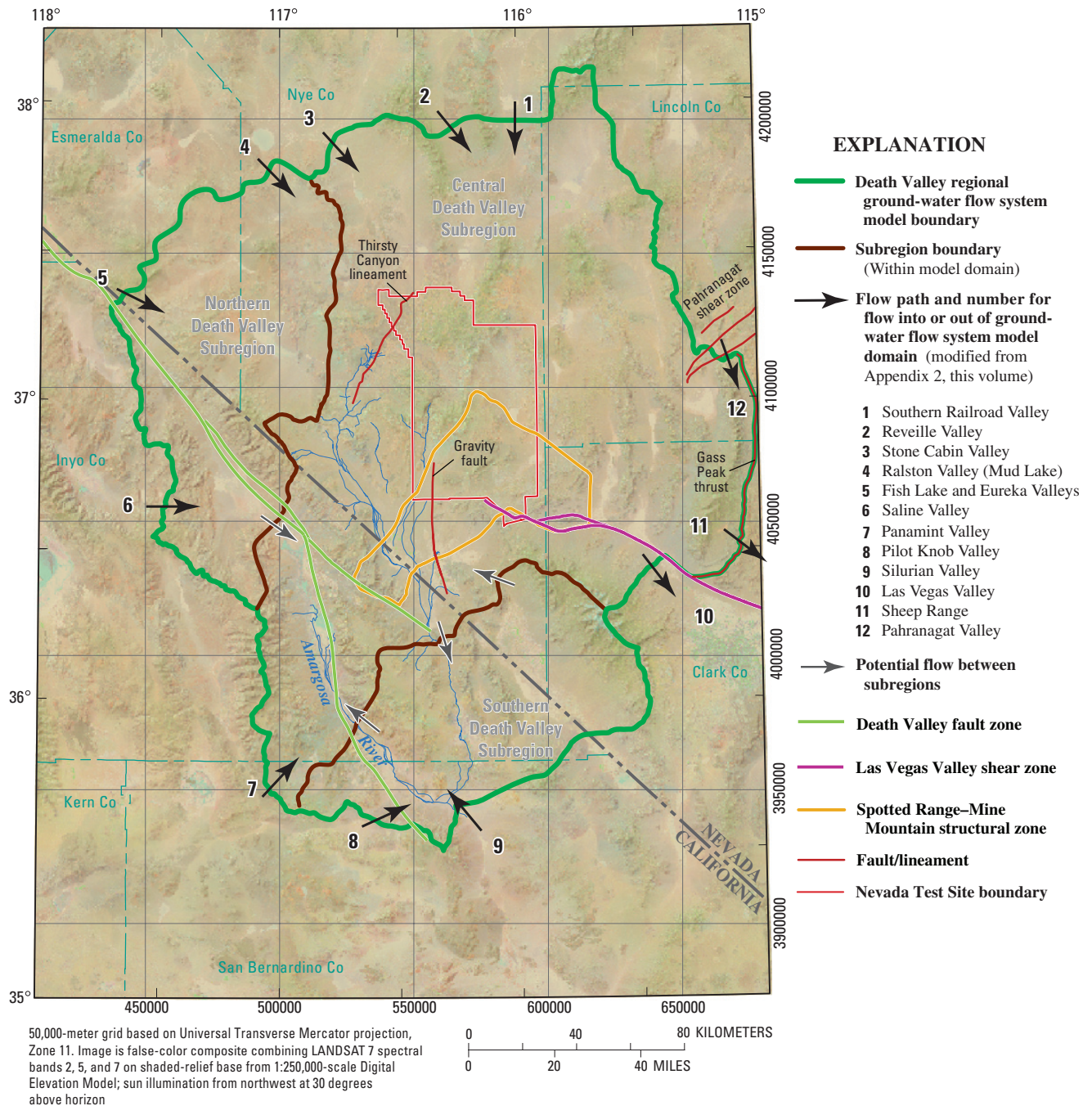


Figure D-5. Subregions and associated flow paths of the Death Valley regional ground-water flow system region.

Northern Death Valley Subregion

Ground water in the northern Death Valley subregion is derived from precipitation on the Montezuma and Panamint Ranges, Slate Ridge, and the Palmetto, Gold, and Stonewall Mountains (fig. D-6). Ground water also may be entering the subregion across the DVRFS model boundary from Eureka Valley and the southern part of Saline Valley and possibly across the northern part of the Panamint Range (Appendix 2, this volume). Much of the ground-water flow is controlled by

northeast-southwest-trending structural zones (Carr, 1984; Chapter B, this volume). Deep regional flow is unlikely because the relatively low-permeability, shallow, intrusive-rock confining unit (ICU), the lower elastic-rock confining unit (LCCU), and the crystalline-rock confining unit (XCU) underlie most of the subregion. Extensive outcrops of the lower carbonate-rock aquifer (LCA) occur in the Grapevine and Cottonwood Mountains in the southern part of the subregion. The LCA has been interpreted to exist in the subsurface

Table D-1. Divisions of the Death Valley regional ground-water flow system.

| Northern Death Valley Subregion |
|--|
| Lida-Stonewall section |
| Sarcobatus Flat section |
| Grapevine Canyon–Mesquite Flat section |
| Oriental Wash section |
| Central Death Valley Subregion |
| Pahute Mesa–Oasis Valley ground-water basin |
| Southern Railroad Valley section |
| Kawich Valley section |
| Oasis Valley section |
| Ash Meadows ground-water basin |
| Pahrangat section |
| Tikaboo Valley section |
| Indian Springs section |
| Emigrant Valley section |
| Yucca–Frenchman Flat section |
| Specter Range section |
| Alkali Flat–Furnace Creek ground-water basin |
| Fortymile Canyon section |
| Amargosa River section |
| Crater Flat section |
| Funeral Mountains section |
| Southern Death Valley Subregion |
| Pahrump Valley section |
| Shoshone–Tecopa section |
| California Valley section |
| Ibex Hills section |

in the southern part of the subregion (Grose, 1983; Sweetkind and others, 2001), including the southern part of Sarcobatus Flat and in the vicinity of Grapevine Springs in the northern part of Death Valley. Pumpage in the northern Death Valley subregion has been negligible, and the change in the volume of ground-water storage relative to the total amount in storage is negligible (Moreo and others, 2003). The subregion can be divided into four sections: Lida-Stonewall, Sarcobatus Flat, Grapevine Canyon–Mesquite Flat, and Oriental Wash.

The Lida-Stonewall section (section A, fig. D-6) potentially receives recharge by throughflow from Ralston Valley and precipitation on areas along the northern boundary of the subregion. The dominant regional flow path is to the south. Field observation and analysis of satellite imagery reveal that the playas at Stonewall Flat and near Lida Junction have very little phreatophytic vegetation, indicating that the small amounts of ET in these areas are probably from local surface water that infiltrates intermittently. Discharge from the section occurs as throughflow to Sarcobatus Flat and Death Valley.

Ground water in the Sarcobatus Flat section (section B, fig. D-6) may originate on the western part of Pahute Mesa (D’Agnese and others, 1997) and flows southwest as throughflow from the central Death Valley subregion by way of Cactus and Gold Flats. Throughflow from the Lida-Stonewall section also may contribute flow to the section. Precipitation on the Grapevine Mountains may contribute recharge in the western part of Sarcobatus Flat, but is not sufficient to maintain the discharge at Sarcobatus Flat. Other potential sources

of recharge for this area are Pahute Mesa and the Kawich Range to the east. Ground water may flow to the southeast along or parallel to buried structures (Grauch and others, 1999) discharging by ET at areas on or adjacent to the playas of Coyote Hole or Sarcobatus Flat. Recent studies indicate that discharge at Sarcobatus Flat is much greater than previously thought (Lacznik and others, 2001). As a result, throughflow from Ralston Valley and from the central Death Valley subregion may be much greater than described by D’Agnese and others (1997). In addition, uncertainty exists about the potential for ground-water flow through the Bullfrog Hills to Amargosa Desert.

Ground water in the Grapevine Canyon–Mesquite Flat section (section C, fig. D-6) originates as throughflow from the northeast past Sarcobatus Flat (D’Agnese and others, 1997). Additional ground water may enter the flow system from Saline Valley. A small amount of recharge may result from precipitation on the Grapevine Mountains. The Grapevine Canyon–Mesquite Flat section contains a major discharge area that includes Grapevine and Staininger Springs. These high-discharge springs are aligned with northeast-oriented regional structural features (Carr, 1984) and their waters have chemical characteristics indicative of an origin from rocks in the eastern part of the DVRFS region (Steinkampf and Werrell, 2001). In addition, numerous seeps and low-discharge springs in and along the flanks of the Grapevine Mountains reflect structural controls of flow on local recharge and the chemistries of these sources (Steinkampf and Werrell, 2001). Ground water that does not discharge at these springs and seeps continues past this discharge area to flow through Death Valley to discharge at Mesquite Flat or farther down the valley. Potential inflow from Saline Valley may discharge at Mesquite Flat or continue through Death Valley.

Some ground water in the Oriental Wash section (section D, fig. D-6) is from locally derived recharge on the predominantly granitic mountains to the north. In addition, ground water may enter the system as throughflow from Eureka and Saline Valleys. Ground-water flow is apparently directed toward a small-volume and low-temperature spring area at Sand Spring in the northern part of Death Valley along the axis of Oriental Wash. This spring area appears to be associated with a northeast-southwest-trending structural zone (Carr, 1984), and the discharge occurs along the northern terminus of the Death Valley fault zone. Some ground water moving along this flow path may bypass Sand Spring and flow through Death Valley toward Mesquite Flat.

Central Death Valley Subregion

In the central Death Valley subregion, the dominant flow paths have been interpreted to be associated with major regional or intermediate discharge areas and have been grouped into three ground-water basins based on the major discharge areas (fig. D-7): Pahute Mesa–Oasis Valley basin, Ash Meadows basin, and Alkali Flat–Furnace Creek basin (Waddell, 1982; D’Agnese and others, 1997, 2002).

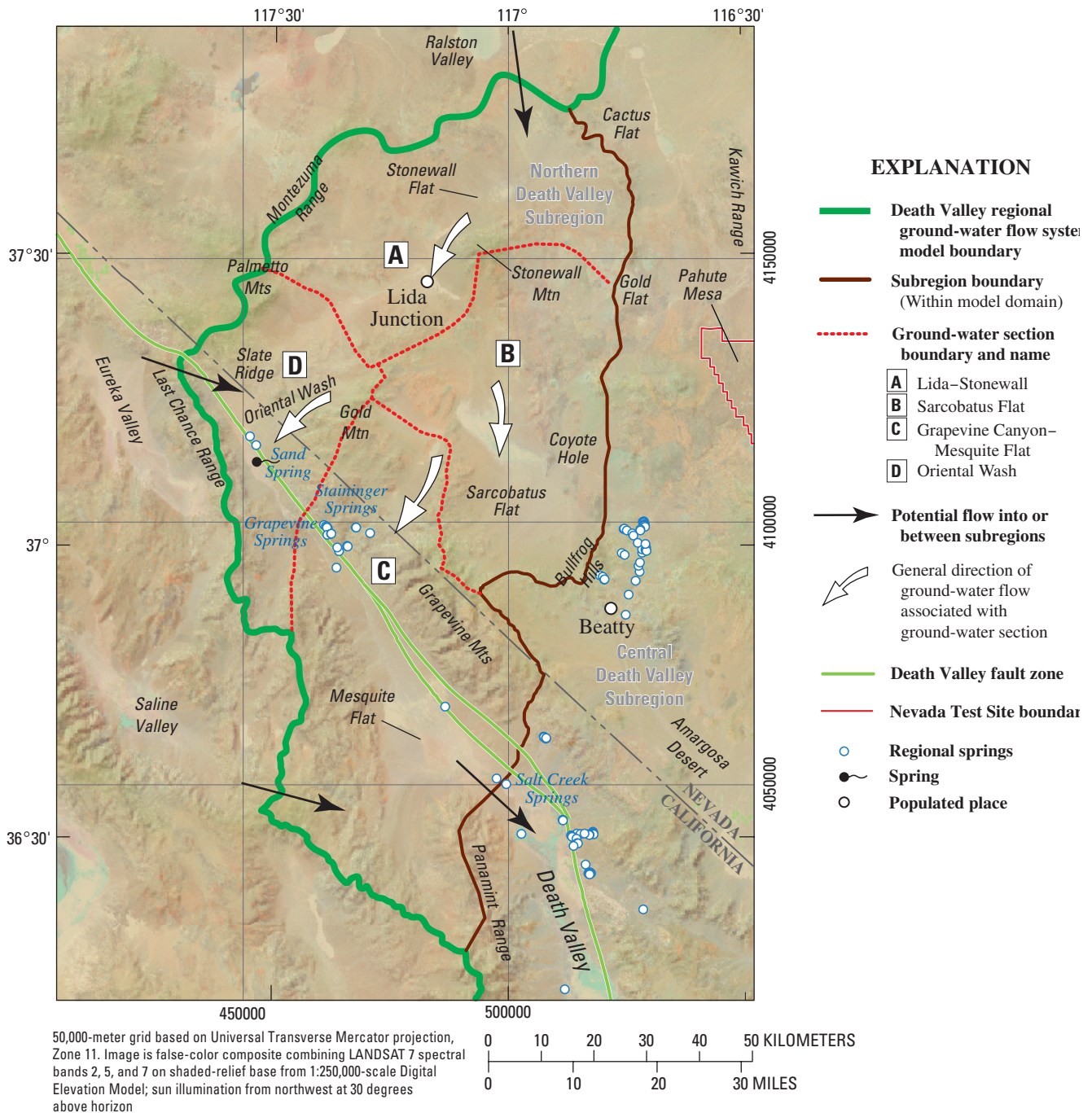


Figure D-6. Northern Death Valley subregion of the Death Valley regional ground-water flow system showing ground-water sections and flow directions.

Pahute Mesa–Oasis Valley Basin

The Pahute Mesa–Oasis Valley ground-water basin is the smallest and northernmost of the three basins and its extent is not well defined (fig. D-7). Ground water is derived primarily from recharge in Pahute Mesa and the Kawich, Cactus, and Belted Ranges (D’Agnese and others, 1997). Additional recharge from within the basin may occur at Black and Quartz Mountains. Throughflow into the Pahute

Mesa–Oasis Valley basin may occur from the southern part of Railroad, Reveille, and Stone Cabin Valleys (Appendix 2, this volume).

At Oasis Valley, ground water is diverted upward by the confining units along faults to discharge by ET and spring flow at and along the flood plain of the Amargosa River and tributary drainages (fig. D-5) (White, 1979; Laczniaik and others, 1996). Mass-balance calculations indicate that about one-half the water that flows to Oasis Valley discharges through ET

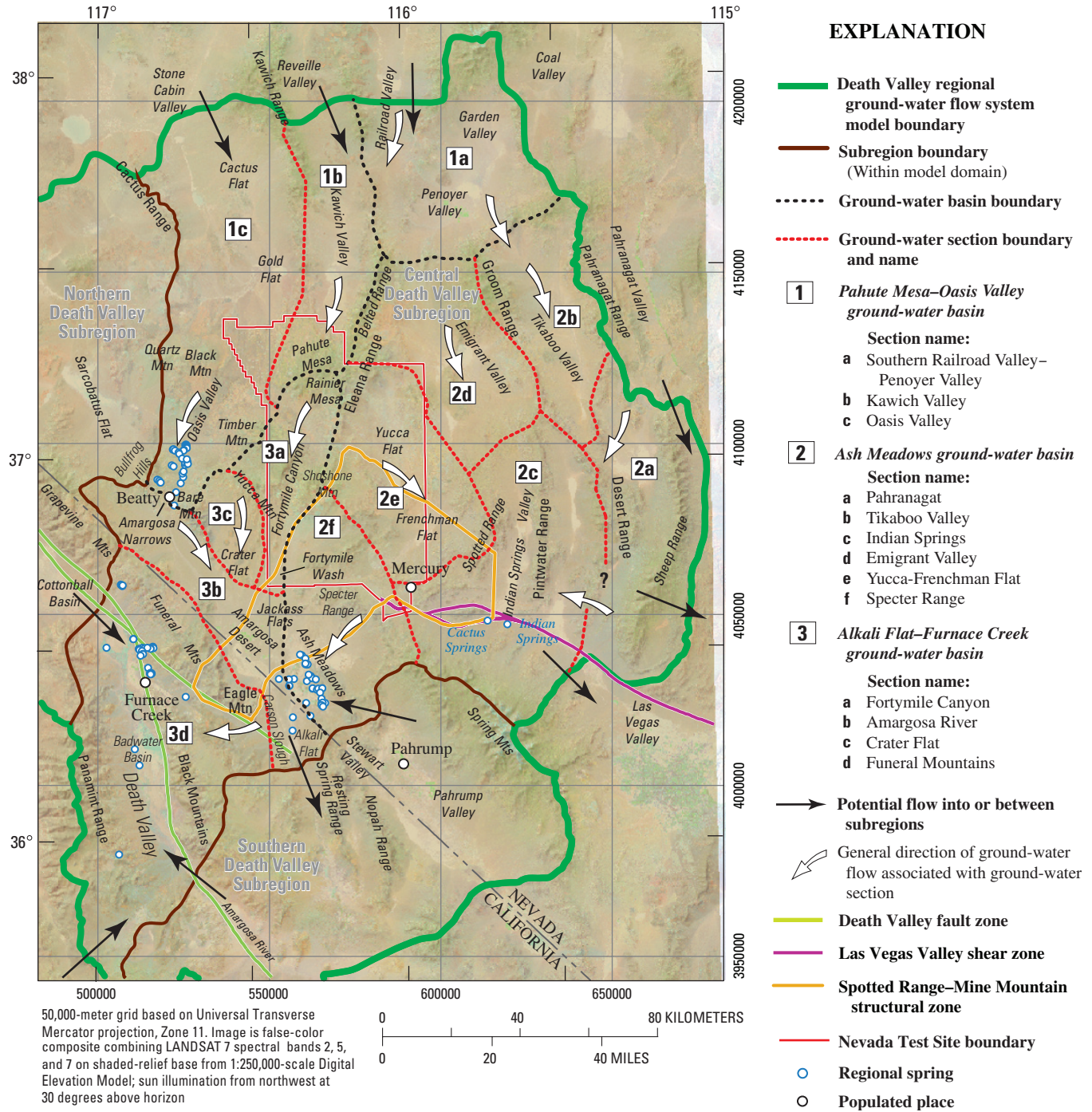


Figure D-7. Central Death Valley subregion of the Death Valley regional ground-water flow system showing ground-water basins, sections, and flow directions.

(White, 1979). Ground water that does not discharge within Oasis Valley flows through a veneer of alluvium or the low-permeability basement rocks at Amargosa Narrows south of Beatty, Nev. (fig. D-7), and into the Alkali Flat–Furnace Creek basin (Waddell, 1982; Lacznik and others, 1996).

Some ground water may not reach Oasis Valley and may flow around the northern part of Bare Mountain toward Crater Flat (fig. D-7). Likewise, some ground water in the

northwestern part of the section (parts of Cactus and Gold Flats) may flow toward the eastern part of Sarcobatus Flat. Based on general flow patterns, the Pahute Mesa–Oasis Valley basin may be divided into three sections: southern Railroad Valley–Penoyer Valley, Kawich Valley, and Oasis Valley.

Ground water in the southern Railroad Valley–Penoyer Valley section originates either as recharge on the flanking mountains or as throughflow from the north (fig. D-7)

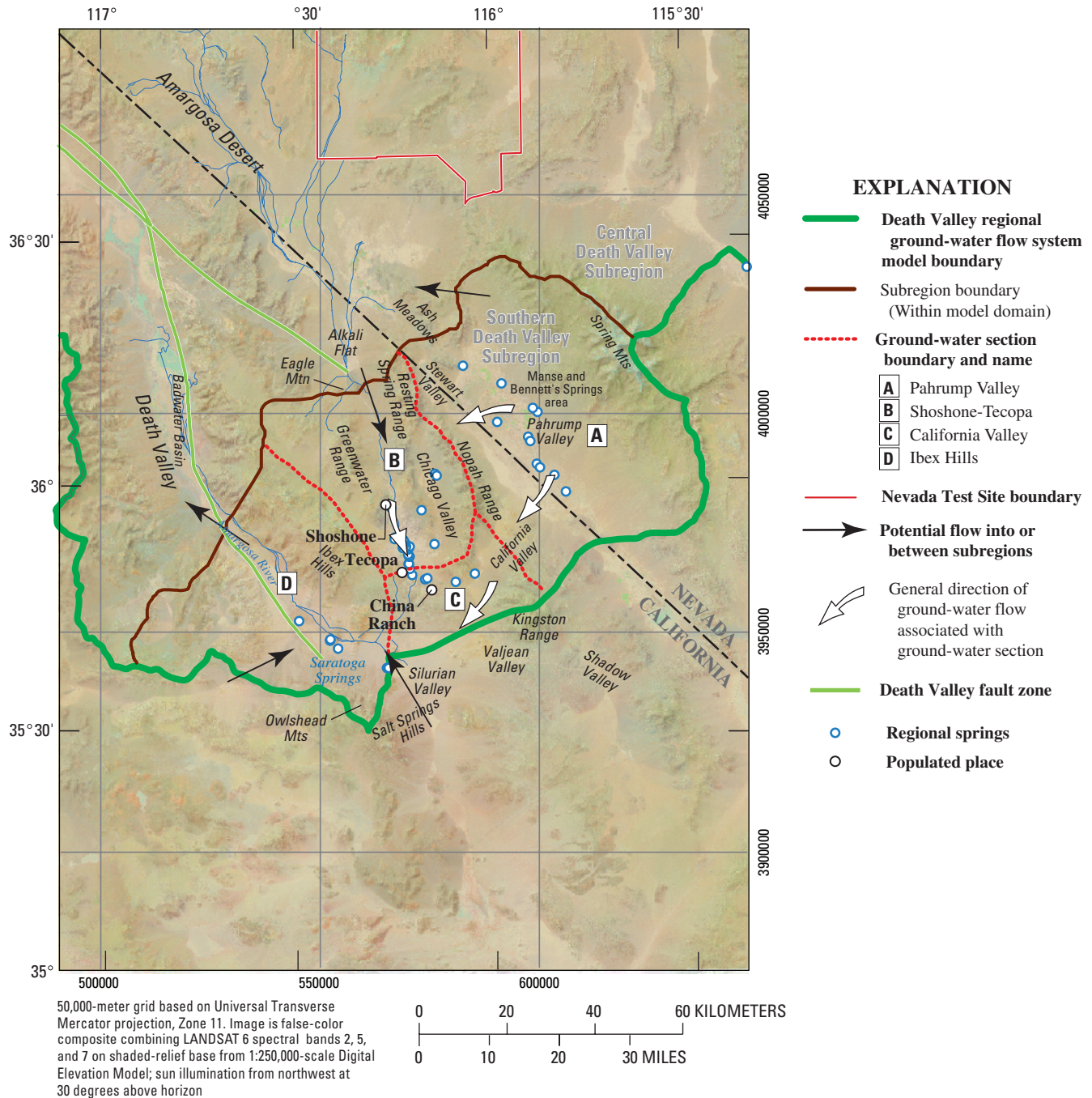


Figure D-8. Southern Death Valley subregion of the Death Valley regional ground-water flow system showing ground-water sections and flow directions.

(D’Agnese and others, 1997; Appendix 2, this volume). Ground water in the section flows dominantly south and southwest toward Kawich Valley and southeast toward Penoyer and Emigrant Valleys. The section has little internal discharge and most, if not all, of the water leaves the system as throughflow. Penoyer Valley traditionally has been characterized as part of the Colorado River ground-water flow system. Some studies indicate that it is possible that the valley is connected to the DVRFS (IT Corporation, 1996). A small discharge area occurs

at the playa in the southern part of Penoyer Valley. Water that is not discharged there may continue to flow south into Emigrant and Tikaboo Valleys.

Ground water in the Kawich Valley section originates mainly as throughflow from the southern Railroad Valley section and as recharge on the Kawich Range and Pahute and Rainier Mesas (fig. D-7). On Pahute and Rainier Mesas, water percolates down and commonly encounters low-permeability volcanic rocks, forming perched and semiperched

water that can be elevated several hundred meters above the regional water table. From the recharge areas, ground water in the Kawich Valley section flows toward a trough in the potentiometric surface beneath the western part of Pahute Mesa (figs. D-2 and D-7) (Waddell and others, 1984). The Thirsty Canyon lineament (fig. D-5) may act as a limited-flow barrier, created by caldera-boundary faults juxtaposing low-permeability rocks on the west and more permeable rocks to the east, diverting westward-moving water to the south (Blankennagel and Weir, 1973, p. 24). The hydraulic gradient across the barrier indicates some eastward flow. The barrier concept is supported by distinct differences in the major anion chemistry of ground-water samples collected on either side of the feature (Laczniak and others, 1996). This section has little internal discharge. Ground water leaving the southern margins of Pahute Mesa flows southwestward in Oasis Valley toward the Amargosa River and south through Fortymile Canyon, ultimately discharging at Oasis Valley, Alkali Flat, and(or) Death Valley.

The Oasis Valley section contains the major discharge area for the basin. The section receives subsurface inflow from the Kawich Valley section, by way of Pahute Mesa, and Gold Flat to the north is the largest source of ground water to the Oasis Valley section (fig. D-7) (Laczniak and others, 1996; White, 1979). The location and nature of the boundary separating the Oasis Valley section from the Alkali Flat-Furnace Creek basin is not well understood, and it is uncertain how much of the water discharging at Oasis Valley actually passes through rocks beneath Pahute Mesa (Laczniak and others, 1996).

Water is withdrawn for irrigation, domestic, and public supply in upper Oasis Valley. Pumping occurred periodically since the 1950's on the Pahute Mesa-Oasis Valley basin part of the Nevada Test Site for water supplies and long- and short-term aquifer tests to help characterize the flow system. Most of this development has been small in scale and likely has had little long-term effect on the system. Similarly, the relatively small amount of pumpage in the area of Penoyer Valley for irrigation likely has had little long-term effect (Moreo and others, 2003).

Ash Meadows Basin

The Ash Meadows basin is the largest basin in the central Death Valley subregion (fig. D-7) (Waddell, 1982). Much of the ground water in this basin is derived from recharge on the Spring Mountains and the Sheep, Pahranaagat, and Belted Ranges. Recharge also may occur within the basin on the Spotted, Pintwater, and Desert Ranges (Laczniak and others, 1996). The Ash Meadows basin is subdivided into six sections: Pahranaagat, Tikaboo Valley, Indian Springs, Emigrant Valley, Yucca-Frenchman Flat, and Specter Range.

The Ash Meadows discharge area (fig. D-7) represents the terminus of the Ash Meadows basin. Water entering Ash Meadows encounters a northwest-southeast trending fault that juxtaposes fine-grained basin-fill sediments and the more

permeable carbonate-rock aquifer (Dudley and Larson, 1976, p. 9-10). The discharge at Ash Meadows occurs at approximately 30 springs along a 16-kilometer (km) long spring line that generally coincides with the trace of the buried fault. All the major springs emerge from circular pools, are relatively warm, and discharged at nearly constant rates from 1953 until agricultural development began in the area in 1969 (Dettinger and others, 1995, p. 79). Most of the spring discharge at Ash Meadows may infiltrate and recharge the basin-fill aquifers, much of this discharging as ET from the alluvium along the Amargosa River, Carson Slough, and Alkali Flat (Czarnecki and Waddell, 1984; Czarnecki, 1997).

Ground water is pumped from wells scattered throughout the Ash Meadows basin. Wells near Ash Meadows tap the basin-fill aquifers adjacent to the carbonate-rock aquifer. Wells on the NTS within the basin are used to supply about 50 percent of the water demand at the NTS (Laczniak and others, 1996). Pumping from basin-fill aquifers around Devils Hole, a collapse feature in the carbonate rock supporting an endemic species of desert pupfish (*Cyprinodon diabolis*) (see fig. A-1), caused water-level declines observed in Devils Hole and the decrease or temporary cessation of flow from several major springs issuing from the carbonate aquifer. After pumping ceased, water levels and spring flow gradually recovered. The effect of pumping on individual springs differed, indicating that a variable degree of hydraulic connection exists between the basin-fill and carbonate-rock aquifers (Dettinger and others, 1995, p. 80).

Previous conceptual models of the Ash Meadows basin indicate significant amounts of flow from Pahranaagat Valley to Ash Meadows. Evaluations of hydrochemical data, however, indicate that the volume of this inflow could be negligible (J.M. Thomas and William Sicke, Desert Research Institute, Reno, Nev., written commun., 2003). Analysis of calcite veins precipitated at Devils Hole (Winograd and others, 1992) also indicates that most, if not all, of the ground water in Ash Meadows originates from the Spring Mountains.

Ground water that bypasses the springs at Ash Meadows may continue as throughflow to Furnace Creek (fig. D-7) or may recharge the basin-fill sediments and join other ground water in the basin-fill sediments to flow southward toward Alkali Flat, where it either discharges or continues south to the southern Death Valley subregion. Three springs at the southern end of the Ash Meadows spring line (Big, Bole, and Last Chance) have elevated strontium values, which may indicate that they receive some flow from a different origin, such as the Pahrump Valley (Peterman and Stuckless, 1992a, p. 70; Peterman and Stuckless, 1992b, p. 712). High-resolution aeromagnetic surveys conducted over the Amargosa Desert and Pahrump indicate a possible hydraulic connection between Pahrump Valley and the Amargosa Desert through Stewart Valley (Blakely and Ponce, 2001).

Ground water recharged on the mountain areas of the Ash Meadows basin flows toward the Spotted Range-Mine Mountain structural zone (fig. D-7). It is generally accepted that ground water in Tikaboo and Emigrant Valleys

and Yucca and Frenchman Flats flows toward a trough in the potentiometric surface beneath Frenchman Flat and the Specter and Spotted Ranges (figs. D-2 and D-7) (Winograd and Thordarson, 1975; Faunt, 1997; D'Agnese and others, 1997). This trough may be a zone of relatively high permeability in the carbonate-rock aquifer associated with the Spotted Range-Mine Mountain structural zone (Carr, 1984; Faunt, 1997; D'Agnese and others, 1998). The Las Vegas Valley shear zone (LVVSZ) bounds the trough on the south and southeast. The flow paths along the trough are directed through the Specter Range area until they encounter the fault at Ash Meadows.

The basin-fill and volcanic-rock aquifers in Emigrant Valley and Yucca and Frenchman Flats (fig. D-7) provide recharge (fig. D-2) to the regional carbonate-rock aquifer by downward percolation (Winograd and Thordarson, 1975; Laczniaik and others, 1996). The water chemistry at Indian Springs Valley indicates that these waters have had little opportunity for contact with volcanic rock or basin-fill sediments composed of volcanic rocks indicating that the ground water beneath Tikaboo and Emigrant Valleys and Yucca and Frenchman Flats is not moving southward toward Indian Springs Valley. The water in the carbonate-rock aquifer in these locations may be moving toward the Amargosa Desert, where the ground water is generally of mixed chemical character and has high levels of sodium (Schoff and Moore, 1964; Winograd and Thordarson, 1975). Ultimately most of the ground water discharges at Ash Meadows.

In the Pahrnatag section, near the Sheep Range, the DVRFS boundary is uncertain and has been postulated in various locations (Harrill and others, 1988; Bedinger and others, 1989; Harrill and Prudic, 1998; D'Agnese and others, 1997, 2002; Appendix 2, this volume). For this study, the DVRFS model boundary was placed along the Gass Peak thrust (fig. D-5; Appendix 2, this volume), the easternmost feature postulated as a boundary. This places the boundary between the Colorado River ground-water flow system and the DVRFS model domain farther east than in most previous studies. Consequently, the deeper carbonate rocks may allow substantial amounts of water to flow to the Colorado River ground-water flow system to the east. If this occurs, then a ground-water divide should exist somewhere near the Desert Range, and flow into the Ash Meadows basin must occur through or north of the northern part of the Sheep Range (fig. D-7; Appendix 2, this volume). Regional-potential data (Appendix 1, this volume) also indicate that the flow-system boundary should be along a divide in the approximate location of the Desert Range (fig. D-7). If this divide exists, a significant amount of discharge from the Pahrnatag section to the east into the Colorado River ground-water system occurs through the carbonate-rock aquifer in the Sheep Range. West of this divide, discharge occurs as throughflow into Indian Springs Valley.

Recharge to the Pahrnatag section occurs partly as throughflow from Tikaboo Valley and in the Sheep Range (fig. D-7). Recharge also may occur at the higher mountains of the Spotted, Pintwater, and Desert Ranges (Laczniaik and

others, 1996). As previously mentioned, hydrochemical data indicate that little or no flow comes into the DVRFS model domain from the Pahrnatag Range. Flow that does come into this section is thought to exit through short pathways to the southeast through the Sheep Range (Appendix 2, this volume).

Recharge to the Tikaboo Valley section occurs in the Pahrnatag Range (fig. D-7). Although the eastern boundary of the Tikaboo Valley section is aligned along the Pahrnatag Range parallel with the boundary of the Colorado River flow system, throughflow may occur along the flow-system boundary at the Pahrnatag Range, especially in the south along the Pahrnatag shear zone (Winograd and Thordarson, 1975) (fig. D-5). Little is known about water levels or flow directions in the basin-fill sediments. The water in the carbonate-rock aquifer in Tikaboo Valley is thought to be moving toward the Amargosa Desert (Workman and others, 2002). On the basis of recent interpretations of regional hydraulic gradients (Appendix 2, this volume), however, some, if not all, flow occurs out of the eastern boundary into the Colorado River flow system.

Regional ground water recharged on the Sheep Range and Spring Mountains flows into the Indian Springs section (fig. D-7) from the south and east and into the potentiometric trough (fig. D-2). Recharge also may occur on higher mountains of the Spotted, Pintwater, and Desert Ranges (Laczniaik and others, 1996), most of which are underlain by carbonate rocks. Most of the water has had little opportunity for contact with volcanic rock or basin-fill sediments composed of volcanic rocks. As a result, hydrochemical data can be useful in delineating flow paths to and from this region.

Potentiometric data for both the basin-fill and carbonate-rock aquifers in the southern part of Indian Springs Valley indicate a prominent east-trending hydraulic barrier between the Nye County line and Indian Springs (fig. D-2) (Winograd and Thordarson, 1968), corresponding to the LVVSZ (fig. D-7). Because no clastic-rock confining units are known within the upper part of the saturated zone in this area, this flow barrier may be created by the LVVSZ (Winograd and Thordarson, 1975), causing discharge at Indian and Cactus Springs. In addition to Indian and Cactus Springs, discharge from the Indian Springs section occurs as throughflow to the Specter Range. Ground-water flow in the section converges in the carbonate-rock aquifer along the trough in the potentiometric surface (fig. D-2) and travels toward the Amargosa Desert, ultimately discharging at Ash Meadows.

Another flow barrier formed by the juxtaposition of the LCCU and the LCA (Winograd and Thordarson, 1968) is postulated approximately 8 km to the north of the LVVSZ. Potentiometric data in the area indicate that flow may be to the north in the basin-fill sediments and to the west between the two flow barriers in the carbonate-rock aquifer north of the barriers.

Recharge to the Emigrant Valley section occurs as throughflow from the north or precipitation to the Belted and Groom Ranges (fig. D-7). Flow is generally to the south in the basin-fill sediments to Yucca Flat but is disrupted at depth by low-permeability clastic-rock units. Basin-fill aquifers

in Emigrant Valley provide recharge to the carbonate-rock aquifer by percolation downward through basin-fill sediments. The western one-half of Emigrant Valley is bordered on the east, south, and southwest by clastic rocks. Geologic mapping indicates that this area of the valley is part of a highly faulted anticline, which, prior to extensional faulting, brought clastic rocks to the surface over a wide region (Winograd and Thordarson, 1968). Gravity surveys indicate that the bedrock beneath western Emigrant Valley is overlain by as much as 1,200 m of basin-fill sediments (Winograd and Thordarson, 1968).

The steep hydraulic gradients on both sides of Emigrant Valley (fig. D-2) are believed to reflect the movement of water through thick clastic-rock confining units (fig. D-4) toward points of lower hydraulic head in Yucca Flat and in the eastern part of Emigrant Valley (Winograd and Thordarson, 1968). The relatively flat hydraulic gradient in Emigrant Valley reflects the large permeability of the basin-fill aquifers. Both the steep and the flat hydraulic gradients probably are caused by a thick sequence of clastic-rock confining units separating the western part of Emigrant Valley from areas of lower ground-water potential to the east and west. The steep hydraulic gradients may be continuous or may represent discontinuous levels within blocks separated by low-permeability faults. Ground-water flow in the carbonate-rock aquifer in Emigrant Valley appears to be moving toward the trough in the potentiometric surface (fig. D-2).

Recharge to the Yucca–Frenchman Flat section is predominantly throughflow from Emigrant Valley to the north and northeast and possibly precipitation on Rainier Mesa and the adjacent Eleana and Belted Ranges (fig. D-7). Water-level contours (fig. D-2) show a southeastern flow component away from Rainier Mesa toward Yucca Flat. The carbonate-rock aquifer beneath the central and northern parts of Yucca Flat is isolated from the carbonate-rock aquifer in adjacent valleys to the north and east by the bordering clastic-rock confining units. Ground water moving between the basins into the carbonate-rock aquifer would have to pass through and would be controlled by the transmissivities of the clastic-rock confining units (Winograd and Thordarson, 1968, p. 43). Discharge from Yucca and Frenchman Flats occurs primarily as throughflow in the carbonate-rock aquifer toward a trough in the potentiometric surface (fig. D-2) near the Spotted Range–Mine Mountain structural zone (fig. D-7), continuing to the southwest toward the Amargosa Desert.

Recharge to the Specter Range section is mostly from throughflow in the carbonate-rock aquifer along the trough in the potentiometric surface (fig. D-2). The distribution of precipitation and the resulting infiltration indicates that ground water moves long distances through different HGUs before reaching Ash Meadows. Ground water flows through the Specter Range section along the trough in the potentiometric surface and ultimately discharges at Ash Meadows.

Alkali Flat–Furnace Creek Basin

The Alkali Flat–Furnace Creek basin lies south and west of the Ash Meadows and Pahute Mesa–Oasis Valley basins and covers a large part of the western one-half of the NTS (fig. D-7). Ground water in this basin is derived from recharge on Pahute Mesa, Timber and Shoshone Mountains, and the Grapevine and Funeral Mountains. Additional recharge to this basin may occur as throughflow from Sarcobatus Flat, Oasis Valley, and Ash Meadows. Recharged ground water from throughflow and local recharge moves through volcanic-rock aquifers in the north and basin-fill and carbonate-rock aquifers in the south toward discharge areas in the southern and southwestern parts of the basin. Subsurface outflow follows the general course of the Amargosa River drainage through a veneer of alluvium near Eagle Mountain into the southern Death Valley subregion (Walker and Eakin, 1963). As with the other basins, the location of the boundary of the Alkali Flat–Furnace Creek basin is neither well established nor fully understood. The Alkali Flat–Furnace Creek basin is divided into four sections: the Fortymile Canyon, Amargosa River, Crater Flat, and Funeral Mountains sections.

The Alkali Flat–Furnace Creek basin supplies water to rural communities in the Amargosa Desert and to private recreational establishments and Federal facilities within Death Valley National Park, Calif. (Lacznik and others, 1996; see fig. A-1)). Domestic and smaller scale irrigation withdrawal started in the 1970's and continues to the present in the western Amargosa Desert. The withdrawal has caused local water-level declines. Withdrawal connected with mining operations south of Beatty has caused lower water levels in the northwestern arm of the Amargosa Desert (Moreo and others, 2003).

The main discharge area in the basin is the springs in the Furnace Creek area (fig. D-7) including Texas, Travertine, and Nevares springs (see fig. C-2). Hydrochemical data indicate that spring flow in the major springs at the Furnace Creek area likely derives from the carbonate-rock aquifer (Winograd and Thordarson, 1975, p. C95). Similar hydrochemistry between spring waters at Ash Meadows and the Furnace Creek area (Czarnecki and Wilson, 1991; Steinkampf and Werrell, 2001) indicate a hydraulic connection between these two discharge areas through the regional carbonate-rock aquifer by way of large-scale fractures or channels in the carbonate-rock aquifer (Winograd and Pearson, 1976).

Downgradient from the Furnace Creek springs, the remaining ground water and reinfiltreated spring flow moves toward the Death Valley saltpan and is transpired either by stands of mesquite on the lower part of the Furnace Creek fan or is evaporated from the saltpan in Badwater Basin (fig. D-7). The Death Valley saltpan is the largest playa in the region (fig. D-3), and despite the low rate of ET from the saltpan proper, the great area of this feature results in a significant amount of discharge (DeMeo and others, 2003). In addition, the saltpan is surrounded by alluvial fans and numerous springs fringed with vegetation. Ground water is shallow near

the distal end of most of the fans sloping from the mountains ringing Death Valley and in the areas between them. Marshes, phreatophytes, and small springs that occur at the base of the fans discharge local recharge from the surrounding mountains and throughflow from adjacent basins.

Recharge to the Fortymile Canyon and Fortymile Wash section is primarily from throughflow from the volcanic rocks of the eastern part of Pahute Mesa and the western part of Rainier Mesa (fig. D-7). Infiltration of surface runoff in the alluvium of the upper reaches of Fortymile Canyon and Fortymile Wash during periods of moderate to intense precipitation may be another source of locally important recharge (Czarnecki and Waddell, 1984; Laczniaik and others, 1996; Savard, 1998; Hevesi and others, 2003). Hydraulic gradients based on sparse water-level data indicate that the principal flow direction in the section is southward from the eastern part of Pahute Mesa and western part of Rainier Mesa. Data from the northern part of this section are insufficient to assess whether flow continues south beneath Timber Mountain or is diverted around it toward Shoshone Mountain, Yucca Mountain, and Jackass Flats. The southern part of the Fortymile Canyon and Wash section includes Yucca Mountain. At and near Yucca Mountain, hydraulic gradients are dominantly upward in the volcanic-rock units from the carbonate-rock aquifer (Luckey and others, 1996). From Fortymile Wash, flow continues southward as throughflow into the Amargosa River section (Laczniaik and others, 1996).

Recharge to the Amargosa River section is predominantly by throughflow in the basin-fill sediments from the Oasis Valley, Crater Flat, Fortymile Canyon and Wash, and Specter Range sections (fig. D-7). Recharge to the carbonate-rock aquifer also occurs by throughflow from the Specter Range and Fortymile Canyon and Wash sections. In the northwestern part of the Amargosa River section, intermediate ground-water movement is dominantly lateral and downward toward regional flow paths (Czarnecki and Waddell, 1984; Sinton, 1987; Kilroy, 1991). In the south-central parts of the basin, near the Nevada-California border, regional ground-water movement is mostly upward from the carbonate-rock aquifer into the intermediate system and toward discharge areas along the Amargosa River, Carson Slough, and Alkali Flat (Czarnecki and Waddell, 1984; Czarnecki, 1997). Hydrochemical data suggest that water in the carbonate-rock aquifer to the north and northeast and in volcanic-rock aquifers to the north and northwest flows toward the Amargosa Desert, where ground water generally is of mixed chemical character and has a large amount of sodium (Schoff and Moore, 1964).

Hydraulic and hydrochemical data indicate that water in the regional flow system in the southern part of Amargosa Desert (fig. D-7) either may flow southwest toward Death Valley through fractures in the southeastern end of the Funeral Mountains or flow southward and toward the surface at Alkali Flat (or Franklin Lake playa), deflected by the low-permeability quartzites of the Resting Spring Range (fig. D-7) (Czarnecki and Waddell, 1984; Czarnecki and Wilson, 1991). The carbon-

ate rocks beneath the Funeral Mountains also might provide preferential conduits or drains for flow from the basin-fill sediments beneath the Amargosa Desert toward Death Valley (Czarnecki and Waddell, 1984; Luckey and others, 1996, p. 14).

Recharge to the Funeral Mountains section is thought to be predominantly from throughflow in the carbonate-rock aquifer in the southern part of the Funeral Mountains (fig. D-7). Additional ground water enters Death Valley as throughflow from Panamint Valley and the Owlshhead Mountains in the southern Death Valley subregion. Local precipitation in the Panamint Range and in the Black and Funeral Mountains, and to a lesser extent in the Greenwater Range, supports mountain-front recharge as surface water seeps into the ground when it reaches alluvial fans ringing the floor of Death Valley. In addition, a small amount of throughflow originating in the northern and southern Death Valley subregions may occur in the relatively fine-grained basin-fill sediments in Death Valley. The Funeral Mountains section contains the major discharge area at the Furnace Creek area for the Alkali Flat-Furnace Creek basin.

Southern Death Valley Subregion

Ground water in the southern Death Valley subregion primarily is derived from recharge at the Spring Mountains and to a lesser extent from recharge at the Nopah, Kingston, and Greenwater Ranges (fig. D-8). Ground water also may be entering the system as throughflow in the basin-fill sediments of the Silurian Valley and valleys adjacent to the Owlshhead Mountains (Appendix 2, this volume). Additional minor ground-water inflow may occur across the boundary from the Alkali Flat-Furnace Creek basin south of Alkali Flat (fig. D-8). The largest discharge area in the subregion is in Pahrump Valley, which contains a broad playa with several springs. The subregion contains four sections: Pahrump Valley, Shoshone-Tecopa, California Valley, and Ibox Hills, each with a significant discharge area. The Valjean section of D'Agnese and others (1997) is thought to have very little flow into the DVRFS model domain and is not used in this study (Appendix 2, this volume). The interconnection between the four sections is much more apparent than sections in the northern and central subregions.

Before extensive development, the playa area in Pahrump Valley contained some phreatophytic vegetation and was surrounded by sparse shrubland vegetation rising into alluvial fans. Ground-water withdrawals accompanying large-scale agricultural development in the Pahrump Valley section has caused cessation of flow of some major springs in the area during withdrawal, with the gradual recovery of spring flow after some withdrawal stopped. Historically, Manse and Bennetts Springs discharged along the base of the broad alluvial fans at the foot of the Spring Mountains. Ground-water withdrawal in the valley caused these springs to cease flowing in the 1970's. In the late 1990's, Manse Spring began to flow again, perhaps due to changes in the amount of agriculture and

agricultural practices in the valley. Withdrawal in the valley does continue for domestic uses and small-scale agriculture uses (Moreo and others, 2003).

Ground water in the Pahrump Valley section that does not discharge at Pahrump Valley flows either west toward Stewart Valley and the northern end of Chicago Valley, or southwest toward California Valley (fig. D-8). Direct ground-water flow to Death Valley from Pahrump Valley is unlikely because of low-permeability quartzites of the Resting Spring Range (Winograd and Thordarson, 1975; Grose, 1983, Sweetkind and others, 2001) that may bifurcate ground-water flow. Some of the ground water flowing toward the south and west is consumed by ET from playas in Stewart and Chicago Valleys.

In the Shoshone-Tecopa section, recharge predominantly is throughflow from adjacent sections with some contribution from local recharge in the Nopah Range (fig. D-8). Ground-water throughflow from Pahrump Valley mixes with ground water flowing south from Alkali Flat. Discharge occurs from ET and springs along the flood plain of the Amargosa River between the towns of Shoshone and Tecopa, Calif. Discharge in the Shoshone-Tecopa section may be from (1) basalt flows to the west damming shallow ground water, (2) normal faults beneath the Amargosa River south of Eagle Mountain forcing ground-water upward (Steinkampf and Werrell, 2001, p. 20), and(or) (3) a shallow (less than 10 km deep) intrusive body influencing the flow of ground water (Steinkampf and Werrell, 2001, p. 20). Ground water that does not discharge in the Shoshone-Tecopa area may continue flowing to the southwest into the Ibex Hills section through faulted and fractured crystalline rocks. Ground water continues flowing south in the alluvium along the Amargosa River channel into the California Valley section.

In addition to this throughflow from Pahrump Valley, recharge to the California Valley section is from precipitation on the Kingston Range and ground water that flows south from the Shoshone-Tecopa section (fig. D-8). South of Tecopa, Calif., a structural uplift brings ground water to the surface and feeds a perennial reach of the Amargosa River. Ground water leaves the California Valley section as surface-water flow or throughflow in the alluvium along the Amargosa River.

In addition to throughflow from the Shoshone-Tecopa section, flow into the Ibex Hills section also occurs along the Amargosa River channel as surface water or ground water in the associated alluvium (fig. D-8). Some additional ground water may enter the section as throughflow from Valjean, Shadow, and Silurian Valleys (which drain an extensive area south of the Kingston Range) and adjacent to the Owlshead Mountains. Discharge occurs primarily as ET and spring flow in the Saratoga Springs area. This area is supported by ground-water discharge from the regional carbonate-rock aquifer and includes adjacent areas of shallow ground water along the flood plain of the Amargosa River. A small amount of ground-water flow may continue north past Saratoga Springs to the central Death Valley subregion and discharge at Badwater Basin.

Surface-Water Hydrology

In the DVRFS region, perennial streamflow is sparse. Most surface water in the region is either runoff or spring flow discharge. Precipitation falling on the slopes of the mountains (such as the Panamint Range or the Black and Funeral Mountains), forms small, intermittent streams that quickly disappear and infiltrate as ground-water recharge. In addition, several streams originate from snowmelt in the high altitudes of the Spring and Magruder Mountains. Both of these types of streams have highly variable base flows and in dry years have almost imperceptible discharges. Springs maintain perennial flow for short distances in some of the drainages.

Surface-water flows in the DVRFS region have been categorized on the basis of hydrologic units (fig. D-9) that are the basic units used by State and local agencies for water-resources planning (Seaber, 1987). Hydrologic units are delineated primarily on the basis of topography and geologic structures and generally correspond to major surface drainages.

Drainage Areas

The Death Valley watershed contains two primary drainage basins—the Amargosa River basin in the south and the Salt Creek basin in the north. The Amargosa River Basin drainage area composes approximately two-thirds of the 22,100-km² Death Valley watershed and has the largest drainage basin discharging into Death Valley (Grasso, 1996). The Amargosa River is the only large perennial stream in the DVRFS region, originating in the mountains of southwestern Nevada and flowing south and west, terminating in the sinks and playas of Death Valley (fig. D-9). Despite the large drainage area, most of the Amargosa River and its tributaries are ephemeral.

Salt Creek drains the northwest part of Death Valley, an area of about 5,700 km² (fig. D-9). Although Salt Creek drains only one-third as much area as does the Amargosa River, it discharges more surface water to the Death Valley saltpan than does the Amargosa River (Hunt, 1975). Ground water discharging as seeps and spring flow from Mesquite Flat feeds Salt Creek (Hunt, 1975). Though Mesquite Flat is without perennial surface water, an extensive growth of phreatophytes is supported by shallow ground water.

Springs

There are four principal kinds of springs in the DVRFS model domain: those discharging along (1) high-angle faults, (2) low-angle faults, (3) low-permeability structural barriers, and (4) lithologic gradations into less-permeable material (Hunt and others, 1966). The largest and most significant springs for this study are those discharging along the high-angle faults, for example, Travertine, Texas, and Nevares

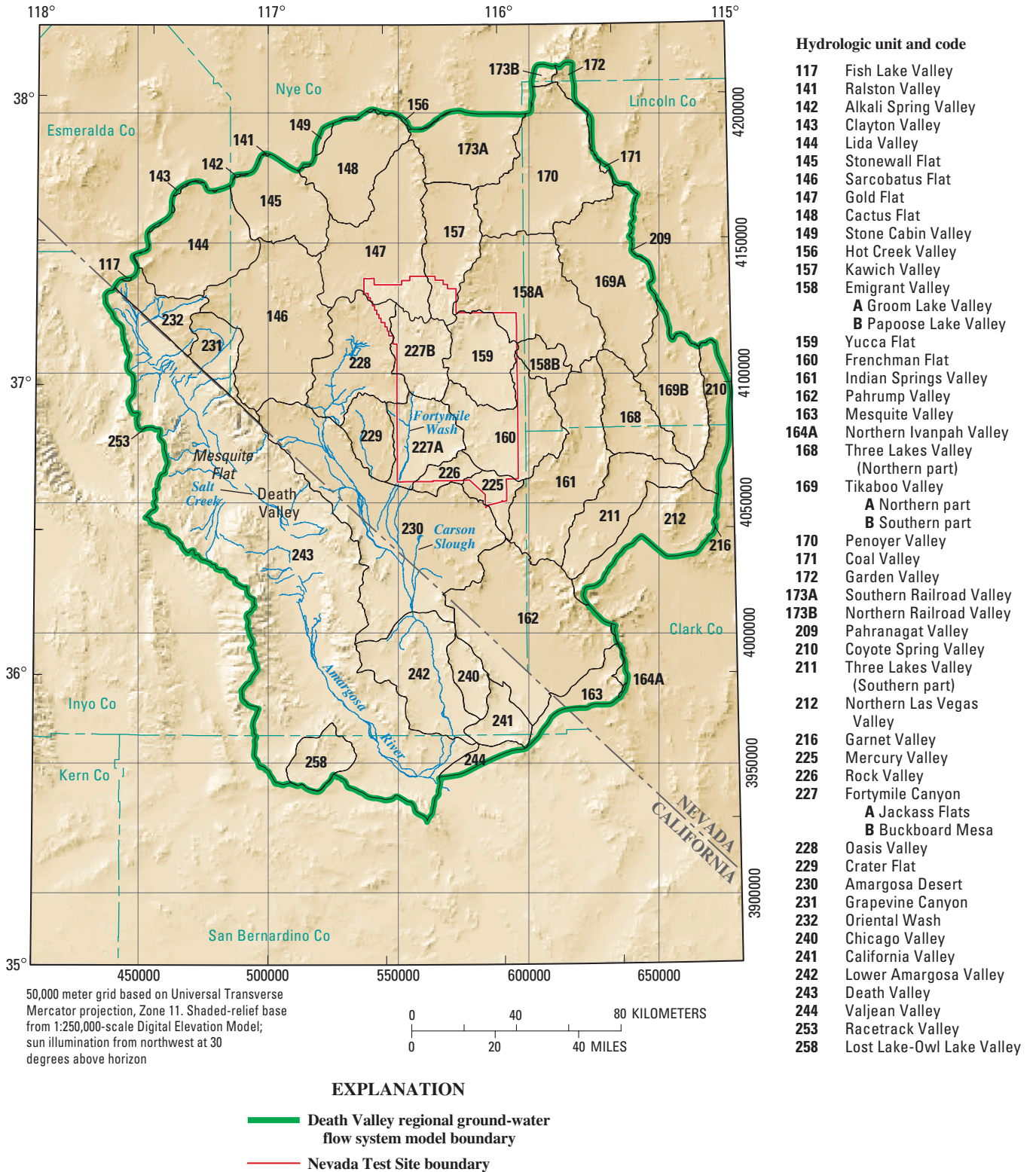


Figure D-9. Hydrologic units for the Death Valley regional ground-water flow system.

Springs along the Furnace Creek fault zone (Hunt and others, 1966), and the springs at Ash Meadows (fig. D-10) (Laczniak and others, 1999). In the mountains, springs discharge at low-angle faults no more than a few gallons per minute (Hunt, 1975). Most of the springs in the Panamint Range are of this type. The third type of spring occurs where ground water is ponded behind a low-permeability structural barrier, such as the spring area at Mesquite Flat. The fourth type of spring is found at the edge of the Death Valley floor where ground water is ponded in the gravel and sand of the fans as they grade into silt under the valley floor. Larger volume and higher temperature springs that occur along major faults are generally considered to be regional springs.

Paleohydrology

Ground-water flow systems respond to and change with climate. The modern ground-water flow system may not be in equilibrium with the modern climate and most likely contains relics of past climates. Forester and others (1999) indicate that during the last glacial cycle [peaking 12,000 years ago (12 ka)], moisture fluxes were greater than current fluxes, and water tables were higher throughout the region (Quade and others, 1995). There is strong evidence that, during Quaternary time, there has been a steady decline in the regional potentiometric surface (Winograd and Szabo, 1988). Stands of mesquite in Death Valley, which are dependent on ground water of fairly good quality, have been dying and are not being replaced, which may indicate that the water supply is continuing to diminish. Whether this decline is because of a decrease in the supply of water or an increase in salinity, or both, is uncertain (Hunt, 1975).

Fossil, isotopic, and petrographic data provide evidence of past changes in precipitation, temperature, and evaporation, which are the manifestations of large-scale climate changes. In this study, climate change is of interest because of the effect of past climates on water levels. For example, plant macrofossils in the DVRFs region indicate that the mean annual precipitation in the past 40 to 10 ka was variable but was typically as much as twice the modern mean annual precipitation (Forester and others, 1999). These plant macrofossil data, together with aquatic fossils, indicate lower mean annual temperature than today (Forester and others, 1999). The increased precipitation and cooler temperatures resulted in a greater than modern level of effective moisture. Greater than modern levels of effective moisture resulted in regional aquifer recharge that was much higher during past pluvial periods (40 to 10 ka; Forester and others, 1999) than today (Benson and Kleiforth, 1989).

Evidence for a higher regional water table at some time in the past has been suggested on the basis of many lines of evidence. J.B. Paces (U.S. Geological Survey, written commun., 2004) points out that records of climate change that may indicate higher water levels can be categorized into three groups: (1) surface features (paleolimnology, paleobotany, and sedimentology); (2) saturated-zone features (paleohydrographs

and paleorecharge); and (3) unsaturated-zone features (pore water and secondary hydrogenic minerals). The data indicate that the water table may have been 10 to 30 meters (m) higher in the past; some researchers postulate the water table may have been as much as 120 m higher.

Extensive paleodischarge deposits and paludal sediments were identified by Swadley and Carr (1987). The location and description of these deposits were refined on the basis of secondary mineral occurrences (Levy, 1991) and strontium isotopic variations from calcite collected from boreholes (Marshall and others, 1993) by Forester and others (1999) and Paces and Whelan (2001). Synchronous paleodischarge at numerous paleodischarge sites distributed over a broad area with heterogeneous hydrogeological conditions indicates the likelihood of a widespread rise in the regional water table (Forester and others, 1999) (fig. D-10). Under these wetter climate conditions, discharge from all sources probably greatly exceeded that which occurred during historical time.

Wetlands from the past pluvial periods of 40 to 10 ka, such as those represented by the deposits at Cactus, Cow Creek, and Tule Springs, were supported by discharge from both the ground-water and surface-water systems. Increased recharge in the Spring Mountains and Sheep Range probably resulted in spring discharge from the alluvial fans at the foot of the mountain ranges.

Deposits in the northern part of Amargosa Desert and the southern part of Crater Flat (fig. D-10) probably also represent an area of focused ground-water discharge during the late Pleistocene (40–12 ka) (Forester and others, 1999). Deposits north of Death Valley Junction, Calif., adjacent to the southern end of the Funeral Mountains (fig. D-10), show an interplay of surface flow and spring discharge as do the deposits in the Amargosa Desert. Interpretations of paleodischarge deposits are not available for Ash Meadows. Quade and others (1995) have identified and studied late Pleistocene wetland deposits in the Coyote Springs and Pahrump Valleys. Extensive spring-discharge and wetland deposits are known from the Pahrump Valley, and according to Quade and others (1995), deposits from about 21 ka and older probably do exist there.

Pluvial lakes occupied many basins in the central and eastern Great Basin during the late Pleistocene (Forester and others, 1999). Within the region, shallow (less than 1.3 m deep) lakes existed in Gold Flat and Emigrant and Kawich Valleys. Fortymile Wash and the Amargosa River were probably perennial streams that helped supply Lake Manly. To produce and maintain this lake would have required either (1) a sizable increase in the volume of precipitation over the saltpan and runoff from the watershed, (2) a substantial decrease in temperature to reduce annual lake evaporation, or (3) a combination of these climatic changes (Grasso, 1996).

Hydrologic models that are based on assumed increased recharge during Pleistocene time (Czarnecki, 1985; D'Agnese and others, 1999) seem to confirm these observations. D'Agnese and others (1999) have reported on a conceptual model of the paleohydrology, based on their climate

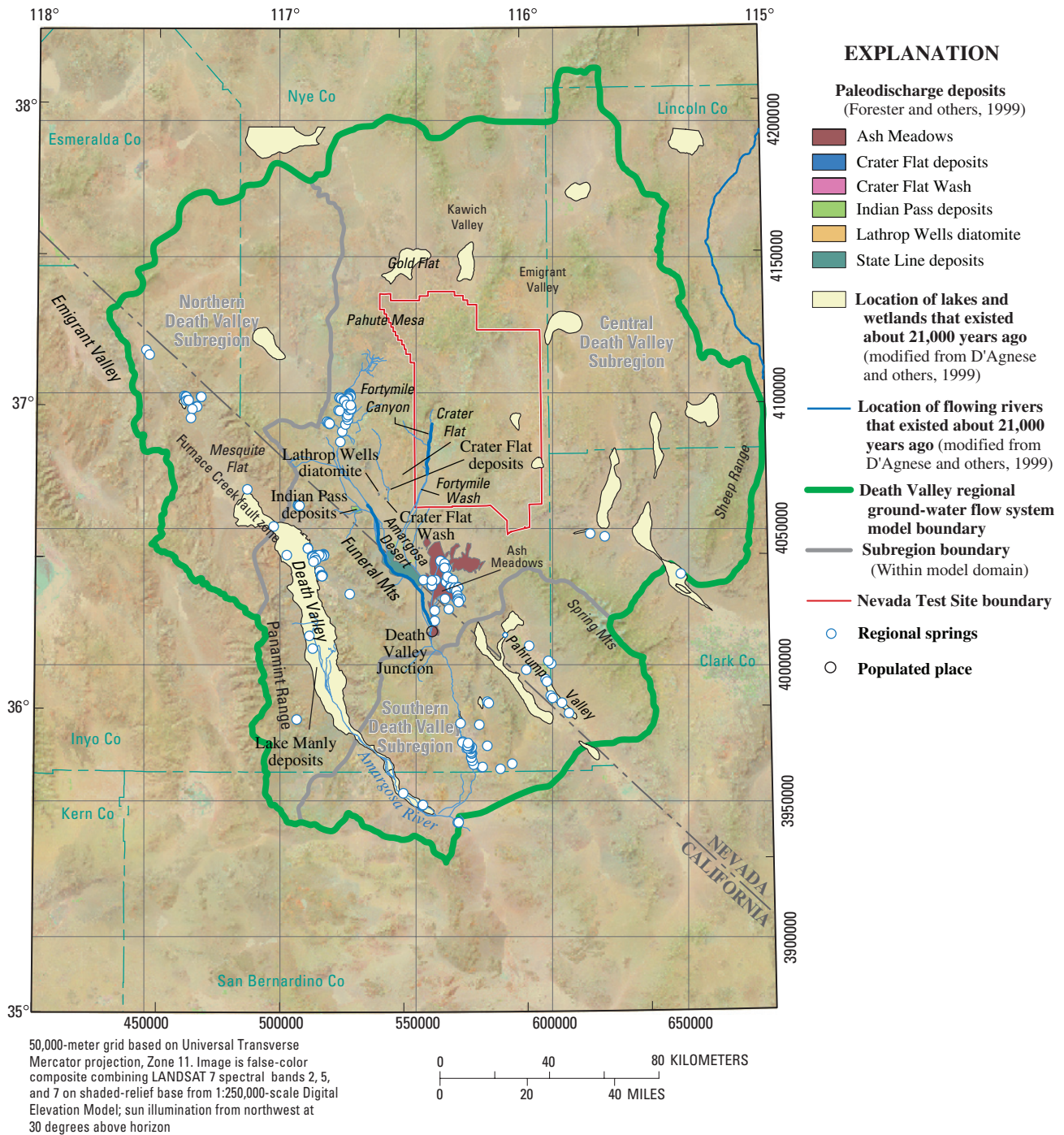


Figure D-10. Location of paleodischarge areas and regional springs in the Death Valley regional ground-water flow system region.

simulation of the Yucca Mountain Project/Hydrologic Resource Management Program (YMP/HRMP) regional ground-water flow model (D'Agnes and others, 1997). In this simulation, the region was assumed to be much cooler and wetter than present, and the lakes and greater discharges described above were supported. It must be remembered, however, that these models have many limitations, not the least of which is the representation of the system as steady state.

Summary

Ground water in the Death Valley region occurs in several interconnected, extremely complex ground-water flow systems. The water moves along relatively shallow and localized flow paths that are superimposed on deeper, regional flow paths. Regional ground-water flow is predominantly through conduits in the carbonate rocks. This flow field is

influenced by complex geologic structures created by regional faulting and fracturing that can create conduits or barriers to flow.

Infiltration of precipitation and runoff on high mountain ranges is the largest source of ground-water recharge. Springs and evapotranspiration are the dominant natural ground-water discharge processes. Discharge related to human activities is associated with ground-water pumping for agricultural, commercial, and domestic uses and is not negligible.

The water table is the upper boundary of the flow system and both no-flow and flow boundaries exist at the lateral extent of the defined flow system. The lower boundary surface of the Death Valley regional ground-water flow system model (DVRFS) domain is the depth at which ground-water flow is dominantly horizontal or parallel to the lower surface and generally corresponds with the upper surface of low-permeability basement rock. Ground-water inflow to the DVRFS model domain occurs in the vicinities of Garden, Coal, Stone Cabin, the southern part of Railroad, Eureka, and Saline Valleys, and the Panamint Range, with possibly small amounts in the Owshead Mountains. Ground-water outflow occurs at the Sheep Range and parts of the Pahrnagat Range, and the western part of Las Vegas Valley and, to a small degree, Silurian Valley.

The region is subdivided into the northern, central, and southern subregions. Ground water flows between these subregions, each which of has distinctive characteristics.

In the northern Death Valley subregion, water levels indicate that much of the ground-water flow is shallow, as the area is underlain by low-permeability bedrock. Ground-water flow is controlled by northeast-southwest-trending structural zones through the mountain ranges east of Death Valley. Ground water entering the subregion as throughflow from the northern boundary or recharge from precipitation flows south to Sarcobatus Flat and Death Valley. Some of this flow discharges at Grapevine and Staininger Springs. These springs result from the intersection of high- and low-permeability structures.

The central Death Valley subregion includes the major discharge areas of Oasis Valley, Ash Meadows, and Alkali Flat–Furnace Creek. These major discharge areas result from flow paths that are complicated by ground water possibly entering the subregion in the vicinities of Stone Cabin, Garden, Coal, and the southern part of Railroad Valleys. Ground-water flow is generally from Pahute Mesa toward Oasis Valley or from the north toward the potentiometric trough north-northeast of Ash Meadows. The major flow paths in the subregion appear to coincide with high-permeability zones created by regional fault or fracture zones. Some of the ground water that originates as recharge in mountain areas or as inflow to the subregion discharges at Ash Meadows. Some continues south and discharges in the Alkali Flat–Furnace Creek basin.

Ground-water movement in the central Death Valley subregion is dominantly lateral and downward toward regional flow paths in the northwestern parts of the Amargosa Desert. Near Yucca Mountain and in areas immediately to the south,

vertical gradients are dominantly upward from the carbonate-rock aquifer into the intermediate system and flow is toward discharge areas to the south and southwest. Ground water in the southern Amargosa Desert may either flow through fractures in the southeastern end of the Funeral Mountains and discharge in the Furnace Creek area or flow southward and discharge at Alkali Flat.

The southern Death Valley subregion is dominated by flow derived primarily from precipitation and subsequent infiltration on the Spring Mountains. Water moves toward the major discharge areas in Pahrump Valley. Springs on the distal edges of alluvial fans in Pahrump Valley have diminished flow, which might result from local ground-water use. Ground water that is not intercepted in Pahrump Valley flows southwest toward discharge areas in Chicago and California Valleys and, ultimately, Saratoga Springs.

In the DVRFS model domain, the entire ground-water system is not in equilibrium. The system has been modified by generally local pumping in (1) Pahrump Valley, (2) Amargosa Desert, (3) Penoyer Valley, and, to a lesser extent, (4) the Nevada Test Site. Although there are virtually no perennial streams in the region, there is evidence for surface-water features, such as perennial streams, lakes, and marshes as well as higher ground-water levels, resulting from wetter climates in the past. Residual effects from past climate change during the Pleistocene, although identifiable in some areas, are thought to be negligible.

References Cited

- Bedinger, M.S., Langer, W.H., and Reed, J.E., 1989, Ground-water hydrology, *in* Bedinger, M.S., Sargent, K.A., and Langer, W.H., eds., *Studies of geology and hydrology in the Basin and Range Province, southwestern United States, for isolation of high-level radioactive waste—Characterization of the Death Valley region, Nevada and California: U.S. Geological Survey Professional Paper 1370-F*, p. 28–35.
- Benson, L.V., and Kleiforth, H., 1989, Stable isotopes in precipitation and ground water in the Yucca Mountain region, southern Nevada—Paleoclimatic implications, *in* Peterson, D.H., ed., *Aspects of climate variability in the Pacific and the western Americas: American Geophysical Union Monograph 55*, p. 41–59.
- Blakely, R.J., Jachens, R.C., Calzia, J.P., and Langenheim, V.E., 1999, Cenozoic basins of the Death Valley extended terrane as reflected in regional gravity anomalies, *in* Wright, L.A., and Troxel, B.W., eds., *Cenozoic basins of the Death Valley Region: Geological Society of America Special Paper 333*, p. 1–16.

- Blakely, R.J., and Ponce, D.A., 2001, Map showing depth to pre-Cenozoic basement in the Death Valley ground-water model area, Nevada and California: U.S. Geological Survey Miscellaneous Field Studies Map, MF-2381-E, 1 sheet, 1:250,000-scale sheet, 6 pages of explanatory text.
- Blankennagel, R.K., and Weir, J.E., Jr., 1973, Geohydrology of the eastern part of Pahute Mesa, Nevada Test Site, Nye County, Nevada: U.S. Geological Survey Professional Paper 712-B, 35 p.
- Carr, W.J., 1984, Regional structural setting of Yucca Mountain, southwestern Nevada, and late Cenozoic rates of tectonic activity in part of the southwestern Great Basin, Nevada and California: U.S. Geological Survey Open-File Report 84-854, 114 p.
- Czarnecki, J.B., 1997, Geohydrology and evapotranspiration at Franklin Lake Playa, Inyo County, California: U.S. Geological Survey Water-Supply Paper 2377, 75 p.
- Czarnecki, J.B., 1985, Simulated effects of increased recharge on the ground-water flow system of Yucca Mountain and vicinity, Nevada-California: U.S. Geological Survey Water-Resources Investigations Report 84-4344, 33 p.
- Czarnecki, J.B., and Waddell, R.K., 1984, Finite-element simulation of ground-water flow in the vicinity of Yucca Mountain, Nevada-California: U.S. Geological Survey Water-Resources Investigations Report 84-4349, 38 p.
- Czarnecki, J.B., and Wilson, W.E., 1991, Conceptual models of the regional ground-water flow and planned studies at Yucca Mountain, Nevada: *Hydrological Science and Technology*, v. 7, no. 1-4, p. 15-25.
- D'Agnese, F.A., Faunt, C.C., and Turner, A.K., 1998, An estimated potentiometric surface of the Death Valley region, Nevada and California, using geographic information systems and automated techniques: U.S. Geological Survey Water-Resources Investigations Report 97-4052, 15 p., 1 plate.
- D'Agnese, F.A., Faunt, C.C., Turner, A.K., and Hill, M.C., 1997, Hydrogeologic evaluation and numerical simulation of the Death Valley regional ground-water flow system, Nevada, and California: U.S. Geological Survey Water-Resources Investigations Report 96-4300, 124 p.
- D'Agnese, F.A., O'Brien, G.M., Faunt, C.C., Belcher, W.R., and San Juan, C.A., 2002, A three-dimensional numerical model of predevelopment conditions in the Death Valley regional ground-water flow system, Nevada and California: U.S. Geological Survey Water-Resources Investigations Report 02-4102, 114 p. Accessed September 22, 2004, at <http://pubs.water.usgs.gov/wri024102/>.
- D'Agnese, F.A., O'Brien, G.M., Faunt, C.C., and San Juan, C.A., 1999, Simulated effects of climate change on the Death Valley regional ground-water flow system, Nevada and California: U.S. Geological Survey Water-Resources Investigations Report 98-4041, 40 p.
- DeMeo, G.A., Lacznik, R.J., Boyd, R.A., Smith, J.L., and Nylund, W.E., 2003, Estimated ground-water discharge by evapotranspiration from Death Valley, California, 1997-2001: U.S. Geological Survey Water-Resources Investigations Report 03-4254, 27 p.
- Dettinger, M.D., Harrill, J.R., and Schmidt, D.L., 1995, Distribution of carbonate-rock aquifers and the potential for their development, southern Nevada and adjacent parts of California, Arizona, and Utah: U.S. Geological Survey Water-Resources Investigations Report 91-4146, 100 p.
- Dudley, W.W., Jr., and Larson, J.D., 1976, Effect of irrigation pumping on desert pupfish habitats in Ash Meadows, Nye County, Nevada: U.S. Geological Survey Professional Paper 927, 52 p.
- Eakin, T.E., Price, Don, and Harrill, J.R., 1976, Summary appraisals of the Nation's ground-water resources—Great Basin region: U.S. Geological Survey Professional Paper 813-G, 37 p.
- Faunt, C.C., 1997, Effect of faulting on ground-water movement in the Death Valley region, Nevada and California: U.S. Geological Survey Water-Resources Investigations Report 95-4132, 42 p.
- Forester, R.M., Bradbury, J.P., Carter, C., Elvidge-Tuma, A.B., Hemphill, M.L., Lundstrom, S.C., Mahan, S.A., Marshall, B.D., Neymark, L.A., Paces, J.B., Sharpe, S.E., Whelan, J.F., and Wigand, P.E., 1999, The climatic and hydrologic history of southern Nevada during the late Quaternary: U.S. Geological Survey Open-File Report 98-0635, 63 p.
- Franke, O.L., Reilly, T.E., and Bennett, G.D., 1987, Definition of boundary and initial conditions in the analysis of saturated ground-water flow systems—An introduction: U.S. Geological Survey Techniques of Water-Resources Investigations, book 3, chap. B5, 15 p.
- Freeze, R.A., and Cherry, J.A., 1979, *Ground water*: Englewood Cliffs, N.J., Prentice-Hall, Inc., 604 p.
- Grauch, V.J.S., Sawyer, D.A., Fridrich, C.J., and Hudson, M.R., 1999, Geophysical framework of the southwestern Nevada volcanic field and hydrogeologic implications: U.S. Geological Survey Professional Paper 1608, 39 p.
- Grasso, D.N., 1996, Hydrology of modern and late Holocene lakes, Death Valley, California: U.S. Geological Survey Water-Resources Investigations Report 95-4237, 53 p.

- Grose, T.L., 1983, Thirty-two geologic cross sections, Clark, Esmeralda, Lincoln, Mineral and Nye Counties, Nevada and adjacent areas in California: Nevada Bureau of Mines and Geology Open-File Report 83-13.
- Harrill, J.R., Gates, J.S., and Thomas, J.M., 1988, Major ground-water flow systems in the Great Basin region of Nevada, Utah, and adjacent States: U. S. Geological Survey Hydrologic Investigations Atlas HA-694-C, 2 sheets.
- Harrill, J.R., and Prudic, D.E., 1998, Aquifer systems in the Great Basin region of Nevada, Utah, and adjacent States—A summary report: U.S. Geological Survey Professional Paper 1409-A, 66 p.
- Hevesi, J.A., Flint, A.L., and Flint, L.E., 2003, Simulation of net infiltration and potential recharge using a distributed parameter watershed model of the Death Valley region, Nevada and California: U.S. Geological Survey Water-Resources Investigations Report 03-4090, 161 p.
- Hunt, C.B., 1975, Death Valley geology, ecology, and archaeology: Los Angeles, University of California Press, 234 p.
- Hunt, C.B., Robinson, T.W., Bowles, W.A., Washburn, A.L., 1966, Hydrologic basin, Death Valley, California: U.S. Geological Survey Professional Paper 494-B, 138 p.
- IT Corporation, 1996, Underground test area subproject phase I, Data analysis task, volume VI—Groundwater flow model data documentation package: Las Vegas, Nev., Report ITLV/10972-81 prepared for the U.S. Department of Energy, 8 volumes, various pagination.
- Kilroy, K.C., 1991, Ground-water conditions in Amargosa Desert, Nevada-California, 1952-87: U.S. Geological Survey Water-Resources Investigations Report 89-4101, 91 p.
- Laczniak, R.J., Cole, J.C., Sawyer, D.A., and Trudeau, D.A., 1996, Summary of hydrogeologic controls on ground-water flow at the Nevada Test Site, Nye County, Nevada: U.S. Geological Survey Water-Resources Investigations Report 96-4109, 59 p.
- Laczniak, R.J., DeMeo, G.A., Reiner, S.R., Smith, J.L., and Nylund, W.E., 1999, Estimates of ground-water discharge as determined from measurements of evapotranspiration, Ash Meadows area, Nye County, Nevada: U.S. Geological Survey Water-Resources Investigations Report 99-4079, 70 p. Accessed September 1, 2004 at: <http://water.usgs.gov/pubs/wri/wri994079/>
- Laczniak, R.J., Smith, J.L., Elliott, P.E., DeMeo, G.A., Chatigny, M.A., and Roemer, G.J., 2001, Ground-water discharge determined from estimates of evapotranspiration, Death Valley regional flow system, Nevada and California: U.S. Geological Survey Water-Resources Investigations Report 01-4195, 51 p.
- Luckey, R.R., Tucci, Patrick, Faunt, C.C., Ervin, E.M., Steinkampf, W.C., D'Agnese, F.A., and Patterson, G.L., 1996, Status of understanding of the saturated-zone ground-water flow system at Yucca Mountain, Nevada as of 1995: U.S. Geological Survey Water-Resources Investigations Report 96-4077, 71 p.
- Levy, S.S., 1991, Mineralogic alteration history and paleo-hydrology at Yucca Mountain, Nevada, *in* High Level Radioactive Waste Management, Proceedings of the Second Annual International Conference, Las Vegas, Nevada, April 28-May 3, 1991: La Grange Park, Ill., American Nuclear Society, p. 477-485.
- Marshall, B.D., Peterman, Z.E. and Stuckless, J.S., 1993, Strontium isotopic evidence for a higher water table at Yucca Mountain, *in* Proceedings of the High Level Radioactive Waste Management Fourth Annual International Conference, Las Vegas, Nevada, April 26-30, 1993: La Grange Park, Ill., American Nuclear Society, p. 1948-1952.
- Moreo, M.T., Halford, K. J., La Camera, R.J., and Laczniak, R.J., 2003, Estimated ground-water withdrawals from the Death Valley regional flow system, Nevada and California, 1913-98: U.S. Geological Survey Water-Resources Investigations Report 03-4245, 28 p.
- Paces, J.B., and Whelan, J.F., 2001, Water-table fluctuations in the Amargosa Desert, Nye County, Nevada, *in* High-Level Radioactive Waste Management, Proceedings of the Ninth International Conference, Las Vegas, Nev., April 29-May 3, 2001: LaGrange Park, Ill., American Nuclear Society, published on CD-ROM.
- Peterman, Z.E., and Stuckless, J.S., 1992a, Applications of strontium and other radiogenic tracer isotopes to paleo-hydrologic studies—Paleohydrogeological methods and their applications: Proceedings of a Nuclear Energy Agency Workshop, Paris, France, November 9-10, 1992, p. 59-84.
- Peterman, Z.E., and Stuckless, J.S., 1992b, Strontium isotope characterization of flow systems in southern Nevada, USA: *Mineralogical Magazine*, v. 58A, p. 711-712.
- Potter, C.J., Sweetkind, D.S., Dickerson, R.P., and Kilgore, M.L., 2002, Hydrostructural maps of the Death Valley regional flow system, Nevada and California: U.S. Geological Survey Miscellaneous Field Studies MF-2372, 2 sheets, 1:250,000 scale, 14 p.
- Quade, Jay, Mifflin, M.D., Pratt, W.L., McCoy, William, and Burckle, Lloyd, 1995, Fossil spring deposits in the southern Great Basin and their implications for changes in water-table levels near Yucca Mountain, Nevada, during Quaternary time: *Geological Society of America Bulletin*, v. 107, p. 213-230.

- Savard, C.S., 1998, Estimated ground-water recharge from streamflow in Fortymile Wash near Yucca Mountain, Nevada: U.S. Geological Survey Water-Resources Investigations Report 97-4273, 30 p.
- Schoff, S.L., and Moore, J.E., 1964, Chemistry and movement of ground water, Nevada Test Site: U.S. Geological Survey Trace Elements Report 838, 75 p.
- Seaber, P.R., Kapinos, F.P., and Knapp, G.L., 1987, Hydrologic unit maps: U.S. Geological Survey Water-Supply Paper 2294, 63 p., 1 pl.
- Sinton, P.O., 1987, Three-dimensional, steady-state, finite-difference model of the ground-water flow system in the Death Valley ground-water basin, Nevada-California: Golden, Colorado School of Mines, Master's thesis, 145 p.
- Steinkampf, W.C., and Werrell, W.E., 2001, Ground-water flow to Death Valley, as inferred from the chemistry and geohydrology of selected springs in Death Valley National Park, California and Nevada: U.S. Geological Survey Water-Resources Investigations Report 98-4114, 37 p.
- Swadley, W.C., and Carr, W.J., 1987, Geologic map of the Quaternary and Tertiary deposits of the Big Dune quadrangle, Nevada-California: U.S. Geological Survey Miscellaneous Investigations Series Map I-1767, scale 1:48,000, 1 sheet.
- Sweetkind, D.S., Dickerson, R.P., Blakely, R.J., and Denning, P.D., 2001, Interpretive geologic cross sections for the Death Valley regional flow system and surrounding areas, Nevada and California: U.S. Geological Survey Miscellaneous Field Studies Map MF-2370, 3 plates, 32 pages of explanatory text. Accessed September 1, 2004 at: <http://greenwood.cr.usgs.gov/pub/mf-maps/mf-2370/>
- Waddell, R.K., 1982, Two-dimensional, steady-state model of ground-water flow, Nevada Test site and vicinity, Nevada-California: U.S. Geological Survey Water-Resources Investigations Report 84-4267, 72 p.
- Waddell, R.K., Robison, J.H., and Blakennagel, R.K., 1984, Hydrology of Yucca Mountain and vicinity, Nevada-California—Investigative results through mid-1983: U.S. Geological Survey Water-Resources Investigations Report 84-4267, 72 p.
- Walker, G.E., and Eakin, T.E., 1963, Geology and ground water of Amargosa Desert, Nevada-California: Carson City, Nevada Department of Conservation and Natural Resources, Ground-Water Resources-Reconnaissance Series Report 14, 45 p.
- White, A. F., 1979, Geochemistry of ground water associated with tuffaceous rocks, Oasis Valley, Nevada: U.S. Geological Survey Professional Paper 712E, p. E1-E25.
- Winograd, I.J., Copeland, T.B., Landwehr, J.M., Riggs, A.C., Ludwig, K.R., Simmons, K.R., Szabo, B.J., Kolesar, P.T., and Revesz, K.M., 1992, Continuous 500,000-year climatic record from vein calcite in Devils Hole, Nevada: *Science*, v. 258, p. 255-260.
- Winograd, I.J., and Pearson, F.J., Jr., 1976, Major carbon-14 anomaly in a regional carbonate aquifer—Possible evidence for megascale channeling, south-central Great Basin: *Water Resources Research*, v. 12, p. 1125-1143.
- Winograd, I.J., and Szabo, B.J., 1988, Water-table decline in the south-central Great Basin during the Quaternary period—Implications for toxic waste disposal, *in* Carr, M.D., and Yount, J.C., eds., *Geologic and hydrologic investigations of a potential nuclear waste disposal site at Yucca Mountain, southern Nevada*: U.S. Geological Survey Bulletin 1790, p. 147-152.
- Winograd, I.J., and Thordarson, William, 1968, Structural control of ground-water movement in miogeosynclinal rocks of south-central Nevada, *in* Eckel, E.B., ed., *Nevada Test Site: Geological Society of America Memoir 110*, p. 35-48.
- Winograd, I.J., and Thordarson, William, 1975, Hydrologic and hydrochemical framework, south-central Great Basin, Nevada-California, with special reference to the Nevada Test Site: U.S. Geological Survey Professional Paper 712C, p. C1-C126.
- Workman, J.B., Menges, C.M., Page, W.R., Taylor, E.M., Ekren, E.B., Rowley, P.D., Dixon, G.L., Thompson, R.A., and Wright, L.A., 2002, Geologic map of the Death Valley ground-water model area, Nevada and California: U.S. Geological Survey Miscellaneous Field Studies Map MF-2381-A. Accessed September 1, 2004 at: <http://greenwood.cr.usgs.gov/pub/mf-maps/mf-2381/>